UNIVERSITY OF CALIFORNIA,
IRVINE

Investigating circadian disruption using real-time longitudinal imaging of the entire *Drosophila* circadian neural network

DISSERTATION

submitted in partial satisfaction of the requirements
for the degree of

DOCTOR OF PHILOSOPHY

in Physiology & Biophysics

by

Ceazar E. Nave

Dissertation Committee:
Todd C. Holmes, PhD, Chair
Tanya Leise, PhD
Devon Lawson, PhD
Francesco Tombola, PhD
Xiangmin Xu, PhD

2020

DEDICATION

To my husband, Sonny:
a source of unconditional love and support.
Our fourteen years together
is worth more than all the riches the Earth can offer.

To my children, Amelia and Ronin:
may the path I pave for you fuel your desire
to make differences in others' lives
and change this world for the better.

TABLE OF CONTENTS

LIST OF FIGURES

Movie Supplement

Supplemental Figures

LIST OF TABLES

ACKNOWLEDGEMENTS

I would like to thank my advisor, Dr. Todd C. Holmes for the opportunity to complete a PhD in his laboratory, and for the years of guidance and support as a graduate student. Thank you for all the invaluable advice your provided, and the morals instilled in me to last a lifetime. Mostly, thank you for allowing me to transform into the scientist that I am today. Year from now, I will always look back and think about the wonderful days spent with each other especially during the coveted Tomato Tuesdays with the Holmes Lab.

I want to express my deepest gratitude to all the members of the Holmes lab (past and present). Thank you for allowing me to be genuine, authentic weird self. You've all created a wonderful and welcoming environment to allow this budding scientist to flourish.

So much of the work presented in this dissertation would not be possible without the incredible hard work, and perseverance of my undergraduate scientists. Jerson, Patrick, Alpha Thanh, Beta Thanh, and Tony – you've done more than help me take on the monumental tasks of experimentation, data analysis, and figure building; you've taught me how to be an effective mentor, and fueled my passion in getting everyone to fall in love with science.

Thank you to my SFSU undergraduate and master's mentors, Dr. Carmen Domingo and Dr. Kimberly Tanner. You both have instilled so much wisdom and compassion in me and I carry it wherever I go. Thank you for being such an inspiration to me and so many others and making a difference in the world…and staying so cool while doing it. Thank you to all my SFSU brigade for the friendship and love you've showered me even after my days at State were long gone. Friendships like what you've provided for me keep me going in this long and arduous PhD adventure in hopes that we will all work together again, just like the old days.

My thesis committee has served as constant support throughout the journey of this dissertation. Thank you to Dr. Tanya Leise, Dr. Devon Lawson, Dr. Francesco Tombola,

and Dr. Xiangmin Xu for the advice you've provided towards the completion of my degree. Additional thanks to Dr. Tanya Leise for all the work you've done in data visualization for the WLS paper and being available for all my annoying requests and questions.

To the Department of Physiology and Biophysics administration. Thank you for all that you do behind all the science. Claire, Duke, Lilian, James, and Janita – thank you for keeping us all afloat and thank you for dealing with all the non-science things that, I otherwise, would butcher.

The UCI School of Medicine Graduate Studies: Leora Fellus, and Associate Dean Klemens Hertel. Thank you for allowing me to discover my passion in helping others achieve their dreams of higher education. Thank you for letting me take on such an important task to highlight and promote the amazing programs that UCI has to offer.

This PhD would not be completed without the love and support from my friends and family. You know who you are, I love you all. My husband and my children, thank you for the unconditional love and support, the sleepless nights, and magical milk barfs.

This work was funded by NIH R35 GM127102 GM102965, GM107405, and GM127102.
Thank you to Cell Press for providing copyright permissions for Chapter 4.

VITA

Ceazar E. Nave

EDUCATION

PhD Physiology & Biophysics. University of California, Irvine	**2015-2020**
MSc Cell & Molecular Biology. San Francisco State University	**2012-2014**
BA Biology (Physiology Emphasis). San Francisco State University	**2008-2012**
BA Liberal Studies (K-12 Ed.). San Francisco State University	**2008-2012**

RESEARCH

PhD Research **2016-2020**

PhD Biomedical Sciences – Physiology & Biophysics, University of California, Irvine

- Advisor: Todd C. Holmes, PhD
- Project: Investigating "Weekend Light Shifts" Using Real-Time Longitudinal Imaging of the Entire *Drosophila* Circadian Neural Network
- Project: Polyglutamine-Huntingtin Expression Selectively Disrupts *Drosophila* Small-Lateral Ventral Neuron Function
- Project: Investigating the Role of *miles-to-go (mtgo)* on Circadian-Modulated Behaviors in *Drosophila*

First-Year Graduate Research **2015-2016**

Cellular & Molecular Biosciences (CMB) Lab Rotations – University of California, Irvine

- CMB First-Year Advisor: Matthew Inlay, PhD
- Winter 2016 Rotation Advisor: Todd C. Holmes, PhD. Dept. of Physiology and Biophysics. Project: Investigating "Social Jet Lag" Using Real-Time Longitudinal Imaging of the Entire *Drosophila* Circadian Neural Network
- Fall 2015 Rotation Advisor: Zeba Wunderlich, PhD. Dept. Developmental Cell Biology. Project: Identifying the Mechanisms of Robustness Driven by Shadow Enhancers in *Drosophila melanogaster*
- Summer 2015 Rotation Advisor: Maksim Plikus, PhD. Dept. Developmental Cell Biology. Project: Characterizing the Role of *FGF5* and *K-14 Noggin* in Murine Hair Regeneration Using Tissue-Specific Gene Ablation

MSc Research **2012-2014**

MSc Cell & Molecular Biology – San Francisco State University

- Advisor: Carmen Domingo, PhD. Dept. of Biology (Developmental Biology).
- Project: Investigating the Role of microRNA-206 During Early Muscle Development in *Xenopus laevis*

- Project: Characterizing the role of Stromal-Derived Factor-1a (SDF-1α) Signaling During Early Muscle Development in *Xenopus laevis*

MSc Research **2013-2014**

Howard Hughes Medical Institute Biology Faculty Explorations in Scientific Teaching – San Francisco State University

- Advisor: Leticia Marquez-Magaña, PhD, and Kimberly D. Tanner, PhD. Dept. of Biology. Project: Increasing Understanding of Science Mentoring in Paired Undergraduate and Master's-Level Course (Biol344/844)

Undergraduate Research **2010-2012**

BA Biology/BA Liberal Studies – San Francisco State University

- Advisor: Carmen Domingo, PhD. Department of Biology (Developmental Biology).
- Project: Investigating the Role of MicroRNA-206 During Early Muscle Development in *Xenopus laevis*
- Project: Characterizing the role of Stromal-Derived Factor-1a (SDF-1α) Signaling During Early Muscle Development in *Xenopus laevis*

TEACHING AND MENTORSHIP

Undergraduate Mentorship **2016-Now**

- **Jerson D. Estrella, BS**. UC Irvine Genetics Honors. UROP Recipient, SURP Recipient. Project: Investigating Circadian Disruption Using Longitudinal and Fluorescence Imaging of the Entire *Drosophila* Circadian Neural Network. Graduated Spring 2019, Columbia University PhD Program 2020-2024
- **Patrick Hwu, BS.** SURP Recipient. Project: Polyglutamine-Huntingtin Expression Selectively Disrupts *Drosophila* Small-Lateral Ventral Circadian Neuron Function. Graduated Fall 2018, UC Irvine PhD Program 2019-2023
- **Thanh C. Vo**. Expected Graduation: Spring 2021. Project: Investigating Circadian Disruption Using Longitudinal and Fluorescence Imaging of the Entire *Drosophila* Circadian Neural Network (Expected graduation Summer 2021)
- **Thanh N. Nguyen.** Expected Graduation: Spring 2021. Project: Polyglutamine-Huntingtin Expression Selectively Disrupts *Drosophila* Small-Lateral Ventral Circadian Neuron Function (Expected Graduation Summer 2021)
- **Tony T. Bui.** Expected Graduation: Summer 2020. Project: Investigating the Role of *miles-to-go (mtgo)* on Circadian-Modulated Behaviors in *Drosophila*. Graduated Spring 2020.

Graduate Teaching Assistant – UC Irvine. Irvine, CA **2016-2017**

- **Graduate Teaching Instructor**: Scientific Writing (Biol100)

Instructor – Los Angeles Valley College. North Hollywood, CA **2015**

- **Instructor**: Introductory Biology, Introductory Chemistry, College Algebra, Introduction to Aseptic Techniques

Science Teaching for Scientists. San Francisco State University. SF, CA **2011-2012**

- Science Education Partnership Assessment Laboratory (SFSU SEPAL)
- Collaboration between SFSU Department of Biology Faculty in assessing undergraduate, and graduate student understanding of classroom objectives
- Development and implementation of retrospective assessments to gain insights in student retention
- Assisted Department of Biology Faculty in addressing student misconceptions during in-class lectures and activities

Science Partnerships: K-12 Ed. San Francisco State University. SF, CA **2009-2010**

- Science Education partnership Assessment Laboratory (SFSU SEPAL)
- Implementation of State of California Science Curriculum Standards in K-12 classrooms
- Development of hands-on Biology and Physical Science curriculum in K-12 classrooms

PRESENTATIONS

Oral Presentations

- **Center for Circadian Biology (CCB) Fall Workshop on Biological Timing, San Diego, CA.** Investigating Circadian Disruption Using Real-Time Longitudinal Imaging of the Entire *Drosophila* Circadian Neural Network — **Nov 2018**
- **2016 *Drosophila* Interest Group, Irvine, CA.** Investigating "Social Jet Lag" Using Real-Time Longitudinal Imaging of the Entire *Drosophila* Neural Network — **May 2016**
- **San Francisco State University Research Symposium, San Francisco, CA.** Time-Lapse Imaging of Muscle Formation in *Xenopus laevis* Embryos — **Aug 2011**

Poster Presentations

- **2020 Society for Research in Biological Rhythms. Online Conference.** Weekend Light Shifts Evoke Persistent *Drosophila* Circadian Neural Network Desynchrony. — **May 2020**
- **2019 Cold Spring Harbor Laboratory Meeting: *Drosophila* Neurobiology, Cold Spring Harbor, NY.** Characterizing the role of *miles-to-go (mtgo)* in *Drosophila* circadian-modulated behaviors — **Oct 2019**

- **2018 Society for Neuroscience Conference, San Diego, CA.** Weekend Light Shifts Evoke *Drosophila* Neural Network Desynchrony **Nov 2018**
- **2018 Society for Research in Biological Rhythms, Amelia Island, FL.** Social Jet Lag Evokes *Drosophila* Neural Network Desynchrony **May 2018**
- **2017 Cold Spring Harbor Laboratory Meeting: *Drosophila* Neurobiology, Cold Spring Harbor, NY.** Social Jet Lag Evokes *Drosophila* Neural Network Desynchrony **Oct 2017**
- **2017 Center for Circadian Biology Symposium: From Cells to Clinic, San Diego, CA.** Social Jet Lag Evokes *Drosophila* Neural Network Desynchrony **Feb 2017**
- **15th International *Xenopus* Genetics Conference, Pacific Grove, CA.** The Role of MicroRNA-206 in *Xenopus laevis* Somite Morphogenesis **Aug 2014**
- **SFSU College of Science and Engineering Student Project Showcase, San Francisco, CA.** Characterizing the Role of SDF-1α Signaling During *Xenopus laevis* Muscle Development **May 2014**
- **2012 Society for the Advancement of Chicanos and Native Americans in Science, Seattle, WA.** MicroRNA-206 is Important for Proper Development of the Notochord-Somite Boundary in *Xenopus laevis* **Oct 2012**
- **SFSU College of Science and Engineering Student Project Showcase, San Francisco, CA.** The Role of MiR-206 During the Formation of the Notochord-Somite Boundary in *Xenopus laevis* **May 2012**

HONORS & AWARDS

- **President's Dissertation Year Fellowship Honorable Mention Award.** University of California, Irvine **May 2019**
- **School of Medicine Dean's Fellowship Award.** University of California, Irvine **Oct 2018**
- **Diversity Research Fellowship.** University of California, Irvine **Aug 2015**
- **15th International *Xenopus* Genetics Conference Travel Award Recipient.** Pacific Grove, CA **Aug 2014**
- **San Francisco State University Distinguished Graduate Student.** San Francisco State University **May 2014**
- **Minority Biomedical Research Support – Research Initiative for Scientific Enhancement (MBRS-RISE) Graduate Fellowship.** San Francisco State University. Director: Frank **2012-2014**

Bayliss, PhD. Department of Biology, San Francisco State University

- **San Francisco State University – Instructionally Related Activities Award (IRA) for Graduate Researchers.** San Francisco State University **2013-2014**
- **Minority Biomedical Research Support – Research Initiative for Scientific Enhancement (MBRS-RISE) Undergraduate Fellowship.** San Francisco State University. Director: Frank Bayliss, PhD. Department of Biology, San Francisco State University **2011-2012**
- **San Francisco State University – instructionally Related Activities Award (IRA) for Undergraduate Researchers.** San Francisco State University **2011-2012**
- **California State University Louis Stokes Alliance for Minority Participation (CSU-LSAMP) Scholarship.** San Francisco State University **2010-2011**

PROFESSIONAL SOCIETIES & ORGANIZATIONS

- **Society for Neuroscience** **2018-Now**
- **Society for Research in Biological Rhythms** **2018-Now**
- **American Association for the Advancement of Science** **2017-Now**
- **University of California, Irvine. School of Medicine Graduate Student Advisory Council.** University of California, Irvine **2016-Now**
- **Diverse Educational Community and Doctoral Experience (DECADE) Executive Student Council – School of Medicine Graduate Student Representative.** University of California, Irvine **2017-2019**
- **Diverse Educational Community and Doctoral Experience (DECADE) Executive Student Council – Public Relations Social Media Chair.** University of California, Irvine **2018**
- **Genetics Society of America** **2014**
- **Society for Developmental Biology** **2013**
- **Society for the Advancement of Chicanos and Native Americans in Science** **2012**

SKILLS

Laboratory

- **Fluorescence microscopy**: Zeiss LSM780 2-photon/excitation microscope, Zeiss Axio-Observer Z1, Zeiss LSM 710 and 700 confocal microscope, Nikon

C1 confocal microscope, Nikon PCM2000 fluorescence compound microscope, Olympus sZX12 microscope, Leica SP8 confocal microscope

- ***Culex fasciatus/Aedes aegypti/Anopheles coluzzii**:* brain dissections, immunohistochemistry, activity monitoring
- ***Drosophila melanogaster***: genetics and genotyping, *Drosophila* brain dissections, neurobiology, circadian biology, sleep analysis, TriKinetics *Drosophila* behavior assays, *Drosophila* brain culture, tissue culture, bioluminescence imaging, *in situ* hybridization and probe design, *Drosophila* embryo cuticle preps, immunocytochemistry (ICC), single-cell RNA sequencing, fluorescence-activated cell sorting (FACS) analysis, RNA and DNA isolation, bacterial transformation
- ***Xenopus laevis***: embryonic micro-dissections, Keller sandwiches, open-faced explants, cell transplantation, tissue culture, in vitro fertilization, oocyte isolation, immunohistochemistry
- ***Mus musculus***: murine genetics and genotyping, epidermal isolation, genotyping, immunohistochemistry

Software

- Microscopy and Digital Processing of Images (Zeiss LSM 710 Confocal Microscope, Zeiss LSM 700 Confocal Microscope, Leica SP8 Confocal Microscope), VOLOCITY, ImageJ/NIH Image/FIJI, Adobe Creative Suite (Photoshop, Illustrator, InDesign), Microsoft Office, MetaMorph Analysis, MATLAB, R/RStudio, IMARIS Image Processing, Leica Image Processing

PUBLICATIONS

- **Weekend Light Shifts Evoke Persistent *Drosophila* Circadian Neural Network Desynchrony.** Authors: Nave, C., Roberts, LR., Hwu, P., Estrella, J.D., Vo, T., Nguyen, T., Bui, T., Rindner, D., Pervolarakis, N., Shaw P., Leise, T., Holmes, T.C. — **Under Review**
- **Polyglutamine-Huntingtin Expression Selectively Disrupts *Drosophila* Small-Lateral Ventral Circadian Neuron Function.** Authors: Vasu, S., Fogle, K.J., Rashid, S., Gudubasha, S., Nave, C., Hwu, P., Holmes, T.C. — **In Preparation**
- **Characterizing the Role of MILES-TO-GO (MTGO) in *Drosophila* Circadian-Modulated Behaviors.** Authors: Nave, C., Hwu, P., Estrella, J.E., Nguyen, T.H., Vo, T.C., Syed, A., Marsh, L., MacGregor, G.R., Holmes., T.C. — **In Preparation**
- **Molecular Basis for Circadian Diurnality And Nocturnality and the Role of the Circadian Clock in Light-Evoked** — **May 2020**

Attraction/Avoidance Behavior in *Aedes aegypti* And *Anopheles coluzzii* Mosquitoes. Authors: Baik, L.S., Nave, C., Au, D.D., Guda, T., Chevez, J.A., Ray, A., Holmes, T.C. Current Biology (2020). Accepted May 2020.

- **Distinct Mechanisms of *Drosophila* CRYPTOCHROME-Mediated Light-Evoked Membrane Depolarization and In Vivo Clock Resetting**. Authors: Baik, L.S., Au, D., Nave, C., Foden, A., Enrriquez-Valdez, W., Holmes, T.C. PNAS (2019). 116 (46) 23339-23344. **Oct 2019**
- **MiR-206 is Required for Changes in Cell Adhesion That Drive Muscle Cell Morphogenesis in *Xenopus laevis***. Authors: Vergara, H.M., Ramirez, J., Rosing, T., Nave, C., Blandino, R., Saw, D., Saraf, P., Peixoto, G., Coombes, C., Adams, M., Domingo, C.R., Developmental Biology (2018). 438(2):94-110 **Mar 2018**
- **The Role of SDF-1α Signaling in *Xenopus laevis* Somite Morphogenesis**. Authors: Leal, M.A., Fickel, S.R., Ramirez, J., Vergara, H.M., Nave, C., Saw, D., Domingo, C.R. Developmental Dynamics (2014). 243, 509-526 **Apr 2014**

ABSTRACT OF THE DISSERTATION

Investigating circadian disruption using real-time longitudinal imaging of the entire *Drosophila* circadian neural network

By

Ceazar E. Nave

University of California, Irvine, 2020

Dr. Todd C. Holmes, Chair

Circadian oscillators are capable of endogenous oscillations in free-running conditions. Many studies show that the coordination of the biological clock with environmental inputs, such as daily solar cycles, is critical for regulating physiological and behavioral activities. Conversely, billions of people worldwide are subjecting themselves to chronic misalignment and disruption of biological clocks with environmental inputs. In this study, we developed an entrainment protocol we call *LD Strobe* that permits us to obtain real-time, longitudinal bioluminescence imaging of the entire *Drosophila* circadian neural circuit in adult cultured brains, *ex vivo.* With the *LD Strobe* schedule, we can now examine circadian disruptions that could potentially lead to the progression of human-related diseases. In the following proposed projects we aim to (1) capture the *Drosophila* circuit-wide responses to Weekend Light Shifts, (2) determine *Drosophila* behavioral outputs generated by circadian-disrupted flies after undergoing a simulated weekend, (3) examine the circuit-wide response of flies in a genetic background with uncharacterized disruptions to circadian-modulated physiology and behavior, and (4) determine the

circadian regulation light-evoked attraction and avoidance behaviors in daytime- and nighttime-biting mosquitos. Due to similarities between mammalian and insect circadian molecular and neural circuits, features of the circadian physiological and behavioral outputs from the proposed projects may be broadly observed and applicable to humans.

CHAPTER 1

Introduction

1.1 Introduction

Almost all walks of life have circadian rhythms: from single-celled bacteria, to complex organisms like mammals. Circadian rhythms are endogenous, biological mechanisms that last for ~24 hours [1,2,48]. These endogenous rhythms control numerous physiological and behavioral aspects of daily life and are entrainment mechanisms that can be synchronized using environmental cues [1,5,8,10,12,14]. For circadian systems, light input from the environment has been shown to be the most powerful zeitgeber to entrain circadian rhythms [16,18,20,22].

In the fruit fly, *Drosophila melanogaster,* the circadian powerhouse overseeing the organism's rhythm are a subset of neurons distributed throughout the fly brain. These neurons are named based on their relative positioning throughout the *Drosophila* brain. There are approximately 150 neurons that express the oscillating molecular clock components and their rhythmic oscillations can be sustained even in the absence of important cues [25,27,33]. All circadian neurons express core clock proteins that are expressed in a cyclic fashion via a transcriptional-translational feedback loop. Generally, clock proteins, PERIOD (PER) and TIMELESS (TIM), form a cytosolic heterodimer that is transported in the nucleus with the help of the casein kinase, DOUBLETIME (DBT). Once in the nucleus, the PER/TIM heterodimer prevent the binding of CLOCK/CYCLE (CLK/CYC) to the E-Box promoter region that encodes production of *per* and *tim* mRNA, thus leading to the inhibition of its own production. However, during daytime, light signals

activate the blue-light sensitive flavoprotein, CRYPTOCHROME (CRY), which degrades TIM resetting the clock. This light-mediated circadian reset occurs in about 50% of clock-protein expressing circadian neurons. Light input signals activate CRY and prevent PER/TIM from repressing CLK/CYC, thus leading to buildup of *per* and *tim* mRNA. PER and TIM proteins then have the opportunity to be produced during nighttime, leading to the process to start all over again. More recently, Rhodopsin-7 (Rh7) is a previously uncharacterized opsin that is shown to contribute to the photosensitivity of *Drosophila* clock neurons [20,29,31,34,65].

The expression of CRY in roughly 50% of the circadian neurons on the fly brain allows for light input to be directly recognized even in the absence of external opsin-based photoreceptors. Circadian rhythmicity remains intact for flies lacking canonical external photoreceptors due to the *eyeless* gene mutation and are comparable to those with intact external photoreceptors [36]. Light input into these circadian neurons lead to the resetting of the circadian clock, however the mechanism on how these circadian neurons (distributed on the surface of the fly brain) synchronize with each other has yet to be elucidated. Work has shown that the mutation of CRY in circadian neurons led to attenuation, but not the complete ablation of the light sensing mechanism of CRY+ circadian neurons [38], leading to speculation of a secondary light input mechanism into the circadian circuit. Recently, Rh7 had recently been identified as a direct light sensor in lateral ventral neurons and was shown to play an integral role in *Drosophila* physiology and behavior [20]. These light input mechanisms into select circadian neurons expressing specific light sensors show region specificity, in that LNvs that exhibit both CRY and Rh7-dependent light response due to their anatomical positioning in the fly brain.

The ~150 pacemaker neurons are distributed throughout the fly brain and are divided into groups based on their sizes and anatomical position in the fly brain. These circadian pacemaker neurons are the master time-keeping system of the organism in that they control clock-modulated daily physiology and behavior.

The anatomical positioning of lateral ventral neurons (LNvs) show their aptitude in receiving light inputs from external opsin-based light photoreceptors. Large-lateral ventral neurons are a subset of circadian neurons that play an important role is light-mediated circuit and behavioral response [38]. Fogle, et al., 2015 found that CRY perturbations led to the disruption in blue light-mediated cellular depolarization. Measurements in l-LNv-mediated depolarization indicated an attenuated response to light in l-LNvs in non-functioning CRY [38]. Additionally, l-LNvs not only play a role in a circuit-wide response to light input, but also are key regulators of circadian-modulated behaviors such as light-induced arousal and sleep [14,20,38,40].

Small-lateral ventral neurons also contribute to light-induced circadian response in that they are key regulators rhythmicity in the absence of photic input and are thus, considered to be the core circadian oscillators [33,42,53]. Interestingly, s-LNvs express CRY for direct photic entrainment, but these circadian subsets also exhibit synaptic communication connecting them to extraretinal photoreceptors, Hofbauer-Buchner (HB) eyelet [25]. Disruptions to s-LNvs lead to the break-down of the free-running clock as well as an absence for the naturally occurring morning and evening anticipatory behaviors, exhibited by increased activity at during dusk and dawn [44,46].

Lateral neurons are adapted for interpreting light due to their expression of CRY as well as their optimal positioning in the fly brain, in proximity to the light-interpreting

compound eye [20,29,33,35,37,65]. Work has shown that CRY-expressing lateral-dorsal neurons are important for mediating evening behavioral peaks. This was shown when functional clocks limited to only LNvs produced sufficient circadian drive, but when circadian function is restored in both LNvs and LNds, both morning and evening anticipation was restored [51]. This event indicates the circuit-wide communication between the neuronal subgroups is integral for the normal function of the circuit.

Exposure to constant light drives the continuous resetting of the circadian clock due to CRY-mediated degradation of TIM [54]. The result of constant light input is an observable behavioral and physiological circadian arrhythmicity [54]. LNvs and LNds have this feature in common with a small subset of Dorsal Neurons (DNs). In *Drosophila,* the DN1 subgroup of dorsal neurons express the light-sensitive CRY, which can control and generate circadian rhythms [55,57]. An addition to how DN1s contribute to circadian-modulated behaviors, recent work shows that inhibition of the DN1 neurons lead to a disruption in the sleep-activity profiles [59]. DN1 neurons along with the canonical circadian neuronal subgroups are connected to the circadian neural circuitry via receiving inputs from the neuropeptide PIGMENT DISPERSING FACTOR (PDF) through PDF-receptors [61,63,66]. A subset of DN1 neurons express PDF-R to receive input from PDF+ lateral ventral neurons [49,67]. DN2s and DN3s are subsets of dorsal neurons that have mRNA production of *cry*, but its circadian-modulating protein is not found in these neurons [68,69]. These circadian neuronal subsets are, thus, considered to be light-blind, and that they must receive light inputs via PDF-circuit-wide transduction.

1.2 Significance

Because clock genes, PER *and* TIM, directly interact with each other for proper circadian network function, I aim to characterize the *in vivo* behavioral outputs of *Drosophila* in environments that challenge circadian rhythmicity. I aim to obtain a juxtaposition between *in vivo behavior* and bioluminescence/expression patterns of core clock proteins in intact adult *Drosophila*, and cultured brains, respectively. More specifically, we aim to capture the oscillatory behaviors of pacemaker cells subjected to a “Weekend Light Shift” schedule setting over an 11-day recording period that encompasses before and after a weekend.

We hypothesize that single-neuron resolution imaging of XLG-PER-Luc and TIM-Luc activity, in a “Weekend Light Shift” condition, driven by light timing changes will reveal the pattern of disruptions and reorganization of whole-network activity. As a control, I will collect data on weekday-weekend light timing schedule under which there is no shift for the weekend. Thus, I will determine numbers for the degree and duration of disrupted circadian processes that billions of people worldwide undergo each week.

1.3 Background and Preliminary Data

The circadian clock controls numerous biological process, and misalignment and disruption in its timing can lead to numerous diseases. The disruption of biological clocks has been linked to numerous ailments like irritability, cognitive and memory impairments. More severely, circadian disruptions have been associated with immune diseases, increased risks of diabetes, heart diseases, and cancers [2,12,70–76]. In turn, several neurodegenerative diseases, like Parkinson's, Alzheimer's, and Huntington's Disease, contributes to disruptions that mimic circadian defects [77–80]. The proposed work aims to understand the importance and the role of the circadian neural circuitry in governing daily physiology and behavior.

Studies show numerous similarities between *Drosophila*, the fruit fly, and human circadian neuronal circuits. The *Drosophila* circadian neurons are distributed throughout the surface of the brain [81–84] and show many similar features to the mammalian central circadian circuit in the suprachiasmatic nucleus (SCN) [10,85]. All animal circadian clocks are characterized by the cyclic synchronization of cell-type-specific clock proteins across networked neurons of the circadian circuit. In *Drosophila*, the core clock proteins include PERIOD (PER) and TIMELESS (TIM) [48,62,86] which reside on the E-box promoter and repress their own transcription by binding to CLOCK and CYCLE, core clock proteins that promote the synthesis of *per* and *tim* mRNA [87–89]. The start of the 24-hour oscillation period of gene expression begins with the UV/blue-light photopigment, CRYPTOCHROME (CRY) degrading the clock protein dimer of PER and TIM in the nucleus, which results in the cycle's daily reset by relief of self-transcriptional repression followed by the eventual accumulation of newly translated PER and TIM[20,36,90–92].

The timing of light in the morning is a potent signal that couples the timing of the circadian clock to its external environment [34,62]. One of our lab's interests is to study how light plays a role in circadian network signaling and entrainments at all levels—from the molecular mechanisms to animal behavior. A great amount of work has been done to study the cycling of clock genes [38,76,93], however, how the circadian network coordinates its activity based on exposure to light signals is yet unclear.

Billions of people around the world undergo weekly weekday-to-weekend light shifts (WLS) that lead to irregular sleep-wake cycles. This includes night-shift workers with inverted schedules, and today's adolescents with shifts up to 3 hours or more [70,71,94]. WLS affects individuals worldwide as a result of exposure to artificial light during odd hours of the day—these are light-induced weekly circadian misalignments between working days and weekends. WLS resembles jet lag caused by trans-meridian flight, where individuals initially travel westward between different time zones, and returning eastward back to their origin. Unlike jetlag, weekend light shifts do not require an individual to travel from one time zone to another to experience desynchrony of internal rhythms when one's internal biological rhythm does not match the environment's solar timing. To investigate the biological consequences of WLS, I must measure how it affects circadian clocks and how long our clock is desynchronized each week. Our lab recently developed a sensitive imaging system that measures whole-circuit circadian circuit clock desynchrony in response to light [95].

From our understanding of the central brain circadian clock, we may then consider how other peripheral clocks in the body adjust to weekly shifts caused by weekend light shifts along with circadian disruptions in everyday metabolic and behavioral functions.

1.4 References

1. Pittendrigh, C.S., and Minis, D. (1964). The Entrainment of Circadian Oscillations by Light and Their Role as Photoperiodic Clocks Colin. Am. Nat. *98*, 261–294.

2. Pittendrigh, C.S., and Daan, S. (1976). A functional analysis of circadian pacemakers in nocturnal rodents. J. Comp. Physiol. A *106*, 223–252. Available at: http://link.springer.com/article/10.1007/BF01417860%5Cnhttp://link.springer.com/content/pdf/10.1007/BF01417860.pdf%5Cnhttp://link.springer.com/10.1007/BF01417860 [Accessed May 4, 2018].

3. Obholz, K.L., Akopyan, A., Waymire, K.G., and MacGregor, G.R. (2006). FNDC3A is required for adhesion between spermatids and Sertoli cells. Dev. Biol. *298*, 498–513.

4. Carrouel, F., Couble, M.-L., Vanbelle, C., Staquet, M.-J., Magloire, H., and Bleicher, F. (2008). HUGO (FNDC3A): a new gene overexpressed in human odontoblasts. J. Dent. Res. *87*, 131–6. Available at: http://www.ncbi.nlm.nih.gov/pubmed/18218838 [Accessed February 6, 2020].

5. Rivas, G.B.S., Teles-de-Freitas, R., Pavan, M.G., Lima, J.B.P., Peixoto, A.A., and Bruno, R.V. (2018). Effects of Light and Temperature on Daily Activity and Clock Gene Expression in Two Mosquito Disease Vectors. J. Biol. Rhythms *33*, 272–288. Available at: http://www.ncbi.nlm.nih.gov/pubmed/29761749 [Accessed August 3, 2020].

6. Syed, A., Lukacsovich, T., Pomeroy, M., Bardwell, A.J., Decker, G.T., Waymire, K.G., Purcell, J., Huang, W., Gui, J., Padilla, E.M., *et al.* (2019). Miles to go (mtgo)

encodes FNDC3 proteins that interact with the chaperonin subunit CCT3 and are required for NMJ branching and growth in Drosophila. Dev. Biol. *445*, 37–53. Available at: https://linkinghub.elsevier.com/retrieve/pii/S0012160618303178 [Accessed December 16, 2018].

7. Ke, J., Zhao, Z., Hong, S.H., Bai, S., He, Z., Malik, F., Xu, J., Zhou, L., Chen, W., Martin-Trevino, R., *et al.* (2015). Role of microRNA221 in regulating normal mammary epithelial hierarchy and breast cancer stem-like cells. Oncotarget *6*, 3709–3721.

8. Yoshii, T., Hermann-Luibl, C., and Helfrich-Föorster, C. (2016). Circadian light-input pathways in Drosophila. Commun. Integr. Biol. *9*.

9. Pavel, M., Imarisio, S., Menzies, F.M., Jimenez-Sanchez, M., Siddiqi, F.H., Wu, X., Renna, M., O'Kane, C.J., Crowther, D.C., and Rubinsztein, D.C. (2016). CCT complex restricts neuropathogenic protein aggregation via autophagy. Nat. Commun. *7*, 1–18.

10. Welsh, D.K., Logothetis, D.E., Meister, M., and Reppert, S.M. (1995). Individual neurons dissociated from rat suprachiasmatic nucleus express independently phased circadian firing rhythms. Neuron *14*, 697–706. Available at: http://journals.sagepub.com/doi/10.1177/0748730419877315 [Accessed October 16, 2019].

11. Yam, A.Y., Xia, Y., Lin, H.T.J., Burlingame, A., Gerstein, M., and Frydman, J. (2008). Defining the TRiC/CCT interactome links chaperonin function to stabilization of newly made proteins with complex topologies. Nat. Struct. Mol.

Biol. *15*, 1255–1262.

12. Roenneberg, T., Allebrandt, K. V, Merrow, M., Line Vetter, C., and Vetter, C. (2012). Social jetlag and obesity. Curr. Biol. *22*, 939–43. Available at: http://www.ncbi.nlm.nih.gov/pubmed/22578422 [Accessed October 25, 2017].

13. Gao, Y., Thomas, J.O., Chow, R.L., Lee, G.H., and Cowan, N.J. (1992). A cytoplasmic chaperonin that catalyzes β-actin folding. Cell *69*, 1043–1050. Available at: https://linkinghub.elsevier.com/retrieve/pii/009286749290622J [Accessed February 21, 2020].

14. Shang, Y., Griffith, L.C., and Rosbash, M. (2008). Light-arousal and circadian photoreception circuits intersect at the large PDF cells of the Drosophila brain. Proc. Natl. Acad. Sci. *105*, 19587–19594. Available at: http://www.pnas.org/content/105/50/19587%5Cnhttp://www.ncbi.nlm.nih.gov/pubmed/19060186%5Cnhttp://www.pnas.org/content/105/50/19587.full.pdf%5Cnhttp://www.pnas.org/content/105/50/19587.short.

15. Hartl, F.U., and Hayer-Hartl, M. (2002). Protein folding. Molecular chaperones in the cytosol: From nascent chain to folded protein. Science (80-.). *295*, 1852–1858.

16. Renn, S.C.P., Park, J.H., Rosbash, M., Hall, J.C., and Taghert, P.H. (1999). A pdf neuropeptide gene mutation and ablation of PDF neurons each cause severe abnormalities of behavioral circadian rhythms in Drosophila. Cell *99*, 791–802.

17. Joachimiak, L.A., Walzthoeni, T., Liu, C.W., Aebersold, R., and Frydman, J. (2014). The structural basis of substrate recognition by the eukaryotic chaperonin

TRiC/CCT. Cell *159*, 1042–1055.

18. Fogle, K.J., Baik, L.S., Houl, J.H., Tran, T.T., Roberts, L., Dahm, N.A., Cao, Y., Zhou, M., and Holmes, T.C. (2015). CRYPTOCHROME-mediated phototransduction by modulation of the potassium ion channel β-subunit redox sensor. Proc. Natl. Acad. Sci.

19. Sheeba, V., Sharma, V.K., Gu, H., Chou, Y.T., O'Dowd, D.K., and Holmes, T.C. (2008). Pigment dispersing factor-dependent and -independent circadian locomotor behavioral rhythms. J. Neurosci. *28*, 217–227.

20. Ni, J.D., Baik, L.S., Holmes, T.C., and Montell, C. (2017). A rhodopsin in the brain functions in circadian photoentrainment in Drosophila. Nature *545*, 340–344. Available at: http://www.nature.com/doifinder/10.1038/nature22325 [Accessed May 4, 2018].

21. Nitabach, M.N., Wu, Y., Sheeba, V., Lemon, W.C., Strumbos, J., Zelensky, P.K., White, B.H., and Holmes, T.C. (2006). Electrical hyperexcitation of lateral ventral pacemaker neurons desynchronizes downstream circadian oscillators in the fly circadian circuit and induces multiple behavioral periods. J. Neurosci. *26*, 479–489.

22. Baik, L.S., Recinos, Y., Chevez, J.A., and Holmes, T.C. (2018). Circadian modulation of light-evoked avoidance/attraction behavior in Drosophila. PLoS One *13*, e0201927. Available at: https://dx.plos.org/10.1371/journal.pone.0201927 [Accessed August 3, 2020].

23. Qiu, J., and Hardin, P.E. (1996). Developmental state and the circadian clock

interact to influence the timing of eclosion in Drosophila melanogaster. J. Biol. Rhythms *11*, 75–86.

24. Skopik, S.D., and Pittendrigh, C.S. (1967). Circadian systems, II. The oscillation in the individual Drosophila pupa; its independence of developmental stage. PNAS *58*, 1862–1869.

25. Veleri, S., Brandes, C., Helfrich-Förster, C., Hall, J.C., and Stanewsky, R. (2003). A Self-Sustaining, Light-Entrainable Circadian Oscillator in the Drosophila Brain. Curr. Biol. *13*, 1758–1767. Available at: https://www.sciencedirect.com/science/article/pii/S0960982203006997 [Accessed June 4, 2018].

26. Blanchardon, E., Grima, B., Klarsfeld, A., Chélot, E., Hardin, P.E., Préat, T., and Rouyer, F. (2001). Defining the role of Drosophila lateral neurons in the control of circadian rhythms in motor activity and eclosion by targeted genetic ablation and PERIOD protein overexpression. Eur. J. Neurosci. *13*, 871–888.

27. Emery, P., Stanewsky, R., Hall, J.C., and Rosbash, M. (2000). A unique circadian-rhythm photoreceptor. *404*, 456–457.

28. Myers, E.M., Jiujiu, Y., and Sehgal, A. (2003). Circadian Control of Eclosion: Interaction between a Central and Peripheral Clock in Drosophila melanogaster. Curr. Biol. *13*, 526–533.

29. Baik, L.S., Recinos, Y., Chevez, J.A., Au, D.D., and Holmes, T.C. (2019). Multiple Phototransduction Inputs Integrate to Mediate UV Light–evoked Avoidance/Attraction Behavior in Drosophila. J. Biol. Rhythms *34*, 391–400.

Available at: http://journals.sagepub.com/doi/10.1177/0748730419847339 [Accessed August 3, 2020].

30. Baik, L.S., Recinos, Y., Chevez, J.A., Au, D.D., and Holmes, T.C. (2019). Multiple Phototransduction Inputs Integrate to Mediate UV Light–evoked Avoidance/Attraction Behavior in Drosophila. J. Biol. Rhythms *34*, 391–400.

31. Kistenpfennig, C., Grebler, R., Ogueta, M., Hermann-Luibl, C., Schlichting, M., Stanewsky, R., Senthilan, P.R., and Helfrich-Förster, C. (2017). A New Rhodopsin Influences Light-dependent Daily Activity Patterns of Fruit Flies. J. Biol. Rhythms *32*, 406–422.

32. Renn, S.C.P., Park, J.H., Rosbash, M., Hall, J.C., and Taghert, P.H. (1999). A pdf neuropeptide gene mutation and ablation of PDF neurons each cause severe abnormalities of behavioral circadian rhythms in Drosophila. Cell *99*, 791–802.

33. Nitabach, M.N., Blau, J., and Holmes, T.C. (2002). Electrical Silencing of Drosophila Pacemaker Neurons Stops the Free-Running Circadian Clock An important area of circadian rhythm research is the relationship between the function of the molecular clock in pacemaker neurons and the central physiological. Cell *109*, 485–495. Available at: https://ac.els-cdn.com/S0092867402007377/1-s2.0-S0092867402007377-main.pdf?_tid=191a407f-2f36-4e51-b468-c0c04bc18151&acdnat=1520814518_8b6e01a8d692d51fc76ec3f96a9757e8.

34. Peschel, N., Chen, K.F., Szabo, G., and Stanewsky, R. (2009). Light-dependent interactions between the Drosophila circadian clock factors cryptochrome, jetlag,

and timeless. Curr. Biol. *19*, 241–7. Available at: http://www.sciencedirect.com/science/article/pii/S0960982208016977 [Accessed January 19, 2016].

35. Baik, L.S., Recinos, Y., Chevez, J.A., and Holmes, T.C. (2018). Circadian modulation of light-evoked avoidance/attraction behavior in Drosophila. PLoS One *13*, 1–14.

36. Fogle, K.J., Parson, K.G., Dahm, N.A., and Holmes, T.C. (2011). CRYPTOCHROME Is a Blue-Light Sensor That Regulates Neuronal Firing Rate. Science (80-.).

37. Collins, B., Mazzoni, E.O., Stanewsky, R., and Blau, J. (2006). Drosophila CRYPTOCHROME is a circadian transcriptional repressor. Curr. Biol. *16*, 441–449.

38. Sheeba, V., Fogle, K.J., Kaneko, M., Rashid, S., Chou, Y.-T., Sharma, V.K., and Holmes, T.C. (2008). Large ventral lateral neurons modulate arousal and sleep in Drosophila. Curr. Biol. *18*, 1537–45. Available at: http://www.pubmedcentral.nih.gov/articlerender.fcgi?artid=2597195&tool=pmcentrez&rendertype=abstract.

39. Konopka, R.J., and Benzer, S. (1971). Clock Mutants of Drosophila melanogaster. Proc. Natl. Acad. Sci. *68*, 2112–2116. Available at: https://www.pnas.org/content/68/9/2112 [Accessed August 3, 2020].

40. Agrawal, P., Houl, J.H., Gunawardhana, K.L., Liu, T., Zhou, J., Zoran, M.J., and Hardin, P.E. (2017). Drosophila CRY Entrains Clocks in Body Tissues to Light

and Maintains Passive Membrane Properties in a Non-clock Body Tissue Independent of Light. Curr. Biol. *27*, 2431-2441.e3. Available at: http://dx.doi.org/10.1016/j.cub.2017.06.064.

41. Myers, M.P., Wager-Smith, K., Wesley, C.S., Young, M.W., and Sehgal, A. (1995). Positional cloning and sequence analysis of the Drosophila clock gene, timeless. Science (80-.). *270*, 805–808. Available at: https://science.sciencemag.org/content/270/5237/805 [Accessed August 2, 2020].

42. Emery, P., Stanewsky, R., Helfrich-Förster, C., Emery-Le, M., Hall, J.C., and Rosbash, M. (2000). Drosophila CRY is a deep brain circadian photoreceptor. Neuron *26*, 493–504.

43. Allada, R., White, N.E., So, W.V., Hall, J.C., and Rosbash, M. (1998). A mutant Drosophila homolog of mammalian clock disrupts circadian rhythms and transcription of period and timeless. Cell *93*, 791–804.

44. Nitabach, M.N., Blau, J., and Holmes, T.C. (2002). Electrical silencing of Drosophila pacemaker neurons stops the free-running circadian clock. Cell *109*, 485–495.

45. Potdar, S., and Sheeba, V. (2018). Wakefulness is promoted during day time by PDFR signalling to dopaminergic neurons in Drosophila melanogaster. eNeuro *5*. Available at: /pmc/articles/PMC6102377/?report=abstract [Accessed August 2, 2020].

46. Park, J.H. (2000). Differential regulation of circadian pacemaker output by separate clock genes in Drosophila. Proc. Natl. Acad. Sci. *97*, 3608–3613.

Available at: http://www.pnas.org/cgi/doi/10.1073/pnas.070036197.

47. Im, S.H., Li, W., and Taghert, P.H. (2011). Pdfr and cry signaling converge in a subset of clock neurons to modulate the amplitude and phase of circadian behavior in Drosophila. PLoS One *6*.

48. Konopka, R.J., and Benzer, S. (1971). Clock mutants of Drosophila melanogaster. Proc. Natl. Acad. Sci. U. S. A. *68*, 2112–2116.

49. Hyun, S., Lee, Y., Hong, S.-T., Bang, S., Paik, D., Kang, J., Shin, J., Lee, J., Jeon, K., Hwang, S., *et al.* (2005). Drosophila GPCR Han Is a Receptor for the Circadian Clock Neuropeptide PDF. Neuron *48*, 267–278.

50. Baik, L.S., Fogle, K.J., Roberts, L., Galschiodt, A.M., Chevez, J.A., Recinos, Y., Nguy, V., and Holmes, T.C. (2017). CRYPTOCHROME mediates behavioral executive choice in response to UV light. Proc. Natl. Acad. Sci.

51. Grima, B., Chélot, E., Xia, R., and Rouyer, F. (2004). Morning and evening peaks of activity rely on different clock neurons of the Drosophila brain. Nature *431*, 869–873.

52. Im, S.H., and Taghert, P.H. (2010). PDF receptor expression reveals direct interactions between circadian oscillators in drosophila. J. Comp. Neurol. *518*, 1925–1945.

53. Helfrich-Förster, C. (2003). The neuroarchitecture of the circadian clock in the brain of Drosophila melanogaster. Microsc. Res. Tech. *62*, 94–102.

54. Myers, M.P., Wager-Smith, K., Rothenfluh-Hilfiker, A., Young, M.W., Myers, M.P.,

Wager-smith, K., Rothenfluh-hilfiker, A., and Young, M.W. (1996). Light-Induced Degradation of TIMELESS and Entrainment of the Drosophila Circadian Clock Published by : American Association for the Advancement of Science Stable URL : http://www.jstor.org/stable/2890841 JSTOR is a not-for-profit service that helps schola. Science (80-.). *271*, 1736–1740.

55. Murad, A., Emery-Le, M., and Emery, P. (2007). A Subset of Dorsal Neurons Modulates Circadian Behavior and Light Responses in Drosophila. Neuron *53*, 689–701.

56. Baik, L.S., Nave, C., Au, D.D., Guda, T., Chevez, J.A., Ray, A., and Holmes, T.C. (2020). Circadian Regulation of Light-Evoked Attraction and Avoidance Behaviors in Daytime- versus Nighttime-Biting Mosquitoes. Curr. Biol.

57. Kunst, M., Hughes, M.E., Raccuglia, D., Felix, M., Li, M., Barnett, G., Duah, J., and Nitabach, M.N. (2014). Calcitonin gene-related peptide neurons mediate sleep-specific circadian output in Drosophila. Curr. Biol. *24*, 2652–2664. Available at: http://dx.doi.org/10.1016/j.cub.2014.09.077.

58. Rhoades, S.D., Nayak, K., Zhang, S.L., Sehgal, A., and Weljie, A.M. (2018). Circadian- and Light-driven Metabolic Rhythms in Drosophila melanogaster. J. Biol. Rhythms *33*.

59. Guo, F., Yu, J., Jung, H.J., Abruzzi, K.C., Luo, W., Griffith, L.C., and Rosbash, M. (2016). Circadian neuron feedback controls the Drosophila sleep-activity profile. Nature *536*, 292–297. Available at: http://www.nature.com/articles/nature19097 [Accessed August 24, 2018].

60. Zhang, L., Chung, B.Y., Lear, B.C., Kilman, V.L., Liu, Y., Mahesh, G., Meissner, R.A., Hardin, P.E., and Allada, R. (2010). DN1p Circadian Neurons Coordinate Acute Light and PDF Inputs to Produce Robust Daily Behavior in Drosophila. Curr. Biol. *20*, 591–599. Available at: http://dx.doi.org/10.1016/j.cub.2010.02.056.

61. Vecsey, C.G., Pirez, N., and Griffith, L.C. (2014). The Drosophila neuropeptides PDF and sNPF have opposing electrophysiological and molecular effects on central neurons. J. Neurophysiol. *111*, 1033–1045. Available at: http://jn.physiology.org/cgi/doi/10.1152/jn.00712.2013.

62. Hall, J.C. (2005). Systems approaches to biological rhythms in Drosophila. Methods Enzymol. *393*, 61–185. Available at: http://www.sciencedirect.com/science/article/pii/S0076687905930048 [Accessed January 19, 2016].

63. Im, S.H., Li, W., and Taghert, P.H. (2011). PDFR and CRY Signaling Converge in a Subset of Clock Neurons to Modulate the Amplitude and Phase of Circadian Behavior in Drosophila. PLoS One *6*, e18974. Available at: https://dx.plos.org/10.1371/journal.pone.0018974 [Accessed August 2, 2020].

64. Harper, R.E.F., Ogueta, M., Dayan, P., Stanewsky, R., and Albert, J.T. (2017). Light Dominates Peripheral Circadian Oscillations in Drosophila melanogaster During Sensory Conflict. J. Biol. Rhythms *32*, 423–432. Available at: http://www.ncbi.nlm.nih.gov/pubmed/28903626 [Accessed July 21, 2020].

65. Rieger, D., Shafer, O.T., Tomioka, K., and Helfrich-Förster, C. (2006). Functional analysis of circadian pacemaker neurons in Drosophila melanogaster. J.

Neurosci. *26*, 2531–2543. Available at: http://rsb.info.nih.gov/ij/ [Accessed August 3, 2020].

66. Hyun, S., Lee, Y., Hong, S.T., Bang, S., Paik, D., Kang, J., Shin, J., Lee, J., Jeon, K., Hwang, S., *et al.* (2005). Drosophila GPCR han is a receptor for the circadian clock neuropeptide PDF. Neuron *48*, 267–278.

67. Mertens, I., Vandingenen, A., Johnson, E.C., Shafer, O.T., Li, W., Trigg, J.S., De Loof, A., Schoofs, L., and Taghert, P.H. (2005). PDF receptor signaling in Drosophila contributes to both circadian and geotactic behaviors. Neuron *48*, 213–219. Available at: https://www.sciencedirect.com/science/article/pii/S0896627305007762 [Accessed August 24, 2018].

68. Benito, J., Houl, J.H., Roman, G.W., and Hardin, P.E. (2008). The blue-light photoreceptor CRYPTOCHROME is expressed in a subset of circadian oscillator neurons in the Drosophila CNS. J. Biol. Rhythms *23*, 296–307. Available at: http://journals.sagepub.com/doi/10.1177/0748730408318588 [Accessed May 4, 2018].

69. Yoshii, T., Todo, T., Wülbeck, C., Stanewsky, R., and Helfrich-Förster, C. (2008). Cryptochrome is present in the compound eyes and a subset ofDrosophila's clock neurons. J. Comp. Neurol. *508*, 952–966. Available at: http://doi.wiley.com/10.1002/cne.21702 [Accessed June 4, 2018].

70. Moore-Ede, M.C., Czeisler, C.A., and Richardson, G.S. (1983). Circadian Timekeeping in Health and Disease. N. Engl. J. Med. *309*, 469–476. Available at:

http://www.nejm.org/doi/abs/10.1056/NEJM198308253090806 [Accessed May 4, 2018].

71. Hastings, M.H., Reddy, A.B., and Maywood, E.S. (2003). A clockwork web: circadian timing in brain and periphery, in health and disease. Nat. Rev. Neurosci. *4*, 649–661. Available at: http://www.nature.com/articles/nrn1177 [Accessed May 4, 2018].

72. Scheer, F.A.J.L., Hilton, M.F., Mantzoros, C.S., and Shea, S.A. (2009). Adverse metabolic and cardiovascular consequences of circadian misalignment. Proc. Natl. Acad. Sci. U. S. A. *106*, 4453–4458. Available at: http://www.pnas.org/content/106/11/4453.full.pdf?with-ds=yes [Accessed October 25, 2017].

73. Filipski, E., Delaunay, F., King, V.M., Wu, M.W., Claustrat, B., Gréchez-Cassiau, A., Guettier, C., Hastings, M.H., and Francis, L. (2004). Effects of chronic jet lag on tumor progression in mice. Cancer Res. *64*, 7879–7885. Available at: http://www.ncbi.nlm.nih.gov/pubmed/14612524 [Accessed October 25, 2017].

74. Aschoff, J. (1984). Circadian timing. Ann. N. Y. Acad. Sci. *423*, 442–68. Available at: http://www.ncbi.nlm.nih.gov/pubmed/6588808 [Accessed August 23, 2018].

75. Labrecque, N., and Cermakian, N. (2015). Circadian Clocks in the Immune System. J. Biol. Rhythms *30*, 277–290. Available at: http://journals.sagepub.com/doi/10.1177/0748730415577723 [Accessed August 23, 2018].

76. Hardin, P.E. The Circadian Timekeeping System of Drosophila. Available at:

https://ac.els-cdn.com/S0960982205009395/1-s2.0-S0960982205009395-main.pdf?_tid=c2ef38aa-bc1a-11e7-8466-00000aacb360&acdnat=1509221058_aa45ab1663c2fc7fea4d9e4432809336 [Accessed October 25, 2017].

77. Mimi Lee, W.-C., Yoshihara, M., and Troy Littleton, J. Cytoplasmic aggregates trap polyglutamine- containing proteins and block axonal transport in a Drosophila model of Huntington's disease. Available at: http://www.pnas.org/content/101/9/3224.full.pdf [Accessed September 12, 2017].

78. Morton, A.J. (2005). Disintegration of the Sleep-Wake Cycle and Circadian Timing in Huntington's Disease. J. Neurosci. *25*, 157–163. Available at: http://www.jneurosci.org/cgi/doi/10.1523/JNEUROSCI.3842-04.2005.

79. Askenasy, J.J.M. (2001). Approaching disturbed sleep in late Parkinson's disease: First step toward a proposal for a revised UPDRS. Park. Relat. Disord. *8*, 123–131.

80. Hatfield, C.F., Herbert, J., Van Someren, E.J.W., Hodges, J.R., and Hastings, M.H. (2004). Disrupted daily activity/rest cycles in relation to daily cortisol rhythms of home-dwelling patients with early Alzheimer's dementia. Brain *127*, 1061–1074.

81. Kaneko, M., Helfrich-Förster, C., and Hall, J.C. (1997). Spatial and temporal expression of the period and timeless genes in the developing nervous system of drosophila: Newly identified pacemaker candidates and novel features of clock gene product cycling. J. Neurosci. *17*, 6745–6760.

82. Kaneko, M., and Hall, J.C. (2000). Neuroanatomy of cells expressing clock genes in Drosophila: Transgenic manipulation of the period and timeless genes to mark the perikarya of circadian pacemaker neurons and their projections. J. Comp. Neurol. *422*, 66–94. Available at: http://doi.wiley.com/10.1002/%28SICI%291096-9861%2820000619%29422%3A1%3C66%3A%3AAID-CNE5%3E3.0.CO%3B2-2 [Accessed August 23, 2018].

83. Beckwith, E.J., and Ceriani, M.F. (2015). Communication between circadian clusters: The key to a plastic network. FEBS Lett. *589*, 3336–3342. Available at: http://dx.doi.org/10.1016/j.febslet.2015.08.017.

84. Nitabach, M.N., and Taghert, P.H. (2008). Organization of the Drosophila Circadian Control Circuit. Curr. Biol. *18*, 84–93.

85. Ueda, H.R., Hayashi, S., Chen, W., Sano, M., Machida, M., Shigeyoshi, Y., Iino, M., and Hashimoto, S. (2005). System-level identification of transcriptional circuits underlying mammalian circadian clocks. Nat. Genet. *37*, 187–192.

86. Tei, H., Okamura, H., and Shigeyoshi, Y. (1997). Circadian oscillation of a mammalian homologue of the Drosophila period gene. *389*, 512–516.

87. Allada, R., Emery, P., Takahashi, J.S., and Rosbash, M. (2001). Stopping time: the genetics of fly and mouse circadian clocks. Annu. Rev. Neurosci. *24*, 1091–1119.

88. Duong, H.A., Robles, M.S., Knutti, D., and Weitz, C.J. (2011). A molecular mechanism for circadian clock negative feedback. Science (80-.). *332*, 1436–9.

89. Gonze, D., Bernard, S., Waltermann, C., Kramer, A., and Herzel, H. (2005). Spontaneous synchronization of coupled circadian oscillators. Biophys. J. *89*, 120–9. Available at: http://www.sciencedirect.com/science/article/pii/S0006349505726643.

90. Stanewsky, R., Kaneko, M., Emery, P., Beretta, B., Wager-Smith, K., Kay, S.A., Rosbash, M., and Hall, J.C. (1998). The cryb Mutation Identifies Cryptochrome as a Circadian Photoreceptor in Drosophila. Cell *95*, 681–692. Available at: https://www.sciencedirect.com/science/article/pii/S0092867400816384 [Accessed June 4, 2018].

91. Hunter-Ensor, M., Ousley, A., and Sehgal, A. (1996). Regulation of the Drosophila protein timeless suggests a mechanism for resetting the circadian clock by light. Cell *84*, 677–685. Available at: https://www.sciencedirect.com/science/article/pii/S0092867400810466?via%3Dihub [Accessed August 24, 2018].

92. Zeng, H., Qian, Z., Myers, M.P., and Rosbash, M. (1996). A light-entrainment mechanism for the drosophila circadian clock. Nature *380*, 129–135. Available at: http://www.nature.com/doifinder/10.1038/380129a0 [Accessed August 24, 2018].

93. Sheeba, V. (2008). The Drosophila melanogaster circadian pacemaker circuit. J. Genet. *87*, 485–493.

94. Crowley, S.J., Acebo, C., and Carskadon, M.A. (2007). Sleep, circadian rhythms, and delayed phase in adolescence. Sleep Med. *8*, 602–612. Available at: http://www.ncbi.nlm.nih.gov/pubmed/17383934 [Accessed June 4, 2018].

95. Roberts, L., Leise, T.L.L., Noguchi, T., Galschiodt, A.M.M., Houl, J.H.H., Welsh, D.K.K., and Holmes, T.C.C. (2015). Light Evokes Rapid Circadian Network Oscillator Desynchrony Followed by Gradual Phase Retuning of Synchrony. Curr. Biol. *25*, 858–867. Available at: http://www.ncbi.nlm.nih.gov/pubmed/25754644 [Accessed May 4, 2018].

96. Papagiannakopoulos, T., Bauer, M.R., Davidson, S.M., Heimann, M., Subbaraj, L., Bhutkar, A., Bartlebaugh, J., Vander Heiden, M.G., and Jacks, T. (2016). Circadian Rhythm Disruption Promotes Lung Tumorigenesis. Cell Metab. *24*, 324–331. Available at: http://dx.doi.org/10.1016/j.cmet.2016.07.001 [Accessed September 12, 2017].

97. Hamada, T., LeSauter, J., Venuti, J.M., and Silver, R. (2001). Expression of period genes: Rhythmic and nonrhythmic compartments of the suprachiasmatic nucleus pacemaker. J. Neurosci. *21*, 7742–7750.

98. Yamaguchi, S., Isejima, H., Matsuo, T., Okura, R., Yagita, K., Kobayashi, M., and Okamura, H. (2003). Synchronization of Cellular Clocks in the Suprachiasmatic Nucleus. Science (80-.). *302*, 1408–1412.

99. Azzi, A., Evans, J.A., Leise, T., Myung, J., Takumi, T., Davidson, A.J., and Brown, S.A. (2017). Network Dynamics Mediate Circadian Clock Plasticity. Neuron *93*, 441–450. Available at: http://dx.doi.org/10.1016/j.neuron.2016.12.022 [Accessed December 28, 2019].

100. Evans, J.A., Leise, T.L., Castanon-Cervantes, O., and Davidson, A.J. (2013). Dynamic Interactions Mediated by Nonredundant Signaling Mechanisms Couple

Circadian Clock Neurons. Neuron *80*, 973–983.

101. Quintero, J.E., Kuhlman, S.J., and McMahon, D.G. (2003). The biological clock nucleus: A multiphasic oscillator network regulated by light. J. Neurosci. *23*, 8070–8076.

102. Schaap, J., Pennartz, C.M.A., and Meijer, J.H. (2003). Electrophysiology of the circadian pacemaker in mammals. Chronobiol. Int. *20*, 171–188.

103. Moga, M.M., and Moore, R.Y. (1997). Organization of neural inputs to the suprachiasmatic nucleus in the rat. J. Comp. Neurol. *389*, 508–534.

104. Fogle, K.J., Parson, K.G., Dahm, N.A., and Holmes, T.C. (2011). Cryptochrome is a blue-light sensor that regulates neuronal firing rate. Science (80-.). *331*, 1409–1413. Available at: http://www.ncbi.nlm.nih.gov/pubmed/21385718 [Accessed May 4, 2018].

105. Sakai, K., Tsutsui, K., Yamashita, T., Iwabe, N., Takahashi, K., Wada, A., and Shichida, Y. (2017). Drosophila melanogaster rhodopsin Rh7 is a UV-to-visible light sensor with an extraordinarily broad absorption spectrum. Sci. Rep. *7*, 7349. Available at: http://www.ncbi.nlm.nih.gov/pubmed/28779161 [Accessed December 28, 2019].

106. Helfrich-Förster, C., Winter, C., Hofbauer, A., Hall, J.C., and Stanewsky, R. (2001). The circadian clock of fruit flies is blind after elimination of all known photoreceptors. Neuron *30*, 249–261.

107. Li, M.-T.T., Cao, L.-H.H., Xiao, N., Tang, M., Deng, B., Yang, T., Yoshii, T., and

Luo, D.-G.G. (2018). Hub-organized parallel circuits of central circadian pacemaker neurons for visual photoentrainment in Drosophila. Nat. Commun. *9*, 4247. Available at: http://www.nature.com/articles/s41467-018-06506-5 [Accessed June 9, 2019].

108. Roberts, L., Leise, T.L., Welsh, D.K., and Holmes, T.C. (2016). Functional Contributions of Strong and Weak Cellular Oscillators to Synchrony and Light-shifted Phase Dynamics. J. Biol. Rhythms *XX*, 1–15. Available at: http://journals.sagepub.com/doi/10.1177/0748730416649550 [Accessed May 4, 2018].

109. Hege, D.M., Stanewsky, R., Hall, J.C., and Giebultowicz, J.M. (1997). Rhythmic Expression of a PER-Reporter in the Malpighian Tubules of Decapitated Drosophila: Evidence for a Brain-Independent Circadian Clock. J. Biol. Rhythms *12*, 300–308.

110. Zerr, D.M., Hall, J.C., Rosbash, M., and Siwicki, K.K. (1990). Circadian fluctuations of period protein immunoreactivity in the CNS and the visual system of drosophila. J. Neurosci. *10*, 2749–2762.

111. Maywood, E.S., Reddy, A.B., Wong, G.K.Y., O'Neill, J.S., O'Brien, J.A., McMahon, D.G., Harmar, A.J., Okamura, H., and Hastings, M.H. (2006). Synchronization and maintenance of timekeeping in suprachiasmatic circadian clock cells by neuropeptidergic signaling. Curr. Biol. *16*, 599–605.

112. Johard, H.A.D., Yoishii, T., Dircksen, H., Cusumano, P., Rouyer, F., Helfrich-Förster, C., and Nässel, D.R. (2009). Peptidergic clock neurons in Drosophila: Ion

transport peptide and short neuropeptide F in subsets of dorsal and ventral lateral neurons. J. Comp. Neurol. *516*, 59–73.

113. Shafer, O.T., and Yao, Z. (2014). Pigment-dispersing factor signaling and circadian rhythms in insect locomotor activity. Curr. Opin. Insect Sci. *1*, 73–80. Available at: https://www.sciencedirect.com/science/article/pii/S2214574514000108 [Accessed August 24, 2018].

114. Jones, J.R., Simon, T., Lones, L., and Herzog, E.D. (2018). SCN VIP neurons are essential for normal light-mediated resetting of the circadian system. J. Neurosci. *38*, 7986–7995. Available at: http://www.ncbi.nlm.nih.gov/pubmed/30082421 [Accessed December 28, 2019].

115. Seugnet, L., Suzuki, Y., Stidd, R., and Shaw, P.J. (2009). Aversive phototaxic suppression: evaluation of a short-term memory assay in *Drosophila melanogaster*. Genes, Brain Behav. *8*, 377–389. Available at: http://doi.wiley.com/10.1111/j.1601-183X.2009.00483.x [Accessed May 4, 2018].

116. Emery, P., So, W.V., Kaneko, M., Hall, J.C., and Rosbash, M. (1998). Cry, a Drosophila clock and light-regulated cryptochrome, is a major contributor to circadian rhythm resetting and photosensitivity. Cell *95*, 669–679.

117. Dolezelova, E., Dolezel, D., and Hall, J.C. Rhythm Defects Caused by Newly Engineered Null Mutations in Drosophila's cryptochrome Gene.

118. Hendricks, J.C., Finn, S.M., Panckeri, K.A., Chavkin, J., Williams, J.A., Sehgal, A., and Pack, A.I. (2000). Rest in Drosophila is a sleep-like state. Neuron *25*, 129–

138. Available at: https://www.sciencedirect.com/science/article/pii/S0896627300808776 [Accessed May 4, 2018].

119. Tononi, G. (2000). Correlates of sleep and waking in Drosophila melanogaster. Science (80-.). *287*, 1834–1837. Available at: http://www.ncbi.nlm.nih.gov/pubmed/10710313 [Accessed May 4, 2018].

120. Stickgold, R., Hobson, J.A., Fosse, R., and Fosse, M. (2001). Sleep, learning, and dreams: Off-line memory reprocessing. Science (80-.). *294*, 1052–1057. Available at: http://www.ncbi.nlm.nih.gov/pubmed/11691983 [Accessed May 4, 2018].

121. Donlea, J.M., Thimgan, M.S., Suzuki, Y., Gottschalk, L., and Shaw, P.J. (2011). Inducing sleep by remote control facilitates memory consolidation in Drosophila. Science (80-.). *332*, 1571–1576. Available at: http://www.sciencemag.org/cgi/doi/10.1126/science.1202249 [Accessed May 4, 2018].

122. Shafer, O.T., Rosbash, M., and Truman, J.W. (2002). Sequential nuclear accumulation of the clock proteins period and timeless in the pacemaker neurons of Drosophila melanogaster. J. Neurosci. *22*, 5946–5954.

123. Baik, L.S., Nave, C., Au, D.D., Guda, T., Chevez, J.A., Ray, A., and Holmes, T.C. (2020). Circadian Regulation of Light-Evoked Attraction and Avoidance Behaviors in Daytime- versus Nighttime-Biting Mosquitoes. Curr. Biol., 1–8. Available at: https://doi.org/10.1016/j.cub.2020.06.010.

124. Baik, L.S., Au, D.D., Nave, C., Foden, A.J., Enrriquez-Villalva, W.K., and Holmes, T.C. (2019). Distinct mechanisms of Drosophila CRYPTOCHROME-mediated light-evoked membrane depolarization and in vivo clock resetting. Proc. Natl. Acad. Sci. U. S. A. *116*, 23339–23344.

125. Barber, A.F., Erion, R., Holmes, T.C., and Sehgal, A. (2016). Circadian and feeding cues integrate to drive rhythms of physiology in Drosophila insulin-producing cells. Genes Dev. *30*, 2596–2606.

126. Cavanaugh, D.J., Geratowski, J.D., Wooltorton, J.R.A., Spaethling, J.M., Hector, C.E., Zheng, X., Johnson, E.C., Eberwine, J.H., and Sehgal, A. (2014). Identification of a circadian output circuit for rest: Activity rhythms in drosophila. Cell *157*, 689–701. Available at: http://dx.doi.org/10.1016/j.cell.2014.02.024.

127. Parisky, K.M., Agosto, J., Pulver, S.R., Shang, Y., Kuklin, E., Hodge, J.J.L., Kang, K., Kang, K., Liu, X., Garrity, P.A., *et al.* (2008). PDF cells are a GABA-responsive wake-promoting component of the Drosophila sleep circuit. Neuron *60*, 672–82. Available at: http://www.sciencedirect.com/science/article/pii/S0896627308009422 [Accessed May 18, 2016].

128. Guo, F., Chen, X., and Rosbash, M. (2017). Temporal calcium profiling of specific circadian neurons in freely moving flies. Proc. Natl. Acad. Sci. U. S. A. *114*, E8780–E8787. Available at: http://www.ncbi.nlm.nih.gov/pubmed/28973886 [Accessed August 24, 2018].

129. Czeisler, C.A., Duffy, J.F., Shanahan, T.L., Brown, E.N., Jude, F., Rimmer, D.W.,

Ronda, J.M., Silva, E.J., Allan, J.S., Jonathan, S., *et al.* (1999). Stability, precision, and near-24-hour period of the human circadian pacemaker. Science (80-.). *284*, 2177–2181.

130. Stothard, E.R., McHill, A.W., Depner, C.M., Birks, B.R., Moehlman, T.M., Ritchie, H.K., Guzzetti, J.R., Chinoy, E.D., LeBourgeois, M.K., Axelsson, J., *et al.* (2017). Circadian Entrainment to the Natural Light-Dark Cycle across Seasons and the Weekend. Curr. Biol. *27*, 508–513. Available at: https://www.sciencedirect.com/science/article/pii/S0960982216315226 [Accessed June 4, 2018].

CHAPTER 2

Weekend Light Shifts Evoke Persistent *Drosophila* Circadian Neural Network Desynchrony

(Nave, Roberts, et al.)

Abstract

Phase-shifting light signals characterized by remaining active later at night and sleeping in late on weekends relative to weekday for up to a 3hr weekend light shift (WLS) disrupt circadian behavior. We compared *Drosophila* whole-circadian circuit responses between un-shifted light/dark schedule and a 3hr WLS schedule at the single-cell resolution in cultured adult *Drosophila* brains using real-time bioluminescence imaging of the PERIOD (PER) protein for 11 days. Circadian circuits show highly synchronous PER and TIMELESS (TIM) oscillations across all major circadian neuronal subgroups in unshifted light schedules. In contrast, WLS significantly dampens oscillator synchrony and rhythmicity in most circadian neurons during and after exposure, with or without eyes present. Lateral ventral neuron (LNv) oscillations are the first to desynchronize in WLS and the last to resynchronize upon returning to a simulated weekday schedule. Surprisingly, one circadian subgroup, the dorsal neuron group-3 (DN3s), robustly increase their within-group synchrony in response to WLS exposure. *In vivo*, WLS induces transient defects in sleep stability, learning, and memory coinciding with circuit desynchrony. In the absence of eyes, CRYPTOCHROME (CRY) is necessary for the light

input signal. Constant light (LL) exposure induces rapid loss of circuit PER cycling coinciding with loss of circadian behavior, while both PER cycling and behavior are resistant to LL disruption in CRY loss of function mutants. Our findings suggest that WLS schedules disrupt circuit-wide circadian neuronal oscillator synchrony for much of the week, thus leading to observed behavioral defects in sleep, learning, and memory.

2.1 Significance of Work

The circadian clock controls numerous aspects of daily animal physiology, metabolism and behavior. Our understanding of circadian circuit-level oscillations stem from *ex vivo* imaging of mammalian suprachiasmatic nucleus (SCN) brain slices. Humans regularly subject themselves to weekday/weekend light shifts but the effects of phase-shifting light signals cannot be measured in SCN. We measured circuit-level circadian responses to a WLS protocol in light-sensitive *ex vivo Drosophila* whole-brain preparation that shows good temporal coincidence to circadian behavioral events and find robust sub-circuit-specific oscillator desynchrony/resynchrony responses to light that coincide with functional defects in learning and memory, and sleep pattern disruption *in vivo*. Our results reflect that WLS cause circadian-circuit desynchronization and correlate with disrupted cognitive and sleep performance.

2.2 Introduction

Billions of individuals across the world subject themselves to phase-advancing light shifts on Monday morning after staying up later during weekends starting on Friday with phase-delaying light signals that persists throughout the duration of the weekend. Disruptions to circadian rhythmicity is linked to serious physiological illnesses such as heart diseases, diabetes, and cancers [70–72,96]. However, the effects of acute light shifts, like WLS, are not known for any circadian neural circuit.

PERIOD (PER) protein cycling imaging in suprachiasmatic nucleus (SCN) provides detailed functional data on the central neural circuits that govern circadian rhythms. Circuit PER cycling also forms the basis for interpreting the linkage between the timing of clock cycling and circadian physiological outputs in mammals [10,97–100]. Longitudinal optical or electrical recording of large numbers of neurons in SCN slices that are no longer driven by light cues shows that free-running between-oscillator phases are complex and relatively desynchronized [98,101,102]. Mammalian SCN ex vivo slices can be imaged at high spatial-temporal resolution, but their direct responses to environmental light signals cannot be studied due to the absence of retino-hypothalamic pathway input into the SCN in *ex vivo* preparations [10,97,100,103].

The primary light input mechanism for the fly circadian neural circuit is via the blue-light sensitive photoreceptor CRYPTOCHROME (CRY) expressed in roughly half of the fly circadian neurons [69,90,104]. A secondary, and broad spectrally activated photoreceptor Rhodopsin-7 (Rh7) is also expressed in *Drosophila* circadian brain neurons and in photoreceptors [20,31,105]. External, opsin-based photoreceptors provide redundant photic input [106,107]. We took advantage of this feature of cell autonomous

photoreceptors in many central brain circadian neurons to develop an imaging system that measures bioluminescence of PER oscillation at single-cell resolution over many days in a long-term, whole-brain, culture system [95,108]. Bioluminescence imaging of highly light-sensitive circadian neurons avoids all possibility of circuit perturbation by light contamination caused by fluorescence excitation [95,108,109].

Our earlier work reveals single-cell resolution circadian circuit-wide response of PER cycling to a single phase advancing light pulse consists of systematic desynchrony followed by resynchronization of PER cycling that varies between the different neuronal subclasses of the circuit [95,108]. The *Drosophila* whole-brain culture responds to light-cued phase shifts throughout the circadian neural circuit in a very robust and reproducible fashion that is indistinguishable from light cued phase shifts *in vivo* as shown by comparison of whole brain PER bioluminescence cycling with anti-PER immunocytochemistry prepared from whole flies exposed to light shifts *in vivo* [95,108,110]. Here, we use *Drosophila* brains to study neural circuit response to WLS whose timing resembles the weekend/weekday light shifts experienced by many humans and further verify the circuit imaging system by comparative imaging and in vivo behavioral analysis by testing *cryb* mutants and environmental disruption of the circadian clock by constant light. Both mammalian and fly rhythms rely on circadian pacemaker circuit networks coupled by peptide and small molecule neurotransmitters [32,111–114]. Motivated by the many functional similarities between mammalian and fly circadian circuitry, we investigated the effects of light shifts on circadian rhythmicity using *Drosophila*.

2.3 Materials and Methods

Behavioral analysis of day-night entrainment

We employed the TriKinetics *Drosophila* Activity Monitor (DAM) system to record the locomotor activity of adult wild-type (W1118[5905]), XLG-PER-Luc,TIM-Luc, and CRYb-XLG-Luc flies [64,90,95,108]. Individual flies were placed in 5mm Pyrex glass tubes with fly food on one end, and a cotton plug on the other. Each experiment was run with either 32 or 64 adult male flies. The fly-containing tubes are mounted in a DAM5 *Drosophila* Activity Monitor (TriKinetics) which records the number of infrared beam crossings over time, as a measure of activity.

Flies are first entrained under standard 12hrs light: 12hrs dark (12:12LD) conditions for ≥3 days. Following entrainment, flies are then exposed to either the *LD Strobe* protocol that for each hour of “light” 15minLight:45minDark is repeated ever hour for 12 hours superimposed over a 12:12LD; Skeleton Photoperiod (SPP); or standard 12:12LD light protocols with consistent phases and a consistent (white light intensity: of 1.1 mW/cm2) for 8 days. The *LD Strobe* protocol is performed by dividing the 12hrs of daytime entrainment into 12 one-hour cycles of short, intermittent light-dark exposures followed by 12 hours of nighttime darkness. The 15-minute skeleton photoperiod protocol is performed by applying a short light pulse at the transition times of expected lights on (simulated dawn) and lights off (dusk) based on the previous standard entrainment. Initial optimization tests for *LD Strobe* and SPP protocols were determined with light pulse durations of either 5, 15, or 30 m using highest behavioral circadian rhythmicity under subsequent constant darkness (DD) conditions as comparison criteria. Following the 8

days of entrainment by either 12:12LD, *LD Strobe*, or SPP, we examined the free-running circadian activity of the flies for ≥3 days under DD.

Quantification of locomotor activity

FaasX (M. Boudinot and F. Rouyer, Centre National de la Recherche Scientifique) was used for analysis of locomotor activity recorded by the automated TriKinetics *Drosophila* Activity Monitor system. Cycle-P was utilized to quantify period length, amplitude and rhythmicity using 15-minute bins of individual fly locomotor activity. Individual fly rhythmicity is defined rhythmic based on chi-square periodogram analysis with the following criteria (high frequency filter on): power ≥40, width ≥4 hours and period length of 24 ±8 hours. Double-plotted actogram graphs were generated by the software ClockLab (Actimetrics) showing normalized activity over 1-minute intervals.

Bioluminescence imaging

Custom bioluminescence set up is designed and built by Logan Roberts with David Callard, and Jeff Stepkowski (Stanford Photonics) and Todd Holmes. Bioluminescence set up includes custom light filters, LED light set up by Prizmatix, a retooled and light-tight black box, and custom temperature control maze. Bioluminescence imaging is performed using adult, male XLG-PER-Luc transgenic fly brains (line provided by Ralf Stanewsky, University of Münster, Germany, (as described in Veleri et al., 2003), CRYb-XLG-PER-Luc (line provided by Ralf Stanewsky, University of Münster, Germany, [64]) and TIM-Luc (provided by Patrick Emery, University of Massachusetts Medical School ([90]). Transgenic flies (XLG-PER-Luc, TIM-Luc, CRYb-XLG-PER-Luc) are first entrained to ≥3 days of 12:12LD entrainment before dissection. Six whole fly brain explants are dissected

and cultured on a single insert per experiment using a modified version of a previously described protocol (Roberts et al., 2015). For bioluminescence imaging of cultured brains with compound eyes, two sets of brain conditions are imaged simultaneously: three brains without compound eyes are co-cultured adjacent to dissected brains where the compound eye is left attached to the optic lobe of the brain (total of 6 brains per imaging culture).

The cultured brains are mounted on a stage (Applied Scientific Instrumentation) with automated XYZ movement controlled by the software Piper. The stage is connected to an upright Axio Observer.Z1 Microscope (Zeiss) set in a custom light-tight incubator (designed by Alec Davidson, Morehouse School of Medicine, GA) with temperature maintained at 25˚C ±0.5˚C. Bioluminescence from the cultured whole brains is collected by a Zeiss 5x (NA=0.25) objective and transmitted directly to a MEGA-10Z cooled intensified CCD camera (Stanford Photonics) mounted on the bottom port of the microscope. The XY position of the samples is manually set using bright-field illumination. The optimal z-plane of focus for bioluminescence imaging is obtained by performing 10 Z-steps at 40-50 µm intervals with 5-10-minute exposures.

Experimental bioluminescence imaging of the samples is obtained with 15-minute exposures at 30 fps for ≥11 days of recording at single-cell resolution during the hourly dark phase of the *LD Strobe* protocol. Light exposure and entrainment are performed using an *LD Strobe* protocol with the 12 hours of daytime entrainment divided into 12 consecutive cycles of a 15-minute light pulse and 45 minutes of darkness, followed by 12 hours of constant darkness (hereby referred to as “15L45D/*LD Strobe*”). Bioluminescence imaging under LL entrainment uses the same parameters of *LD Strobe* but differs in that there is no 12 hours of constant darkness. For the entirety of the LL period, brains are

exposed to 8 days of consecutive cycles of 15-minute light pulse, followed by 45 minutes of darkness, until the onset of DD.

Images are collected by Piper (Stanford Photonics) and averaged into 45-minute bins by ImageJ before using MetaMorph (Molecular Devices, Sunnyvale, CA), Microsoft Excel and custom MATLAB scripts to measure circadian parameters of bioluminescence cycling with single cell resolution. Only experiments with all six brain explants still healthy, contamination-free, adhering to the insert substrate, and exhibiting bioluminescence for ≥11 days are used for analysis.

Simulating day-night entrainment and weekend light shifts ex vivo

To establish baseline measurements of day-night entrainment, one group (referred to as the control group) consists of whole brain explants exposed to the 15L45D *LD Strobe* schedule that simulates 12:12LD entrainment for 8 days with no phase shifts followed by ±3 days of constant darkness (DD). Stable white light exposure (30μW/cm2, as performed in our previous published work [95,108]using a mic-LED (Prizmatix)) is set to provide a stable light intensity with automated timing set via TTL input from Piper (Stanford Photonics). During intervals of light exposures, the CCD camera is protected by a mechanical shutter controlled via TTL input from Piper to allow for semi-continuous imaging. For samples exposed to a WLS protocol (referred to as WLS LD), the first three recorded “weekdays” (all with the same phase for a simulated “Wednesday” to “Friday”) have parallel phases with the control group. This is followed by a 3-hour phase delay on the evening of the third recorded day (simulated “Friday night”) followed by two “weekend” days but with no changes to the shift obtained from the simulated Friday (simulated “Saturday” through “Sunday”).

Whole brain explants are exposed to a phase advance of three hours on the morning of the sixth day of recording (simulated “Monday” morning) with no phase shifts for the following simulated weekdays (“Monday” through “Wednesday”). Finally, explants are placed in constant darkness (DD) for ≥3 days. Three-hour phase shifts were used because they correspond with social behaviors observed in the general populace regarding weekend light shifts and have been linked to negative health effects. LED light exposure and brain imaging are automated via TTL input through the Piper software provided by Stanford Photonics (control group=208 players, WLS group=214 players). Here, players refer to automated presets (created using the Piper Software) that distinguish when and how long the TTL input will turn on LED lights and/or open or close the CCD camera shutter.

Processing of bioluminescence images

Cosmic rays are removed in real-time using the Piper cosmic ray filter set to discriminate the sum of all pixel values above 800 and reject frames that are >3 standard deviations over the running average (run over 30 frames). ImageJ is used to generate images with bioluminescence images averaged over 45-minute intervals. These images were then further processed using MetaMorph as described in previously work [95,108]. Briefly, noise from dark current and cosmic rays were removed by using a running minimum algorithm to generate new images constructed from pairs of sequential images using the minimum values of each pixel from the two images. MetaMorph was used to generate a stack of images for each experiment with average luminescence intensity over time measured for regions of interest (ROIs) that were manually defined based on a previous protocol [95]. ROIs were classified into canonical circadian neuron groups

(colored-coded: red = s-LNv, yellow = l-LNv, orange = LNd, blue = DN1, green = DN3) based on consistent and classically recognized anatomical locations.

Raw bioluminescence data were then processed in Microsoft Excel and was adjusted for background noise then converted into raw luminescence over time to photons-per-minute as previously described [95,108]. Circadian parameters were analyzed for 11-day recordings using modified versions of previously described MATLAB scripts with the first 12hrs excluded due to initially high amplitude and highly variable bioluminescence following dissection and addition of luciferin [95]. Between circadian neuronal cell group variable bioluminescence persists for several days after dissection. These records are retained to show re-emergence of highly synchronized between circadian cell group rhythms after several days in culture. This is in strong agreement with anti-PER and anti-TIM immunocytochemical “snapshots” of highly synchronous in vivo fly brain PER cycling measured in flies maintained in LD over 24 hours [81,110].

Quantification of circadian oscillator dynamics

Custom MATLAB scripts (version 8.2) were employed to analyze real-time bioluminescence recordings for quantification of order parameter, goodness-of-sine-fit, amplitude, period and phase. The order parameter ‘R’ was used to quantify the synchrony of phase, period and waveform for each circadian neuron subgroup and for ‘all cells’ (summed from all subgroups). Statistical significance was determined by using a bootstrap procedure with the size of each bootstrap sample equivalent to the original number of cells in each data set. Each bootstrap procedure was repeated 4,000 times (except 10,000 for the ‘all cells’ group) to provide 95% and 99% confidence intervals for the difference in R (RWLS- RC) between cells exposed to WLS and cells in control

conditions with no phase shifts with the null hypothesis that there is no difference between conditions. Discrete wavelet-transform (DWT) was used in combination with sine-fit estimates of 2-day sliding windows to provide circadian measures of rhythmicity, period, amplitude and phase. Oscillator rhythmicity was determined as the percentage of variance accounted for by fitting a sine wave to the time series (goodness-of-sine-fit). Oscillators were deemed “reliably rhythmic” if their period was 24 ±8 hours, amplitude was the noise amplitude (mean amplitude of the DWT component associated with periods shorter than 4-hrs), and their goodness-of-sine-fit measure was ≥0.82 as described in [95].

Non-linear embedded phase estimates used to generate phase ensemble animations and validate sine-fit estimates

A time delay embedding protocol was used to confirm that circadian parameter s was reliably measured using sine-fits of wavelet detrended time series. Phase estimates were determined by the polar angle of time series that were embedded in a higher dimension via a 6-hour lag resulting in oscillations circling the origin. Phase plots generated using this nonlinear embedded phase analysis confirmed the same patterns of oscillator dynamics observed in plots generated using sine-fit calculations. Non-linear embedded phase estimates were also used to generate phase ensemble animations as previously described [108].

Fly sleep quantification

Fly activity data was binned into 60-minute time sections. Following binning, activity data was translated to run length encoding and any run of zero activity for five or

greater minutes was scored as sleep. Each fly's total amount of sleep per bin was totaled, and the resultant matrix contained the total amount of sleep by fly per 60-minute increments for the length of the experiment. Flies that died during the experiment registered very long strings of zero activity and were manually removed to prevent over counting sleep amounts. Students two-sided t-test was used to compare differences between bins of experimental groups, with a p-value <0.05 considered to be significant.

Fly learning and memory assay

Flies were evaluated for the effects of the weekend light shift on both sleep and short-term memory [115]. ~6-day old male Canton-S (Cs) flies were used to assess short-term memory (STM) using the Aversive Phototaxic Suppression (APS) assay. Prior to being tested for STM, flies are examined to determine if they exhibit normal photosensitivity and quinine photosensitivity. This step is used to ensure that the changes to sensory thresholds are true changes in associative learning. Photosensitivity is evaluated using a T-maze with one lightened and darkened chambers that appear equal on either side. Flies must make photopositive choices to be considered for post-WLS evaluation of STM. Quinine sensitivity index (QSI) is achieved by determining the duration a fly stay on a side of a T-maze without quinine, as opposed to one side with the aversive stimuli, during a 5-minute period [115]. The learning test to evaluate STM used the APS assay. Flies were subjected to WLS schedule used for bioluminescence and behavior experiments. Flies were tested on the subjective "Tuesday" of the WLS schedule, two days after 3hr phase shifts experienced during the weekend. Flies are individually placed in a T-maze and allowed to choose between a lighted or darkened chamber for over 16 trials. Flies that do not display phototaxis during the first block of four trials are excluded

from further trials. During the 16 trials, flies learn to avoid the lighted chamber paired with aversive stimulus [115]. The performance index is calculated as the percentage of the times the fly choses the dark vial during the last four trials of the 16-trial test. STM is defined as selecting the dark vial on two or more occasions during the final four tests.

2.4 Results

2.4.1 Development of *LD Strobe* to Simulate Day-Night Entrainment

Light is the primary environmental cue for circadian entrainment [62]. Previous studies show that *Drosophila* brains are directly light sensitive due to the expression of cell-autonomous, short-wavelength, light-sensitive photoreceptors. Light-sensitive components CRYPTOCHROME (CRY) and Rhodopsin-7 (Rh7) are expressed in select circadian neuronal subsets and are distributed throughout the fly brain [20,25,68,69,90,104]. The direct sensitivity of the fly brain to light input enables the measurement of physiological photic entrainment using real-time bioluminescence recordings of entire cultured brains [95,108]. In addition to long durations of light, circadian cycles can be entrained using short pulses of light, referred to as “skeleton photoperiods (SPP)” [1,2]. In SPP, light pulses flank the beginning and end of the simulated daytime, which is then followed by long periods of complete darkness (DD) that simulate nighttime. This suggests that obtaining bioluminescence images during simulated daytime is possible. However, circadian locomotor behaviors in DD that follow skeleton photoperiods are relatively weak and differ significantly from the robust circadian behaviors seen in DD following standard 12-hrs light:12-hrs dark (LD) cycles (Figure 1A top row, 1B first column). As circadian behavior in DD reflects the activity of the free-running clock, we established the criteria that DD behavior following light schedules used for imaging conditions must show no statistically significant differences compared to normal LD cycles and developed a novel entrainment protocol we refer to as *LD Strobe* (Figure 1A bottom row, 1B right column, also see methods). *LD Strobe* consists of 15-minute periods of light followed by 45-minute bouts of darkness each hour during the 12-

hour “day”, then 12 hours of darkness during the 12-hour “night.” DD behavior following *LD Strobe* is indistinguishable from that following standard LD (Figure 1B, right column). Thus, *LD Strobe* effectively simulates daytime during 12 hours of alternating periods of light and dark, during which dark periods provide the opportunity to capture circadian circuit bioluminescence.

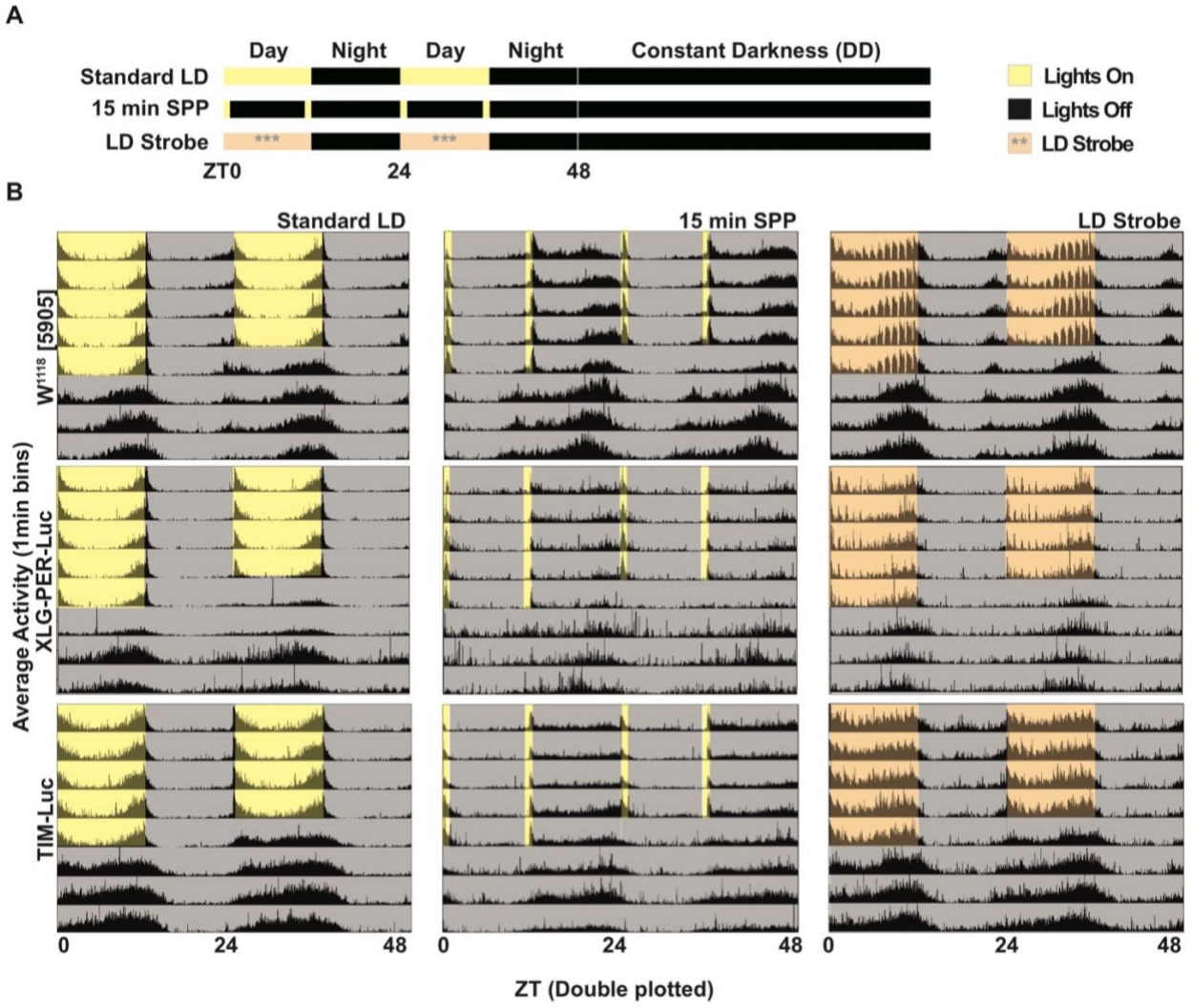

Figure 1. Day-night entrainment of locomotor activity by *LD Strobe* and Skeleton Photoperiod (SPP). Averaged double-plotted locomotor activities of adult *Drosophila* for 5 days of entrainment by various light protocols followed by 3 days of constant darkness (DD). **(A)** All flies are entrained to ≥3 days of 12hr:12hr LD prior to exposure to control Standard LD **(A, first row)**, 15-minute skeleton photoperiod (**A, middle row**; yellow bars indicate 15 minutes of light exposure at caps of each 12-hour day), or *LD Strobe* (**A, bottom row**; orange shade indicates 15-minutes of light followed by 45-minutes of dark for every hour of the 12hr day). Yellow or orange shade indicates windows of light

exposure, black indicates lights off. **(B)** Behavior actograms for three fly genotypes (W1118[5905], top row; XLG-PER-Luc, middle row, and TIM-Luc, bottom row) in three different entrainment schedules (Standard LD, left column; 15-min SPP, middle column; *LD Strobe*, right column). All entrainment schedules involve 5 days of respective light/dark regimes (yellow or orange shade/gray shade), followed by 3+ days of constant darkness (gray shade). See Table 1 for number of flies used.

2.4.2 Synchronized TIMELESS-luciferase rhythmic cycles occur in all major circadian cell groups under *LD Strobe* simulated day/night

We compared *period* and *timeless* clock promoter-driven luciferase transgenic lines, *XLG-PER-Luc* [25,95] and *TIM-Luc*, imaging whole brains under the *LD Strobe* light schedule. The averages of all clock neuron bioluminescence signals of *XLG-PER-Luc* and *TIM-Luc* are highly rhythmic and synchronous for each line in simulated day/night but exhibit minor differences (Figure 2A). The phase of *TIM-Luc* is advanced a few hours and shows lower amplitudes relative to *XLG-PER-Luc* (Figure 2A). The waveform of *TIM-Luc* is asymmetric with a broader and shallow trough compared to the peak while *XLG-PER-Luc* exhibits symmetric peaks and troughs for its waveform (Figure 2A). These properties seen in the averaged clock neuron bioluminescence signals of *TIM-Luc* are seen also in the averaged bioluminescence signals of the individual subgroups: the small- and large-lateral ventral neurons (s-LNvs and l-LNvs), the and lateral-dorsal neurons (LNds), and the dorsal neurons-1 (DN1) and dorsal neurons-3 (DN3) subgroups (Figure 2B, C). Synchrony of phase, period and waveform between individual neurons among subgroups is high as shown by individual superimposed records (Figure 2C) and as quantified by order parameter R, which measures phase, period and coherence (Figure 2D). Statistical comparison of order parameter R between *XLG-PER-Luc* and *TIM-Luc* shows mostly no significant differences to the 95% confidence interval during simulated day/night; however, synchrony and waveform amplitude quickly drop for *TIM-Luc* in DD conditions (Figure 2E). The asymmetric waveform seen for *TIM-Luc* may reflect actual signal or more likely, as the signal, relative to *XLG-PER-Luc* is lower, we may not be able to detect the lowest amplitude time points at the trough. Because we cannot yet distinguish between

these possibilities, we focused the remainder of our analysis using *XLG-PER-Luc* whole brain imaging.

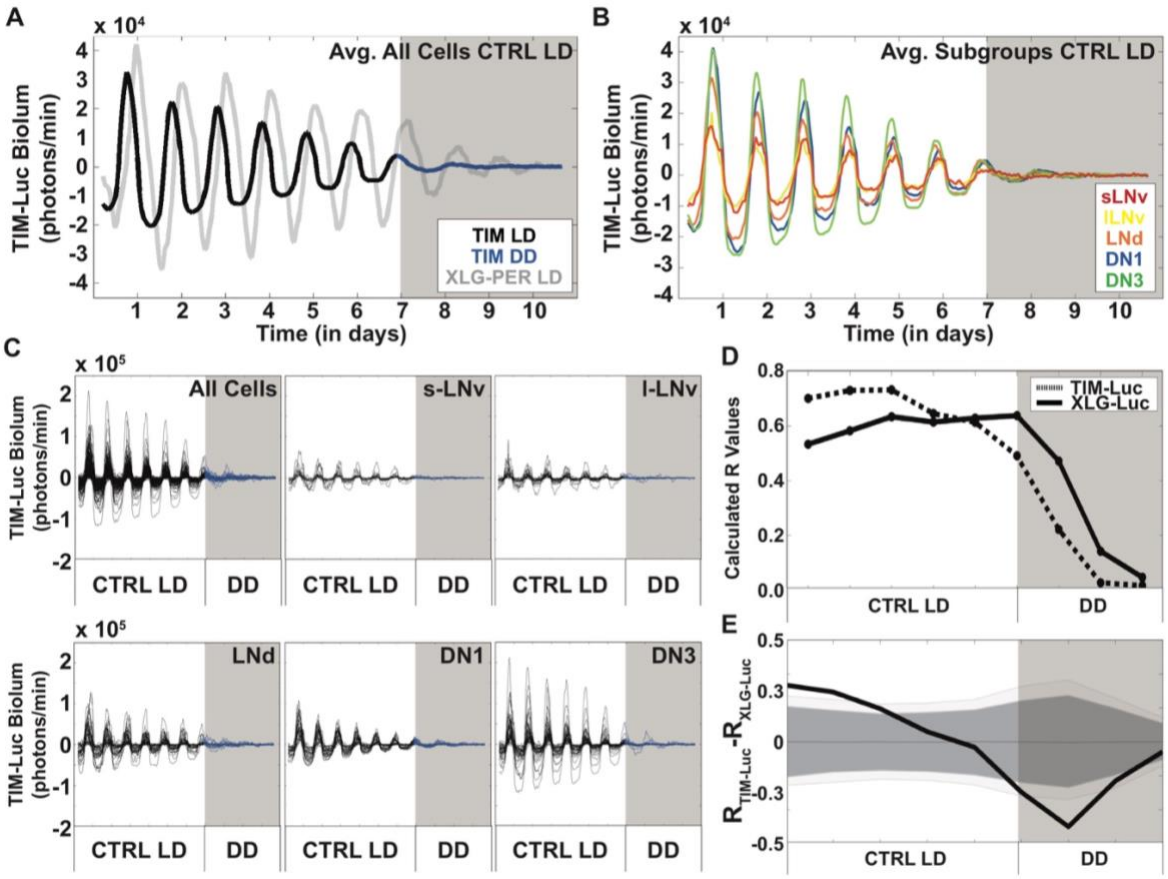

Figure 2. Bioluminescence recording of TIMELESS oscillations in *Drosophila* circadian neurons. Bioluminescence recordings of TIMELESS-Luc in cultured adult *Drosophila* brains (n = 6 brains, 159 cells) under control LD (black trace) followed by complete darkness (blue trace, gray shade). XLG-PER-Luc bioluminescence (gray trace) is overlaid for comparison of oscillations between the two genotypes. **(A)** Averaged bioluminescence traces of all TIM-expressing circadian neurons under 7 days of control LD conditions (black trace) followed by complete darkness (blue trace, gray shade). XLG-PER-Luc expression is overlaid for comparison of the two clock proteins (s-LNv = 18 cells, l-LNv = 19 cells, LNd = 18 cells, DN1 = 27 cells, DN3 = 18 cells). **(B)** Averaged bioluminescence traces of TIM-expression in circadian neuron subgroups under control

LD conditions. Each canonical neuron subgroup is labeled as follows: s-LNv (red), l-LNv (yellow), LNd (orange), DN1 (blue) and DN3 (green) proteins (s-LNv = 15 cells, l-LNv = 24 cells, LNd = 43 cells, DN1 = 35 cells, DN3 = 42 cells). **(C)** TIM bioluminescence traces of individual neurons for all cells (top left panel), s-LNv (top middle panel), l-LNv (top right panel), LNd (lower left panel), DN1 (bottom middle panel), and DN3 (bottom right panel) under control LD conditions. Control LD entrainment involves 7 days of control LD followed by constant darkness (gray shade). **(D)** Calculated synchronization index/order parameter, R values for TIM oscillations (dotted trace) under control LD conditions. XLG-PER-Luc (solid trace), under control conditions is overlaid for comparison. **(E)** Statistical comparisons of overall synchrony between TIM and PER under control LD conditions followed by DD. Difference in order parameter, R, between oscillations of TIM and PER were calculated using bootstrapped analysis (black trace). Dark gray and light gray zones indicate either 95% or 99% confidence zones respectively. Here, the null hypothesis indicates that there is no difference in order parameter, R, between the oscillations of TIM and PER under control LD conditions.

2.4.3 PER cycling in the circadian circuit under simulated LD and in response to light shifts does not differ with the presence or absence of eyes

While CRY is the primary light input channel for circadian neurons, opsin-based external photoreceptors contribute as a secondary light input channel. We measured PER cycling in the circadian circuit under simulated day/night using the *LD Strobe* protocol in whole brain explants with the eyes attached. We sought to determine whether the presence of the eyes, along with CRY, alters circuit cycling. Comparison between the averaged bioluminescence of all cells for brains with or without compound eyes reveals qualitatively no difference in PER oscillations throughout simulated day/night light cycles for a week (Figure 3A, white shade), while PER cycles in brains with compound eyes attached appear to dampen more slowly in DD (Figure 3A, blue dotted trace, gray shade versus blue solid trace, gray shade). PER oscillations in canonical circadian neurons in brains with compound eyes attached or absent are qualitatively similar (Figure 3B). Quantitatively, the calculated order parameter R between the oscillations of PER in brains with or without the compound eye are similar under simulated day/night cycles and in DD conditions (Figure 3C, dotted and solid trace respectively, DD represented by gray shade). We find no significant differences in calculated R-values in PER cycling in cultured brains with and without compound eyes attached during simulated day/night cycles and DD (Figure 3D).

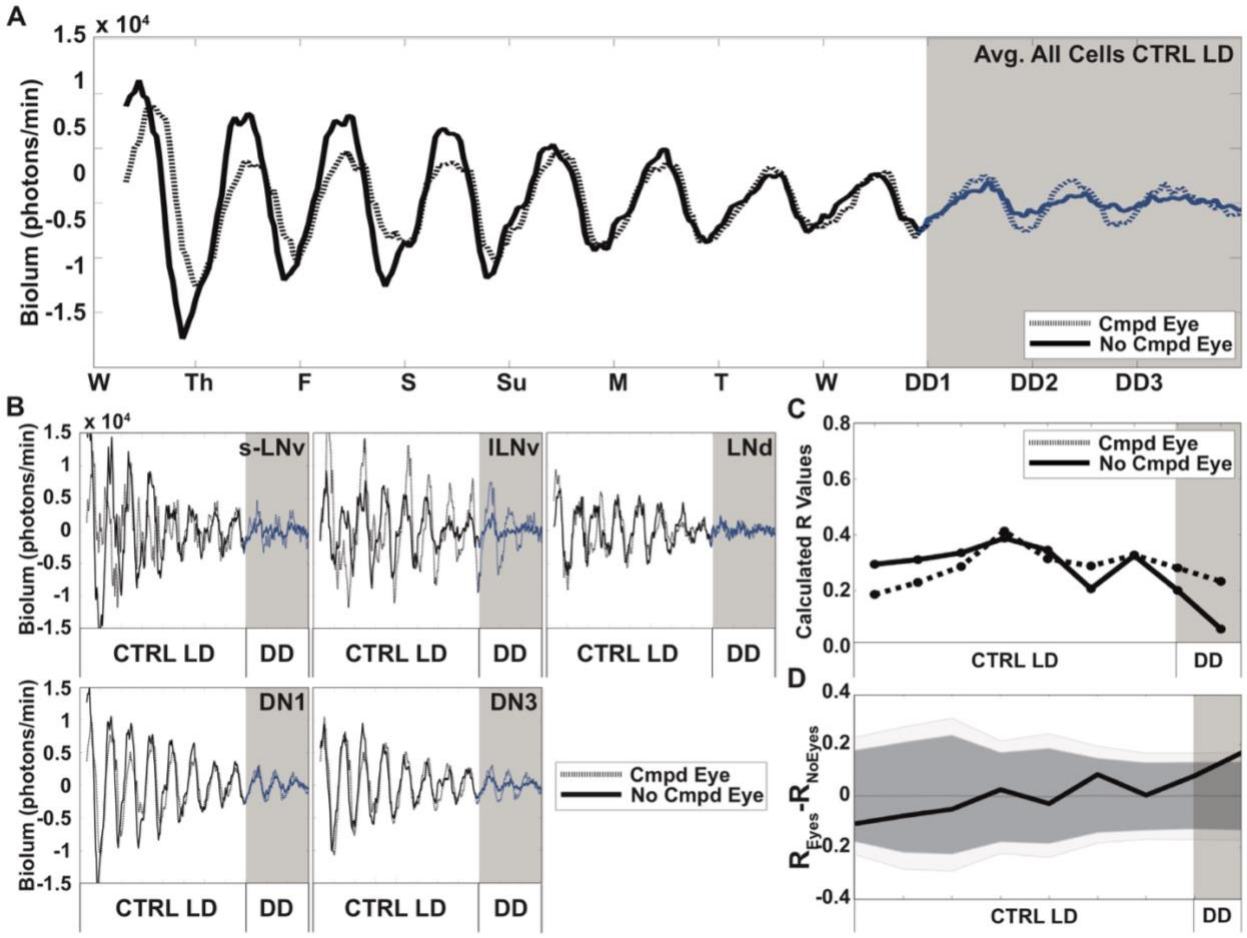

Figure 3. Circadian neuron subgroups are light entrained with either the presence or absence of the compound eyes. Averaged 11-day bioluminescence recordings of cultured *Drosophila* brains with compound eyes attached (n=3 brains, 70 cells, dotted trace) or completely removed (n=3 brains, 63 cells, solid trace) reported by PERIOD from XLG-PER-Luc flies. **(A)** Control LD conditions simulate standard 12L12D entrainment spanning one week without phase shifts for cultured brains with compound eyes (sLNv n=6, lLNv n=5, LNd n=7, DN1 n=30, DN3 n=22) and brains with compound eyes removed (sLNv n=7, lLNv n=7, LNd n=7, DN1 n=29, DN3 n=13) followed by DD (gray shade). **(B)** Averaged bioluminescence traces for individual neuronal subgroups comparing oscillators in brains with or without attached compound eyes. **(C)** Calculated dynamic

changes in synchronization index/order parameter, R, measures the level of synchrony for all circadian neuron subgroups using a one-day rolling window. Comparative differences in the calculated dynamic changes in synchronization index/order parameter, R, in control LD conditions for all neurons in brains cultured with compound eyes (dotted traces), and brains without compound eyes (solid traces). **(D)** Statistical comparisons overall synchrony between brains with or without compound eyes under control LD conditions. Difference in order parameter, R, between brains with or without eyes were calculated using bootstrapped analysis (black trace). Dark and gray zones indicate either 95% or 99% confidence zones, respectively. Here, the null hypothesis indicates that there is no difference in order parameter, R, between brains with or without compound eyes attached under control LD conditions.

2.4.4 Constant light immediately evokes loss of PER oscillations throughout the circadian circuit

Constant light (LL) rapidly evokes circadian behavioral arrhythmicity [2]. However, the detailed linkage between LL induced changes in PER cycling in the circadian circuit and behavioral arrhythmicity is unknown. Prior to LL, we imaged cultured whole brains under standard *LD Strobe* to simulate day/night cycles for three days prior to transitioning to five days of LL, then into complete darkness (Figure 4A, white, red, and gray shade, respectively). Upon entry into LL, averaged PER oscillations from the entire circadian circuit rapidly dampens and persists well into DD (Figure 4A, red and gray shade respectively). LL-induced averaged PER oscillations and amplitudes are dampened for all circadian subgroups (Figure 4B), however, the lateral neurons immediately lose oscillatory behaviors under LL, while DN1 and DN3s have oscillations that persist days after the start of LL (Figure 4B, light red shade). The long-lasting detrimental effects of constant light on PER cycling throughout the circadian circuit continues from the transition from LL to DD (Figure 4A, B, gray shade). Quantitative analysis of the LD-LL-DD transitions show that synchrony of cells within the circuit under an LL environment rapidly decreases in order parameter R (Figure4C, dotted trace) compared to the overall circuit of brains in a control LD environment (Figure 4C, solid trace) and statistically significant differences between the two conditions (Figure 4D). These results further validate the correspondence between circadian circuit wide PER cycling imaged in whole brain to *in vivo* circadian behavior as both dampen almost immediately in response to constant light.

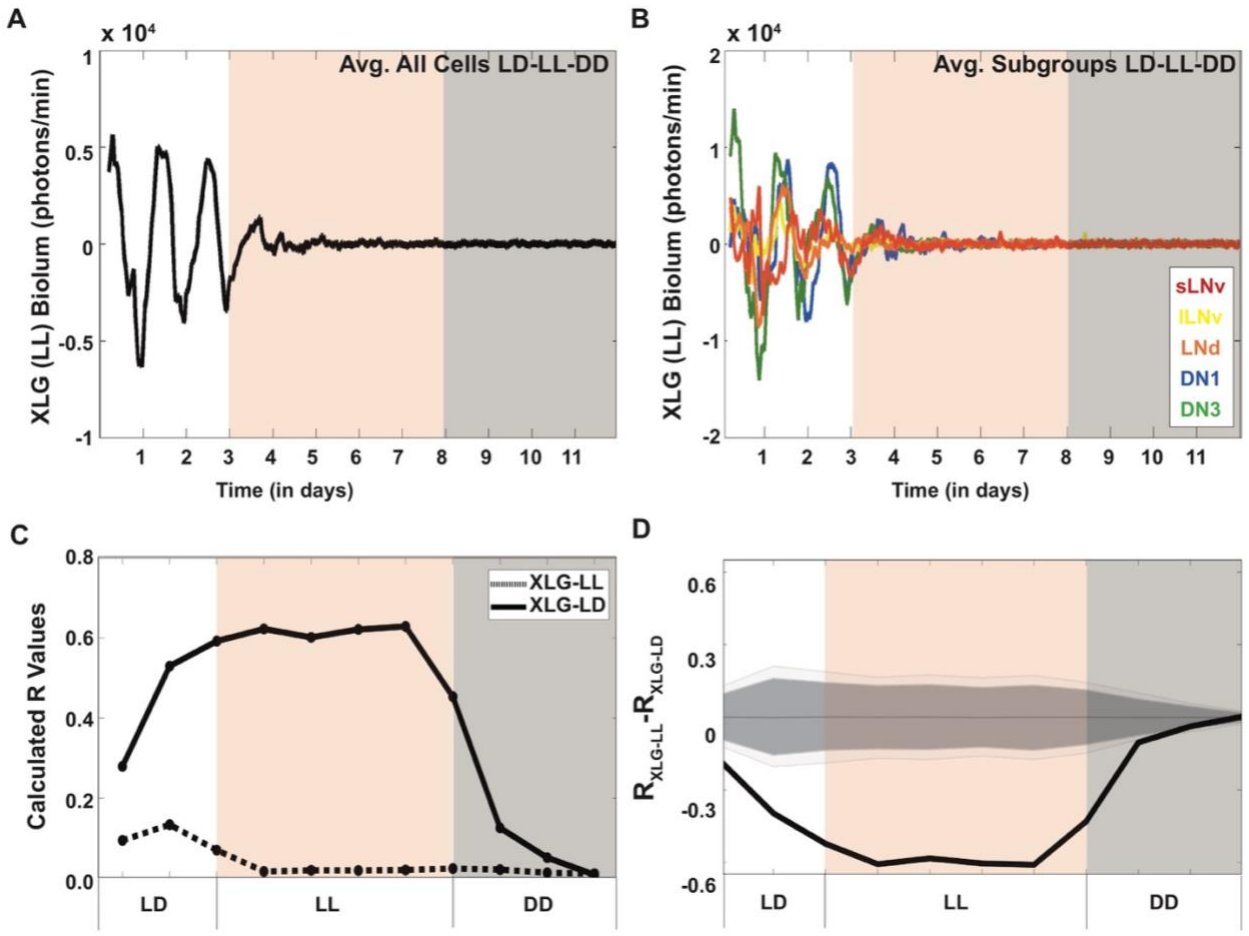

Figure 4. Exposure to constant light dampens PER oscillations in *Drosophila* clock neurons. Bioluminescence recordings of XLG-PER-Luc in cultured adult *Drosophila* brains (n = 6 brains) under 3 days of control LD, followed by 5 days of constant light (LL, red shade), then DD (gray shade). **(A)** Averaged bioluminescence traces of all PER-expressing circadian neurons under 3 days of control LD, followed by 5 days of LL conditions (black trace, red shade) followed by complete darkness (black trace, gray shade). **(B)** Averaged bioluminescence traces of PER-expression in circadian neuron subgroups under control LD-LL-DD conditions. Each canonical neuron subgroup is labeled as follows: s-LNv (red), l-LNv (yellow), LNd (orange), DN1 (blue) and DN3 (green). **(C)** PER bioluminescence traces of individual neurons for all cells (top left panel),

s-LNv (top middle panel), l-LNv (top right panel), LNd (lower left panel), DN1 (bottom middle panel), and DN3 (bottom right panel) under LD-LL-LD conditions (s-LNv = 11 cells, l-LNv = 11 cells, LNd = 22 cells, DN1 =53 cells, DN3 = 44 cells). **(D)** Calculated synchronization index/order parameter, R values for PER oscillations (dotted trace) under LD-LL-DD conditions. XLG-PER-Luc (solid trace), under control conditions is overlaid for comparison (s-LNv = 18 cells, l-LNv = 19 cells, LNd = 18 cells, DN1 = 27 cells, DN3 = 18 cells). **(E)** Statistical comparisons of overall synchrony of PER expression under control LD followed by DD and LD-LL-DD conditions. Difference in order parameter, R, between oscillations of PER in control LD or LD-LL-DD were calculated using bootstrapped analysis (black trace). Dark gray and light gray zones indicate either 95% or 99% confidence zones respectively. Here, the null hypothesis indicates that there is no difference in order parameter, R, between the oscillations of PER under control LD conditions followed by DD and LD-LL-DD.

2.4.5 LL induced PER arrhythmicity is partially rescued mutant flies that lack CRY in *Drosophila* whole brains

CRY plays a crucial role in environmental light entrainment *in vivo* [90,116]. Constant light exposure (LL) disrupts the circadian clock in many animal species, including *Drosophila*, as shown by light intensity-dependent behavioral arrhythmicity [2,27]. In contrast, mutant *cryb* and *cry*-null flies are behaviorally rhythmic in LL, indicating the primacy of CRY as the primary light input channel for circadian neurons [27,117]. We measured the whole brain light response of PER cycling throughout the circadian circuit in the absence of CRY using XLG-PER-Luc in a *cryb* mutant background transgenic line [64] under LD and LL conditions. PER oscillations of *cryb* mutants in LD and LL with control XLG-PER-Luc in CTRL LD (Figure 5A, blue dotted, black solid, and gray solid lines, respectively). Under LD conditions, *cryb* mutant PER oscillations are completely dampened (Figure 5A blue dotted trace). In contrast, *cryb* PER oscillations under LL entrainment exhibit a semblance of oscillations and peak bioluminescence (Figure 5A, black solid trace) comparable to that seen in control XLG-PER-Luc under standard LD entrainment (Figure 5A, gray solid trace). In DD following either LD or LL, both *cryb* conditions show little or no oscillations (Figure 5A, gray shade). The canonical circadian neurons of *cryb* mutants show dampened PER oscillations throughout the entirety of the LL or LD entrainment (Figure 5B) except for the high amplitude oscillations measured in the DN1 subgroup (Figure 5B, black solid trace, fourth panel) under LL conditions. We calculated the order parameter R of *cryb* PER oscillations under LD (Figure 5C, dotted trace) and LL conditions (Figure 5D, dotted trace) and compared these values to R calculated for control XLG-PER-Luc under LD (Figure 5C and D, solid traces) as

entrainment progresses into DD (Figure 5C and D, gray shade). As expected, PER oscillations in *cryb* mutants show no significant synchrony under either LD (Figure 5E) conditions compared to XLG-PER-Luc oscillations, and partial rescue of rhythmicity under LL (Figure 5F).

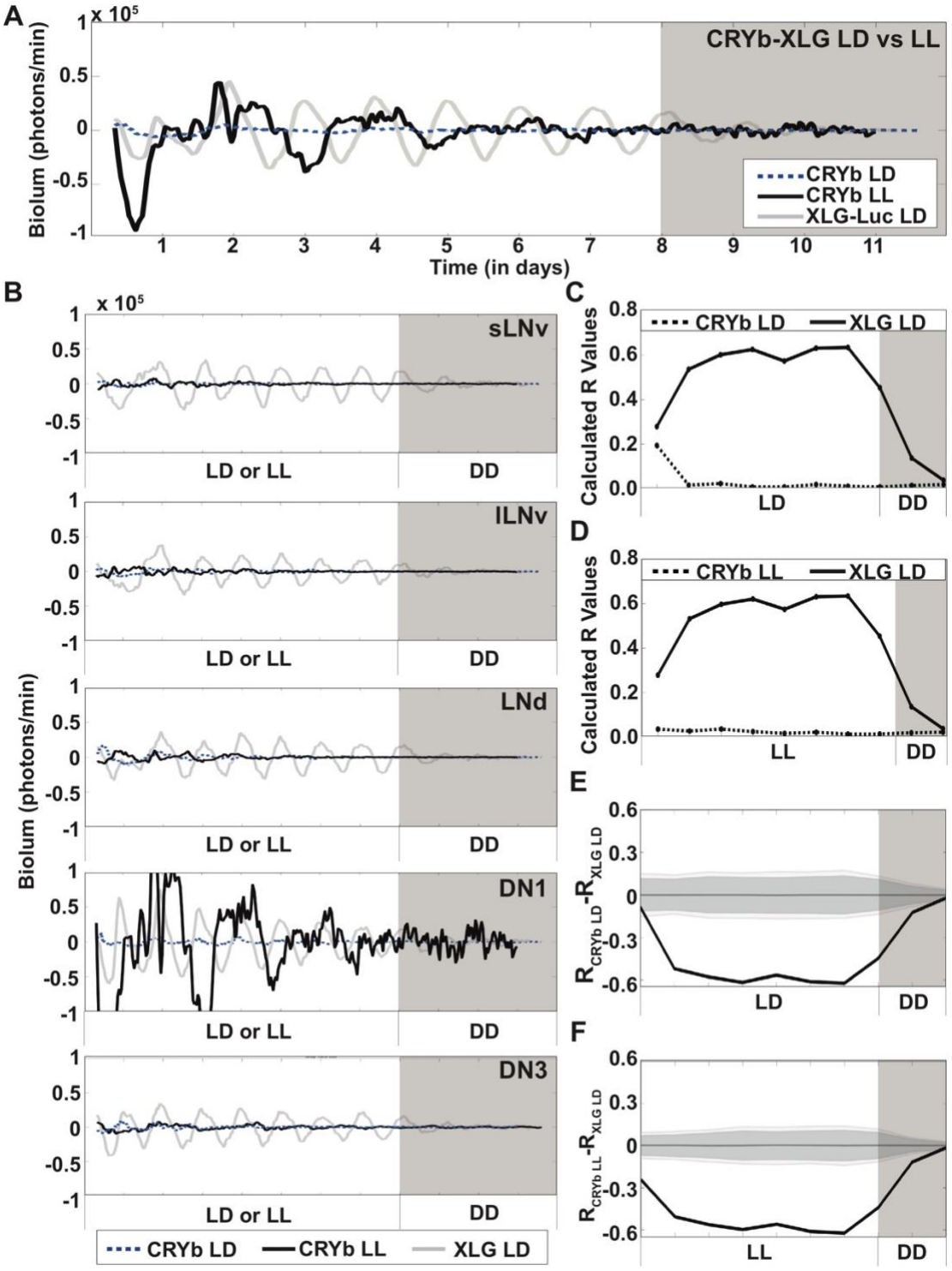
A
x 10^5
Biolum (photons/min)
CRYb-XLG LD vs LL
CRYb LD
CRYb LL
XLG-Luc LD
Time (in days)
B
sLNv
lLNv
LNd
DN1
DN3
LD or LL
DD
Biolum (photons/min)
CRYb LD
CRYb LL
XLG LD
C
Calculated R Values
CRYb LD
XLG LD
LD
DD
D
Calculated R Values
CRYb LL
XLG LD
LL
DD
E
R_CRYb LD-R_XLG LD
LD
DD
F
R_CRYb LL-R_XLG LD
LL
DD

Figure 5. CRYPTOCHROME is required for LD entrainment of cultured fly brains. Bioluminescence recordings of CRYb XLG-PER-Luc in cultured adult *Drosophila* brains under 8 days of control LD (n = 3 brains; blue dotted trace) and 8 days of LL (n = 3 brains, black solid trace), followed by DD (gray shade). XLG-PER-Luc bioluminescence (gray trace) is overlaid for comparison of oscillations between the two genotypes (s-LNv = 18 cells, l-LNv = 19 cells, LNd = 18 cells, DN1 = 27 cells, DN3 = 18 cells). **(A)** Averaged bioluminescence traces of all PER-expressing circadian neurons in a CRYb background under 8 days of control LD (blue dotted trace) (s-LNv = 17 cells, l-LNv = 20 cells, LNd = 11 cells, DN1 = 13 cells, DN3 = 25 cells) or LL (black solid trace), followed by complete darkness (gray shade). XLG-PER-Luc expression is overlaid for comparison of the two clock proteins **(B)** Averaged bioluminescence traces of PER-expression in circadian neuron subgroups in a CRYb background under control LD (blue dotted trace) and LL conditions (black solid trace). Each canonical neuron subgroup undergoes both LD and LL conditions (s-LNv = 29 cells, l-LNv = 20 cells, LNd = 16 cells, DN1 = 30 cells, DN3 = 29 cells). XLG-PER-Luc bioluminescence (gray trace) is overlaid for comparison of oscillations between the two genotypes. **(C)** Calculated synchronization index/order parameter, R values for PER oscillations in CRYb-XLG-Luc under control LD conditions (dotted trace). XLG-PER-Luc (solid trace), under control conditions is overlaid for comparison. **(D)** Calculated synchronization index/order parameter, R values for PER oscillations in CRYb-XLG-Luc under LL conditions (dotted trace). XLG-PER-Luc (solid trace), under control conditions is overlaid for comparison. **(E)** Statistical comparisons of overall synchrony between PER from CRYb-XLG-Luc and PER from XLG-Luc under control LD conditions followed by DD. Difference in order parameter, R, between

oscillations of PER from CRYb-XLG-Luc under control LD and PER from XLG-Luc from control LD conditions were calculated using bootstrapped analysis (black trace). Dark gray and light gray zones indicate either 95% or 99% confidence zones respectively. Here, the null hypothesis indicates that there is no difference in order parameter, R, between the oscillations of PER from CRYb-XLG-Luc and PER from XLG-Luc under control LD conditions. **(F)** Statistical comparisons of overall synchrony between PER from CRYb-XLG-Luc and PER from XLG-Luc under LL and control LD conditions (respectively) followed by DD. Difference in order parameter, R, between oscillations of PER from CRYb-XLG-Luc under LL and PER from XLG-Luc from control LD conditions were calculated using bootstrapped analysis (black trace). Dark gray and light gray zones indicate either 95% or 99% confidence zones respectively. Here, the null hypothesis indicates that there is no difference in order parameter, R, between the oscillations of PER from CRYb-XLG-Luc under LL and PER from XLG-Luc under control LD conditions.

2.4.6 Exposure to weekend light shifts dampen circadian circuit-wide rhythmicity and synchrony

With the ability to study bioluminescence during simulated daytimes, we examined the circadian circuit-wide dynamic response at the single-neuron resolution to compare unshifted to shifted light schedules. For 11 days, we obtained bioluminescence imaging of cultured adult *Drosophila* brains exposed to the *LD Strobe* entrainment schedule. Under control (CTRL), unshifted LD conditions, we find a high level of multi-day synchrony (8 days) between all major circadian neuron subgroups (Figure 6A) along with robust rhythmicity, high amplitude oscillations, and ~24hr. After 8 days of unshifted LD, we challenged the free-running clock by placing brains in constant darkness (DD). Clock cycling amplitude rapidly dampens in DD (Figure 6A, gray shade).

To simulate WLS, we performed light phase shifts by initiating a 3hr phase delay, simulating “staying up late on Friday.” We retained this 3hr phase delayed schedule for two days simulating “sleep in late, stay up late” followed by a 3hr phase advance to simulate “Monday morning.” Similar weekday/weekend schedules, as previously described, are chronically experienced by much of the human populace worldwide. We find that *Drosophila* whole-brain explants exposed to WLS schedules show reduced synchrony between and within canonical circadian neuron subgroups during (Figure 6B, red shade) and after simulated weekend phase shifts (Figure 6B, green shade). Furthermore, circadian neuron subgroups following WLS show an immediate loss in rhythmicity and synchrony during the transition into DD (Figure 6B, green shade), revealing long-lasting circadian neural circuit perturbation three days after the last phase shift that simulates one weekend. This contrasts with the high level of synchrony seen in

DD for unshifted CTRL (Figure 6A, gray shade). Averaged circuit-wide cycling (Figure 6C) is compared between unshifted CTRL (black) and 3hr WLS (red), indicating average oscillator phase recovery does not occur until several days post-shift.

The striking differences in oscillator rhythmicity and phase coherence found in CTRL LD (Movie S1, left) are observed when compared to brains exposed to WLS (Movie S1, right). Phase ensemble animations aid to visualize oscillator dynamics comparing brains in CTRL (left) and WLS (right) schedules averaged as a whole throughout the duration of the experiment (Movie S2), separated into canonical circadian neuron subgroups (Movie S3), and at single-cell level (Movie S4). Differences in inter-subgroup dynamics in CTRL and WLS conditions led us to investigate circadian cycling of individual circadian neuron subgroups at single-cell resolution.

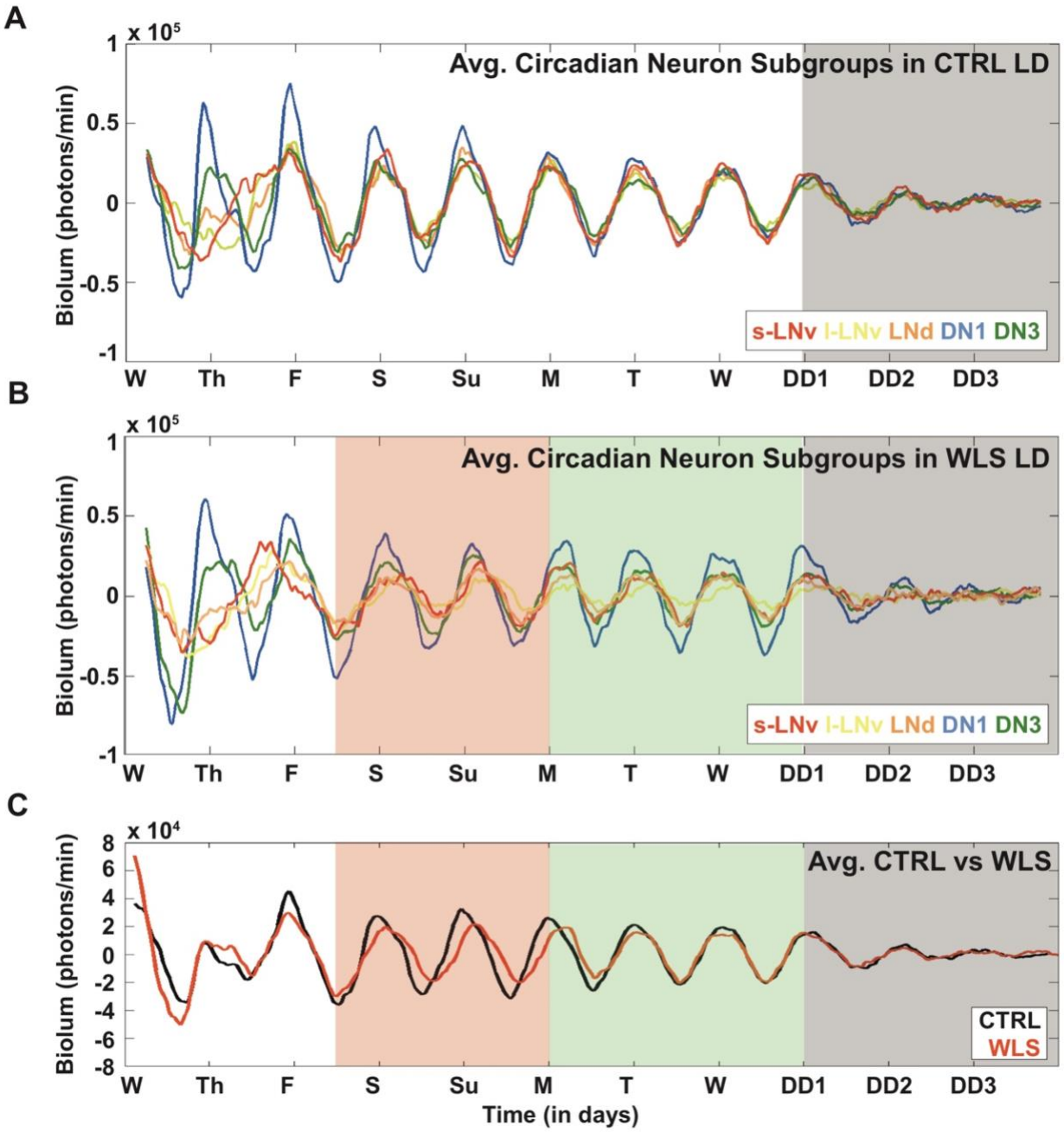

Figure 6. Weekend light shifts dampen circuit-wide rhythmicity and synchrony of *Drosophila* circadian neurons. 11-day bioluminescence recordings of cultured *Drosophila* brains reported by PER-Luciferase (n=6 brains). **(A)** Control *LD Strobe* conditions simulate standard 12hr Light: 12hr Dark (12L12D) spanning 8 days, without

phase-shifting light signals (s-LNv (red) = 18 cells, l-LNv (yellow) = 19 cells, LNd (orange) = 18 cells, DN1 (blue) = 27 cells, DN3 (green) = 18 cells). After the one-week simulation, brains are placed in constant darkness (DD) to challenge the free-running clock (gray shade). **(B)** Weekend light shift (WLS) conditions subject cultured adult *Drosophila* brains to one simulated weekend entailing a 3hr phase delay on Fridays, which persist until Sunday (red shade). Weekends are followed by a 3hr phase advance to simulate the return to a weekday schedule (green shade) and constant darkness (gray shade; s-LNv (red) = 17 cells, l-LNv (yellow) = 17 cells, LNd (orange) = 15 cells, DN1 (blue) = 28 cells, DN3 (green) = 30 cells). **(C)** Averaged bioluminescence traces comparing all cells placed in control LD (black trace) or WLS conditions (red trace). Light shifts are indicated as follows: weekend phase delay (red shade), weekday phase advance (green shade), and complete darkness (gray shade).

2.4.7 Individual circadian neuron subgroups exhibit distinct dynamics of activity under WLS conditions

Under unshifted CTRL LD, circadian neuron subgroups exhibit distinct signatures in rhythmicity, phase coherence and amplitude throughout the duration of entrainment (black traces, Figure 7A), which dampen in DD (blue traces against gray shaded background, Figure 7A). The sLNvs show the highest degree of synchrony over the course of CTRL LD (Figure 7A, first column). The DN1s exhibit the highest amplitude oscillations (Figure 7A, fourth column), and the DN3s exhibit the greatest variability in oscillator amplitude and synchrony in CTRL LD (Figure 7A, fifth column). WLS disrupts rhythmicity and synchronization during (red traces) and after (black traces on green shaded background) shifts affecting all circadian neuron subgroups except for DN3s (Figure 7B) which significantly tighten their amplitude and phase coherence (Figure 7B). Interestingly, DN3s are the only cells that become more synchronized in response to WLS returning to a “weekday” schedule (Figure 7B, fifth column, green shaded background). Averaged waveforms for the s-LNv, l-LNv, LNd, DN1 and DN3 are shown during the WLS on “Saturday, Sunday and Monday” (Figure 8A) and post-WLS on “Monday, Tuesday, Wednesday and Thursday” (Figure 8B).

Quantitatively, s-LNvs and LNds maintain the highest level of synchrony in CTRL conditions as shown by the increasing order parameter R values in simulated LD day/night (black lines, Figure 9A). In DD, following CTRL LD, all neuronal subgroups exhibit a clear and immediate decrease in phase, period and coherence as quantified by order parameter ‘R’ (gray shaded background). Small- and large-LNvs show large changes in relative phase angle (Figure 9B) and significantly lower synchrony in response

to WLS relative to unshifted CTRL LD (Figure 9A, Figure 9C, shaded area represents 95% confidence limit). Conversely in response to WLS, LNds, DN1s, and DN3s maintain relatively more robust synchrony and amplitude, measured by order parameter R (Figure 9A, red traces), smaller changes in relative phase angle (Figure 9B), and few significant differences between control and shifted light conditions (Figure 9C). Despite being cell autonomously light-blind by not expressing CRY or Rh7 like other subgroups [20,68,69], DN3s tend to increase inter-group oscillator synchrony as a response to WLS relative to unshifted CTRL LD (Figure 9A, C).

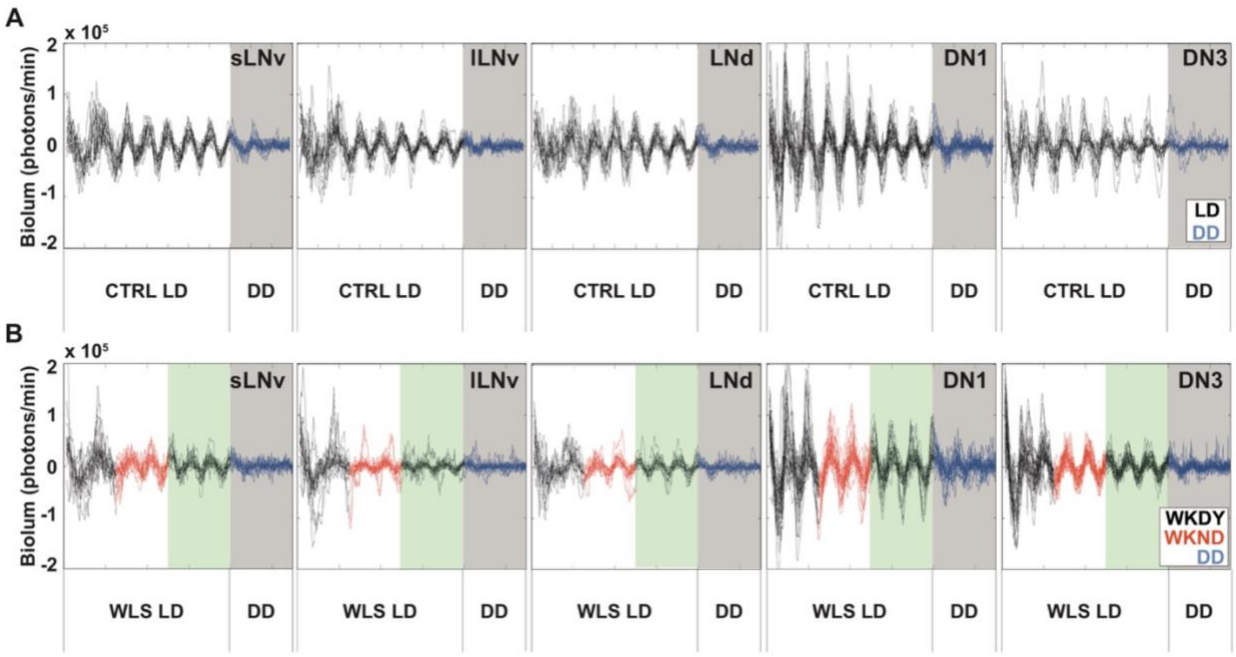

Figure 7. Circadian neuron subgroups exhibit distinct dynamics of activity in response to WLS conditions. Bioluminescence traces for individual cells from each canonical circadian neuron subgroup. Each trace in one panel represents bioluminescence from one individual cell**. (A)** Bioluminescence traces from brains subjected to control LD without phase advancing light signals for 8 days (black traces), then placed in DD conditions (blue traces, gray shade; s-LNv = 18 cells, l-LNv = 19 cells, LNd = 18 cells, DN1 = 27 cells, DN3 = 18 cells). **(B)** Bioluminescence traces from brains subjected to WLS LD conditions. WLS conditions entail pre-WLS (black trace, white shade), WLS (red trace, white shade), post-WLS (black trace, green shade), followed by DD (blue trace, gray shade; s-LNv = 17 cells, l-LNv = 17 cells, LNd = 15 cells, DN1 = 28 cells, DN3 = 30 cells).

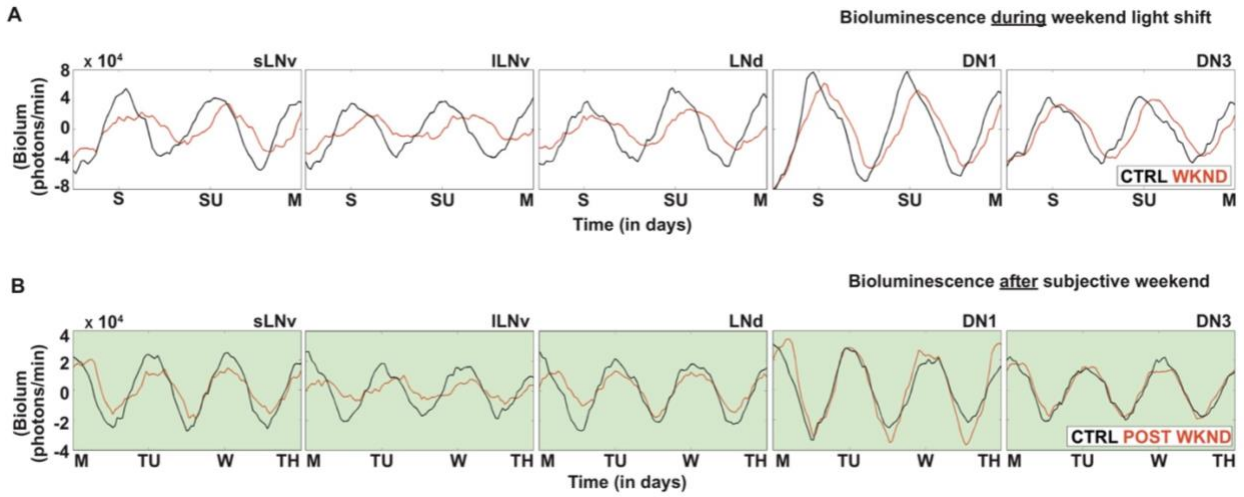

Figure 8. Detailed traces of averaged bioluminescence during and post-exposure to WLS. (A) Averaged bioluminescence traces for each circadian subgroup comparing the "simulated weekends" in control LD (black trace) with WLS conditions (red trace). **(B)** Averaged bioluminescence traces for each circadian subgroup comparing the "post-WLS" weekdays in control LD (black trace) and WLS conditions (red trace). Traces for both control LD and WLS conditions were generated using custom MATLAB scripts. See Methods and Materials for more details.

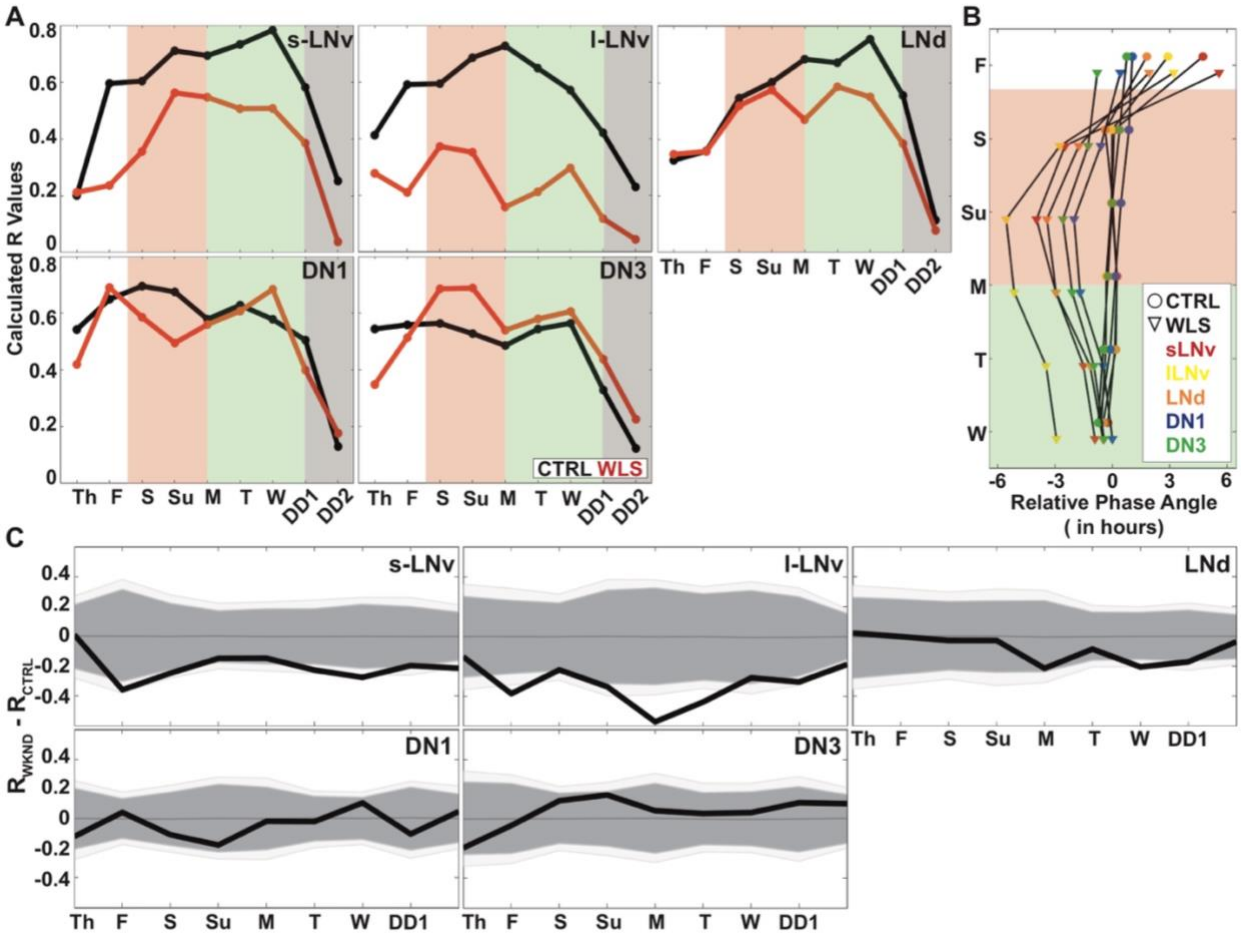

Figure 9. Circadian neuron subgroup synchrony exhibit destabilization in dynamics during WLS and requires days to recover post-shift. Calculated dynamic changes in synchronization index/order parameter, R, measures the level of synchrony for each circadian neuron subgroups using a one-day rolling window. **(A)** Calculated order parameter, R, comparing LD conditions between Control LD with no shifts (black) and WLS LD with 3hr shifts (red). WLS schedule is marked during the following light schedules: pre-shift (white shade), WLS (red shade), post-shift (green shade), and DD (gray shade). **(B)** Comparison of phase angle changes between each circadian neuron subgroups under control LD (circle) and WLS conditions (triangle). WLS conditions are

indicated as follows: pre-shift (white shade), WLS (red shade), post-shift (green shade). Each circadian neuron subgroups for control LD and WLS conditions are as follows: s-LNv (red), l-LNv (yellow), LNd (orange), DN1 (blue), DN3 (green). **(C)** Statistical comparisons of subgroup synchrony between control LD and WLS conditions followed by DD. Difference in order parameter, R, between control and WLS (R_{WLS}-R_{CTRL}) conditions were calculated using bootstrapped analysis (black trace). Dark and gray zones indicate either 95% or 99% confidence zones, respectively. Here, the null hypothesis indicates that there is no difference in order parameter, R, between brains placed in control LD or WLS LD.

2.4.8 Exposure to WLS leads to sleep disruption, and defects in learning and memory

Due to long-lasting post-shift changes in oscillator ensemble activity in circadian neurons following WLS, we measured correlative behavioral outputs under the similar light shift protocols *in vivo*. We exposed whole, intact flies to CTRL LD and WLS schedules used in while-brain imaging while measuring sleep [118,119]. Sleep is stable for unshifted CTRL LD (Figure 10A) as shown by consistent amplitudes (x-axis) and robust waveform (y-axis) across multiple days (z-axis). Flies exposed to WLS have significantly disrupted sleep patterns only during and after phase shifts (Figure 10B, red dots indicate significant hourly difference in sleep compared to CTRL LD). Hourly sleep differences between CTRL LD and WLS groups persist up to six days following the "Monday" phase advance into DD (Figure 10B, gray shade). Though hour-by-hour sleep amounts differ between CTRL LD and WLS groups during days after the phase advancing light shift, the total sleep amount over time does not differ—indicating the eventual effect of sleep homeostasis. Decreased cognitive performance, including learning and memory, is linked to circadian dysregulation and sleep low [120,121]. We tested how WLS affects learning and memory using the Aversive Phototaxic Suppression (APS) assay [115] two days after the phase-advancing light shift. WLS flies show significant impairments in remembering where to avoid aversive stimuli (quinine) in the maze compared to flies in CTRL LD (Figure 10E). This suggests that WLS exposure impairs learning and maintenance of short-term memory days following weekend phase shifts as shown by the inability for conditioning to avoid aversive stimuli, coinciding with persistent post-shift circadian circuit and sleep pattern impairment.

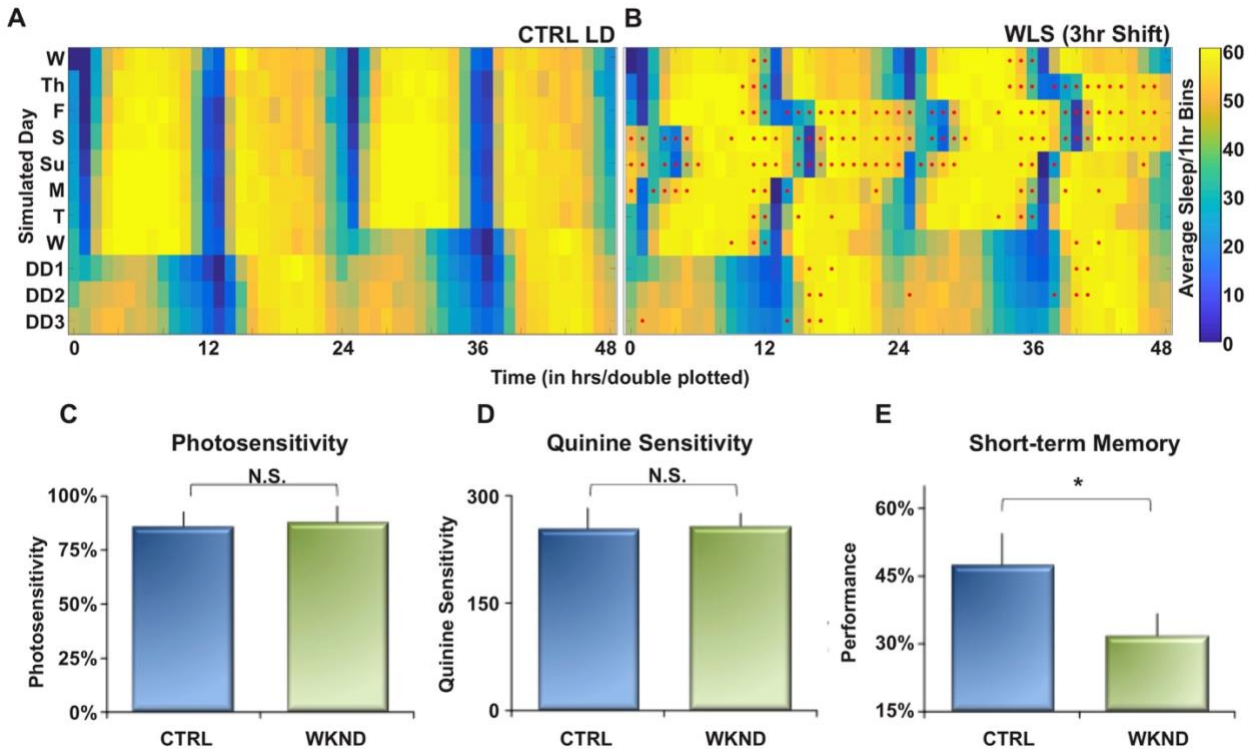

Figure 10. WLS leads to sleep disruption and hinders learning and memory. (A) Double-plotted heat map indicates the average amount of sleep of whole, intact flies per one-hour bins under control LD conditions. Maximum amount of sleep/1hr bin is shown in yellow, and no sleep (0 minutes) is shown in blue. Each row represents elapsed time: two days, 48 hours for double plotting. Control LD includes 8 days of simulated daytime and nighttime followed by 3 days of DD (n = 64 flies). (B) Double-plotted heat map indicating sleep amount of whole, intact flies under a WLS LD schedule. Maximum amount of sleep/1hr bin is shown in yellow, and no sleep (0 minutes) is shown in blue. WLS schedule entails a 3hr phase delay during simulated weekends followed by a 3hr phase advance simulating return to a weekday schedule. Flies are subjected to DD after 8 days of LD. Red dots indicate significant differences in sleep/1hr bin between control LD and WLS LD (n = 64 flies). (**C-E)** Aversive Phototaxic Suppression (APS) assay was

used to determine how WLS affects learning and memory. **(C)** Photosensitivity assay comparing flies exposed to control LD (blue) and WLS conditions, two days after the 3hr phase advance (green) (n = 5 male flies/condition). **(D)** Quinine sensitivity measurements for flies placed in either control LD (blue) and WLS conditions (green) two days after the 3hr phase advance (n = 5 male flies/condition)**. (E)** Measurement of learning and memory for flies exposed to WSL using the APS assay. Performance is measured for fly ability to remember to avoid specific parts of a T-maze two days after exposure to an LD condition. Control LD flies are indicated in blue, post-WLS flies in green (n = 10-11 male flies/condition). Significance for differences between control LD and WLS LD was determined using a t-test a $p \leq 0.05$.

	W1118 [5905]			XLG-PER-Luc			TIM-Luc		
	n	% Rhythmic	Period	n	% Rhythmic	Period	n	% Rhythmic	Period
Std. Entrainment									
LD	60	96.7	23.9	57	100	23.9	61	98.4	24
DD	57	100	23.5	54	90.7	23.3	56	96.4	23.8
30L30D LD Strobe									
LD	54	100	23.8	46	95.7	23.8	49	98	23.8
DD	53	100	23.5	45	64.4	23	47	89.4	23.8
15L45D LD Strobe									
LD	61	100	23.7	41	97.6	23.9	37	94.6	23.9
DD	60	100	23.5	36	75	23.2	28	89.3	23.7
5L55D LD Strobe									
LD	56	98.2	23.6	58	98.3	23.8	56	96.4	23.7
DD	51	94.1	23.4	54	74.1	23.3	52	92.3	23.5
30-min SPP									
LD	61	98.4	23.9	56	94.6	23.9	58	79.3	23.8
DD	59	98.3	23.6	51	82.4	23.3	55	90.9	23.3
15-min SPP									
LD	62	100	23.6	55	74.5	23.8	60	88.3	23.9
DD	61	98.4	23.4	50	54	23.7	59	76.3	23.7
5-min SPP									
LD	63	100	23.6	62	95.2	23.7	57	94.7	23.7
DD	63	98.4	23.3	62	87.1	23.1	56	94.6	23.5

Table 1. Quantification of behavioral entrainment by *LD Strobe* and skeleton photoperiod. FaasX was used for analysis of behavioral experiments. Wild-type W1118 [5905] XLG-PER-Luc and TIM-Luc flies were exposed to 5 days of entrainment (LD) by either *LD Strobe* or skeleton photoperiod protocols with 30, 15 or 5-minute light intervals. Following entrainment, flies were maintained in constant darkness (DD) for 5 days. Cycle-P was used to quantify measures of period length and the percentage of rhythmic flies using 15-minute bins of individual fly locomotor activity. Individual flies were considered rhythmic by chi-square periodogram analysis if they met the following criteria: power ≥ 40, width ≥ 4 hours and period length of 24 ± 8 hours.

2.5 Supplemental Movies

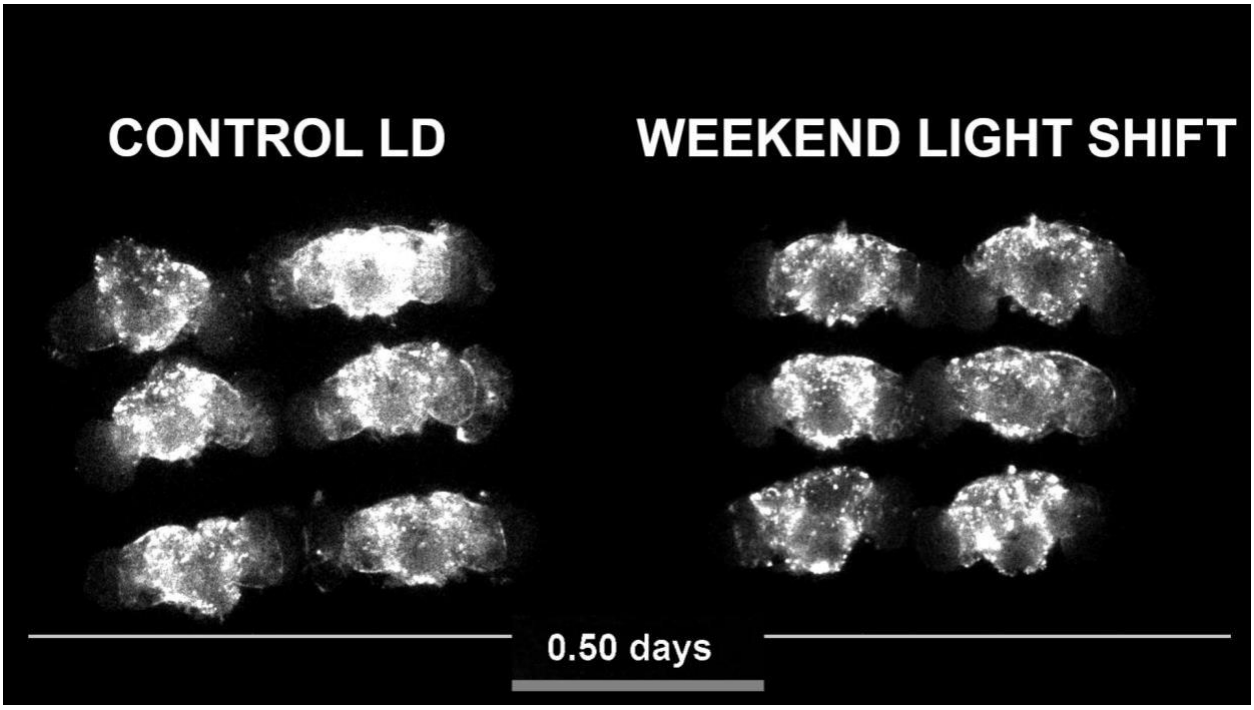

Movie S1: Raw time-lapse bioluminescence recordings of adult XLG-Per-Luc *Drosophila* whole-brain explants cultured for 11 days. Left: Six whole brain culture explants maintained in control conditions (*LD Strobe* with no phase shift) for 9 days followed by 2 days of constant darkness (DD). Right: Six whole brain culture explants exposed to weekend light shifts for 9 days followed by transfer to DD for the final 2 days. See Materials and Methods for more details.

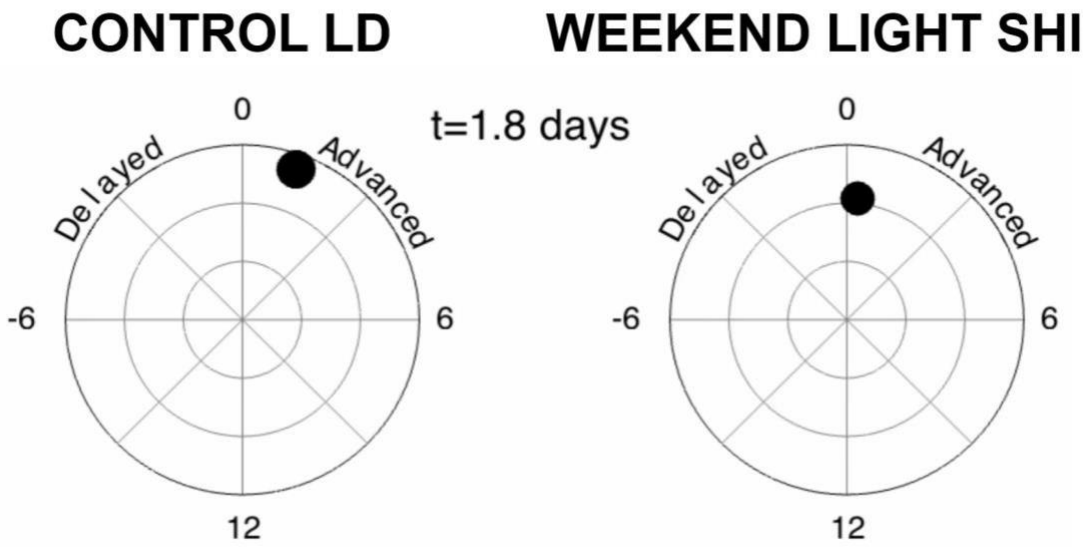

Movie S2: The animations show changes in the relative phase and amplitude of XLG-Per-Luc bioluminescence activity for "all cells" (averaged from all neuronal subgroups) in either control (left) or WLS (right) conditions. Mean network phase is standardized so that the mean network phase is set to ZT 0 on Day 3 when entrainment is most stable. The angle of the disks represents the relative phase shift over time such counterclockwise movement indicates a phase delay whereas clockwise movement indicates a phase advance. The drift of the disks towards the center of the circle and the size of the disks indicates reduction in amplitude. See Materials and Methods for more details.

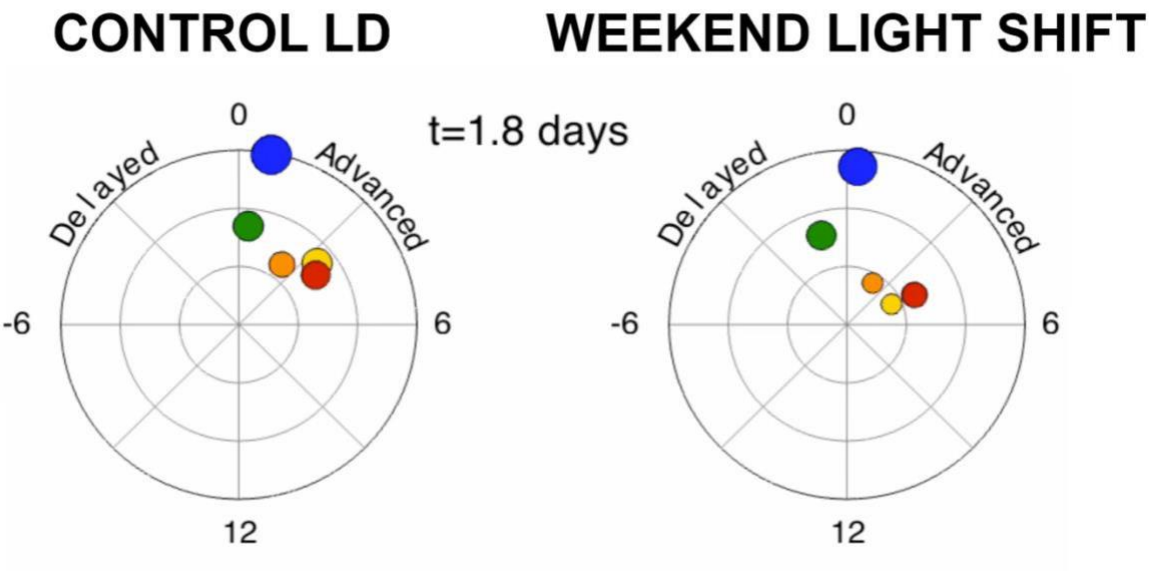

Movie S3: The animations show dynamic changes in relative phase shifts and amplitude for each neuronal subgroup in either control conditions (left) or in response to WLS (right). The mean phase shift for each neuron subgroup is represented by polar angle of the disks whereas amplitude is represented by the size and proximal distance of the disks from the center of the circles. The disks are colored according to neuronal subgroup for the s-LNvs (red), l-LNvs (yellow), LNds (orange), DN1s (blue) and DN3s (green).

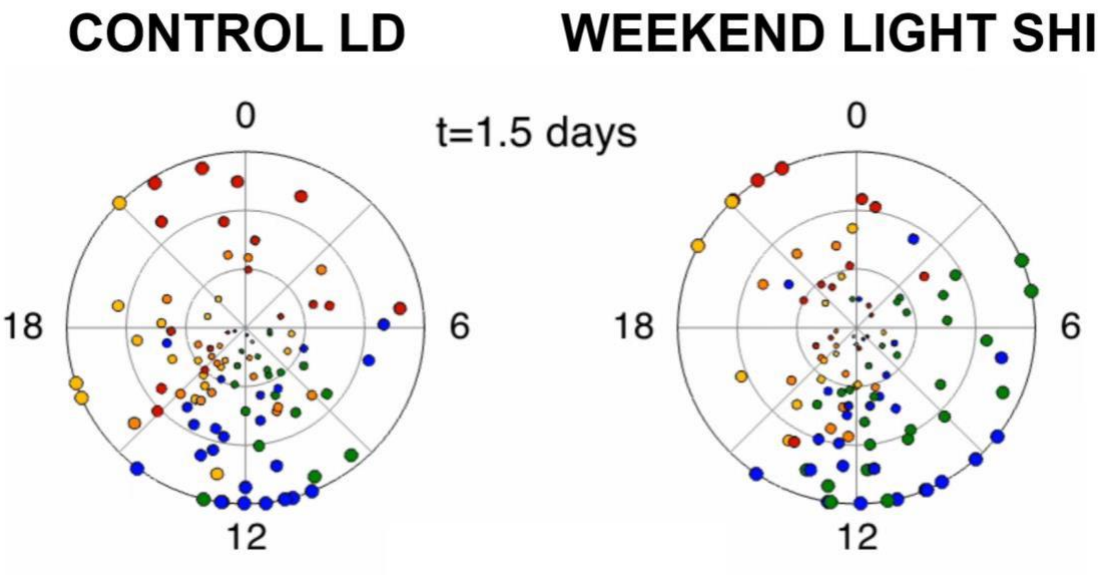

Movie S4: The animations show changes in the phase and amplitude of XLG-PER-Luc bioluminescence activity for individual neuron oscillators from all neuronal subgroups in either control conditions (Left) or in response to WLS (Right). The angle of the disks represents oscillator phase and drift of the disks towards the center of the circle and the size of the disks indicates reduction in amplitude. The disks are colored according to neuronal subgroup for the s-LNvs (red), l-LNvs (yellow), LNds (orange), DN1s (blue) and DN3s (green).

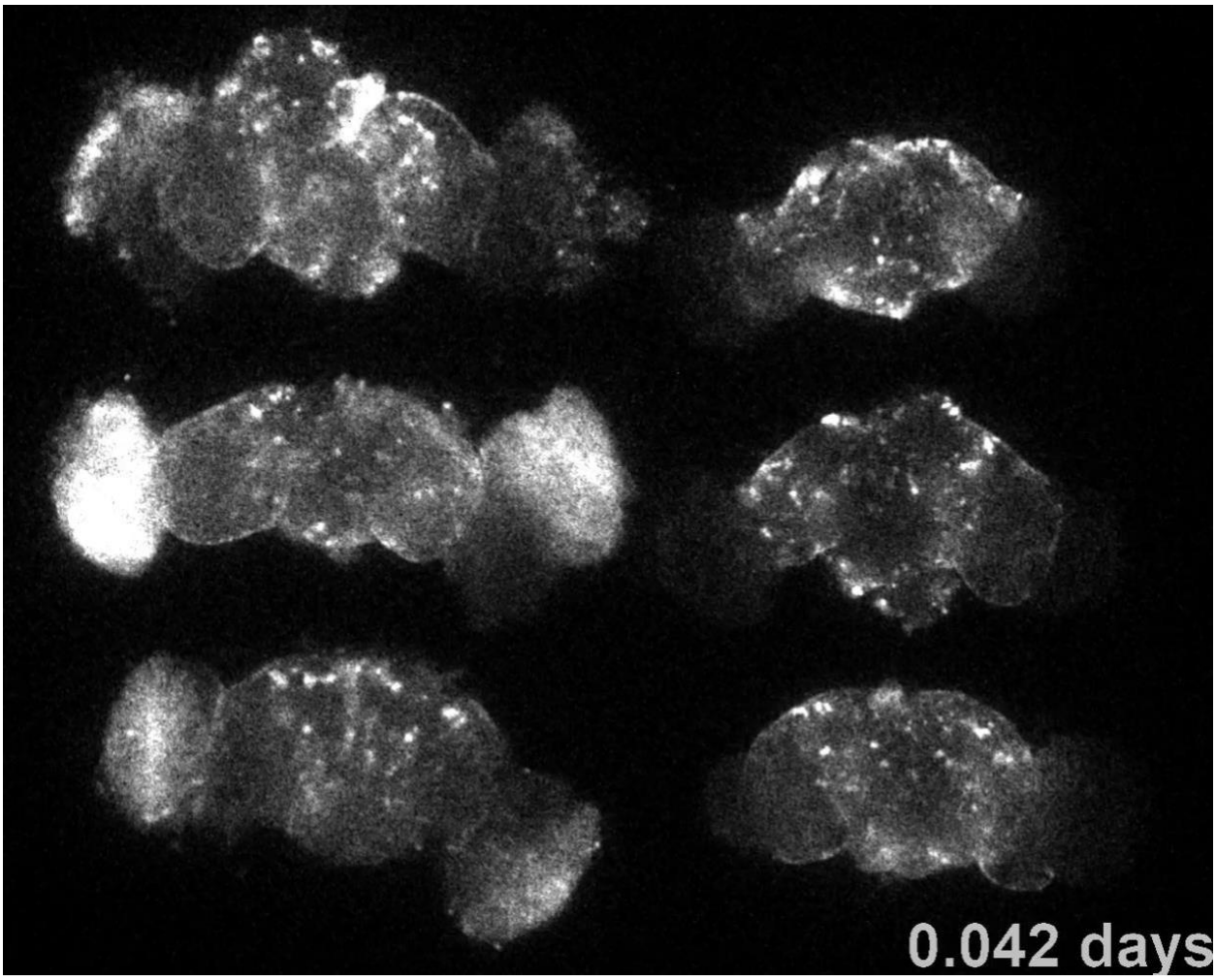

Movie S5: Raw time-lapse recordings of adult XLG-Per-Luc *Drosophila* whole-brain explants comparing bioluminescence of brains with and without compound eyes in CTRL LD. Left: three whole brain culture explants with compound eyes attached maintained in control conditions (*LD Strobe* with no phase shift) for 9 days followed by 2 days of constant darkness (DD). Right: three whole brain culture explants with compound eyes removed maintained in control conditions (*LD Strobe* with no phase shift) for 9 days followed by 2 days of constant darkness (DD). See Materials and Methods for more details.

2.6 Discussion

Well-established work on skeleton photoperiods inspired us to test fragmented light/dark periods that permit bioluminescence imaging without disruption of the circadian clock [1,2]. Based on the strict criteria of no measurable differences in circadian free running behavior, the *LD Strobe* light schedule faithfully replicates standard 12h:12h light-dark cycles. Our whole-circuit imaging using *LD Strobe* provides longitudinal multi-day bioluminescence recordings of the entire circadian neural network at single-cell resolution with reporters for PER and TIM. The relative phase peaks of PER and TIM are separated by approximately 3 hours, consistent with very highly time resolved immunocytochemical (ICC) “snapshots” for anti-PER and anti-TIM taken at one hour intervals that show sequential nuclear accumulation of PER and TIM [122]. The relative phasing of PER and TIM is one of many independent lines of evidence that the clock reporter cycling in whole brain reflect the in vivo circadian clock circuit. In a previous study, we compared a matrix of whole brain imaged PER cycles of five different circadian neuronal sub-groups (sLNv, lLNv, LNd, DN1 and DN3) with six different time matched light conditions that were strategically chosen to test predictions of PER peaks or troughs across 3 days with anti-PER ICC analysis of brains collected from behaving flies. Our detailed whole brain dynamic PER cycling results predicted all less time resolved ICC results for the 5 x 6 matrix, with a statistical confidence value of 10^{-27} [95]. LL rapidly induces circadian behavioral rhythmicity [2,35,123]. Circadian rhythmicity in LL is preserved in mutant flies lacking functional CRY [27,117,124]. In close agreement with these well characterized LL *in vivo* behavioral responses, PER-cycling rapidly dampens throughout the circadian circuit in response to LL exposure in imaged whole brains, thus providing another line of

validation for the whole brain imaging method. In *cryb* mutants, circadian circuit persistence of PER cycling occurs in LL, centered in the DN1 cell group and to a lesser degree in the LNds. This result is noteworthy as the DN1s act as output neurons for the circadian circuit [125,126]. Thus, whole brain imaged PER cycling responses to LL are validated by both genetic and environment challenges to the circadian circuit as compared to in vivo behavioral responses. Environmental light shift conditions that closely approximate WLS coincide with the disruption of the circadian regulated behavioral of sleep and learning and memory *in vivo* (more below), thus showing strong linkage between the imaged whole brain PER cycling and in vivo behavior for all measures tested.

Under simulated LD cycles, we obtained detailed circuit responses to unshifted regular light: dark cycles and light shifts approximating weekday and weekend light shift conditions. We find coherent mean circadian network phase in response to alternating light pulses of *LD Strobe*. This indicates that properly timed Zeitgebers at the start and end of daytime hours, with standard night-time darkness are the most critical light input features for proper entrainment, consistent with earlier studies employing skeleton photoperiod protocols [2]. In contrast, oscillators exhibit immediate damping in rhythmicity and synchrony when transitioning from LD to DD indicating that steady photoentrainment is critical for maintenance of robust oscillator synchrony and physiological rhythmicity [95,108].

Different anatomically defined subgroups of circadian neuronal oscillators exhibit differences in timing in response, varying degrees of change in inter- and intra-subgroup synchrony and amplitude and timing of recovery in response the WLS phase delay followed by a light phase advance days later. Single-cell resolution analysis reveals that

rhythmicity and synchrony in s-LNvs, l-LNvs, and LNds immediately dampens by initial “Friday” phase delay to mark the start of WLS. Taking the LD and DD data together, the s-LNVs are the most stable of all circadian subgroups in the absence of light shifts but are most labile in response to changes in light entrainment evoking the “first out, last back in” phase destabilization [108]. In contrast, DN1s while showing light-induced phase shifts, maintain greater rhythmicity and synchrony in response to the phase delays. Surprisingly, the DN3s increase their synchrony in response to phase delays in addition to the striking reduction in oscillator amplitude variance. LNds and the light blind DN3s immediately restore rhythmicity faster than other subgroups after exposure to a simulated weekend. Remarkably, the DN3s increase in phase synchrony and amplitude coherence during and after WLS entrainment. The DN3s could code for the initial time phase before light induced shift to a new phase, thus acting as a temporal placeholder. The LNds and DN3s may play a critical role in prompting the remaining circadian neural network into a new state of adaptation of the phase-shifted synchrony, consistent with earlier evidence indicating LNDs track phase-advance shifts more rapidly than other subgroups [95,108].

Furthermore, light input from external photoreceptors, such as the compound eye, also modulate clock entrainment [106]. Light from either input channel in the absence of the other (CRY/Rh7 versus external opsin expressing photoreceptors) yields identical behavioral light circadian phase shift responses [20,106], indicating these input channels are functionally redundant and the circadian circuit likely encodes their input in a similar if not identical fashion. Electrophysiological light responses can be recorded in circadian neurons using light stimulus parameters that are optimized for opsin activation in eyes but are insufficient in duration (and perhaps amplitude) for CRY activation (Li et al., 2018;

see Baik et al., 2019 for detailed light parameters for CRY activation). As expected, we find that overall circuit entrainment by direct light is comparable whether the compound eye is present or is completely removed. This confirms the functional redundancy of internal cell autonomous photoreceptors and external opsin-based photoreceptors.

The significant loss in amplitude and synchrony between oscillators following WLS relative to CTRL transitioning to DD suggests long-lasting residual circadian circuit instability is masked by light inputs into the neural circuit. Together, the data show long-lasting desynchrony of the circadian circuit during and after phase delays and advances of the WLS “weekend.” The circadian circuit is likely destabilized for the greater part of the week for individuals that shift every weekend as a matter of lifestyle. Considering the correlative defects in post-WLS sleep stability, learning, and memory, this poses the critical question of whether these defects are cumulative and can be detrimental over time. Phase shifts due to “jetlag” disrupt the timing of both arousal/wake and sleep. Circadian neurons functionally segregate to control arousal (s-LNvs, l-LNvs) versus sleep (DN1s) [14,38,59,127]. *In vivo* luciferase calcium monitoring at circadian neuronal subgroup spatial and temporal resolution confirms that the s-LNv and l-LNv intracellular calcium signaling exhibit biphasic morning and late day peaks corresponding to arousal while a subset DN1s coincide highest intracellular calcium levels with sleep [59,128]. This innovative imaging approach yields robust records of circadian signal transduction occurring in these neurons in the absence of potential contaminations from light excitation necessary for fluorescence imaging.

Circadian clocks regulate numerous aspects daily animal physiology and behavior. Light is the primary environmental zeitgeber for circadian entrainment for many animals,

including *Drosophila* [106] and humans [129]. Many humans have increased their exposure to artificial light starting with the invention of electric light, now accelerated by increasing expose to screened devices, thus leading to misalignment of circadian clocks to the external environment [130]. In adolescents, this weekly weekday-to-weekend light shifts in sleep-wake cycles are chronic, and prevalent, with light shifts lasting from 3 hours or more [94].

Light shift conditions that closely approximate WLS lead to persistent desynchrony in most of the adult *Drosophila* circadian neural network measured at the single-cell resolution for over a simulated week *ex vivo* strongly coincides with the disruption of circadian regulated behavioral outputs *in vivo*. Adult flies exposed to WLS exhibit transient defects in memory, learning, and sleep stability between 5-6 days of the week. This suggests that for weekly repeated WLS, functional consequences downstream to circadian desynchrony are present during most days of the week. The detriments of clock disruption through light shifts may underlie more severe complications due to cumulative weekly repetitions that may span throughout an individual's life. Based on the many molecular and circuit-circuit organizational similarities between *Drosophila* and mammals, the circadian neural network responses we measure to weekend light shift conditions may be instructive for understanding light shifts in humans and other animals.

2.7 References

1. Pittendrigh, C.S., and Minis, D. (1964). The Entrainment of Circadian Oscillations by Light and Their Role as Photoperiodic Clocks Colin. Am. Nat. *98*, 261–294.

2. Pittendrigh, C.S., and Daan, S. (1976). A functional analysis of circadian pacemakers in nocturnal rodents. J. Comp. Physiol. A *106*, 223–252. Available at: http://link.springer.com/article/10.1007/BF01417860%5Cnhttp://link.springer.com/content/pdf/10.1007/BF01417860.pdf%5Cnhttp://link.springer.com/10.1007/BF01417860 [Accessed May 4, 2018].

3. Obholz, K.L., Akopyan, A., Waymire, K.G., and MacGregor, G.R. (2006). FNDC3A is required for adhesion between spermatids and Sertoli cells. Dev. Biol. *298*, 498–513.

4. Carrouel, F., Couble, M.-L., Vanbelle, C., Staquet, M.-J., Magloire, H., and Bleicher, F. (2008). HUGO (FNDC3A): a new gene overexpressed in human odontoblasts. J. Dent. Res. *87*, 131–6. Available at: http://www.ncbi.nlm.nih.gov/pubmed/18218838 [Accessed February 6, 2020].

5. Rivas, G.B.S., Teles-de-Freitas, R., Pavan, M.G., Lima, J.B.P., Peixoto, A.A., and Bruno, R.V. (2018). Effects of Light and Temperature on Daily Activity and Clock Gene Expression in Two Mosquito Disease Vectors. J. Biol. Rhythms *33*, 272–288. Available at: http://www.ncbi.nlm.nih.gov/pubmed/29761749 [Accessed August 3, 2020].

6. Syed, A., Lukacsovich, T., Pomeroy, M., Bardwell, A.J., Decker, G.T., Waymire, K.G., Purcell, J., Huang, W., Gui, J., Padilla, E.M., *et al.* (2019). Miles to go (mtgo)

encodes FNDC3 proteins that interact with the chaperonin subunit CCT3 and are required for NMJ branching and growth in Drosophila. Dev. Biol. *445*, 37–53. Available at: https://linkinghub.elsevier.com/retrieve/pii/S0012160618303178 [Accessed December 16, 2018].

7. Ke, J., Zhao, Z., Hong, S.H., Bai, S., He, Z., Malik, F., Xu, J., Zhou, L., Chen, W., Martin-Trevino, R., *et al.* (2015). Role of microRNA221 in regulating normal mammary epithelial hierarchy and breast cancer stem-like cells. Oncotarget *6*, 3709–3721.

8. Yoshii, T., Hermann-Luibl, C., and Helfrich-Föorster, C. (2016). Circadian light-input pathways in Drosophila. Commun. Integr. Biol. *9*.

9. Pavel, M., Imarisio, S., Menzies, F.M., Jimenez-Sanchez, M., Siddiqi, F.H., Wu, X., Renna, M., O'Kane, C.J., Crowther, D.C., and Rubinsztein, D.C. (2016). CCT complex restricts neuropathogenic protein aggregation via autophagy. Nat. Commun. *7*, 1–18.

10. Welsh, D.K., Logothetis, D.E., Meister, M., and Reppert, S.M. (1995). Individual neurons dissociated from rat suprachiasmatic nucleus express independently phased circadian firing rhythms. Neuron *14*, 697–706. Available at: http://journals.sagepub.com/doi/10.1177/0748730419877315 [Accessed October 16, 2019].

11. Yam, A.Y., Xia, Y., Lin, H.T.J., Burlingame, A., Gerstein, M., and Frydman, J. (2008). Defining the TRiC/CCT interactome links chaperonin function to stabilization of newly made proteins with complex topologies. Nat. Struct. Mol.

Biol. *15*, 1255–1262.

12. Roenneberg, T., Allebrandt, K. V, Merrow, M., Line Vetter, C., and Vetter, C. (2012). Social jetlag and obesity. Curr. Biol. *22*, 939–43. Available at: http://www.ncbi.nlm.nih.gov/pubmed/22578422 [Accessed October 25, 2017].

13. Gao, Y., Thomas, J.O., Chow, R.L., Lee, G.H., and Cowan, N.J. (1992). A cytoplasmic chaperonin that catalyzes β-actin folding. Cell *69*, 1043–1050. Available at: https://linkinghub.elsevier.com/retrieve/pii/009286749290622J [Accessed February 21, 2020].

14. Shang, Y., Griffith, L.C., and Rosbash, M. (2008). Light-arousal and circadian photoreception circuits intersect at the large PDF cells of the Drosophila brain. Proc. Natl. Acad. Sci. *105*, 19587–19594. Available at: http://www.pnas.org/content/105/50/19587%5Cnhttp://www.ncbi.nlm.nih.gov/pubmed/19060186%5Cnhttp://www.pnas.org/content/105/50/19587.full.pdf%5Cnhttp://www.pnas.org/content/105/50/19587.short.

15. Hartl, F.U., and Hayer-Hartl, M. (2002). Protein folding. Molecular chaperones in the cytosol: From nascent chain to folded protein. Science (80-.). *295*, 1852–1858.

16. Renn, S.C.P., Park, J.H., Rosbash, M., Hall, J.C., and Taghert, P.H. (1999). A pdf neuropeptide gene mutation and ablation of PDF neurons each cause severe abnormalities of behavioral circadian rhythms in Drosophila. Cell *99*, 791–802.

17. Joachimiak, L.A., Walzthoeni, T., Liu, C.W., Aebersold, R., and Frydman, J. (2014). The structural basis of substrate recognition by the eukaryotic chaperonin

TRiC/CCT. Cell *159*, 1042–1055.

18. Fogle, K.J., Baik, L.S., Houl, J.H., Tran, T.T., Roberts, L., Dahm, N.A., Cao, Y., Zhou, M., and Holmes, T.C. (2015). CRYPTOCHROME-mediated phototransduction by modulation of the potassium ion channel β-subunit redox sensor. Proc. Natl. Acad. Sci.

19. Sheeba, V., Sharma, V.K., Gu, H., Chou, Y.T., O'Dowd, D.K., and Holmes, T.C. (2008). Pigment dispersing factor-dependent and -independent circadian locomotor behavioral rhythms. J. Neurosci. *28*, 217–227.

20. Ni, J.D., Baik, L.S., Holmes, T.C., and Montell, C. (2017). A rhodopsin in the brain functions in circadian photoentrainment in Drosophila. Nature *545*, 340–344. Available at: http://www.nature.com/doifinder/10.1038/nature22325 [Accessed May 4, 2018].

21. Nitabach, M.N., Wu, Y., Sheeba, V., Lemon, W.C., Strumbos, J., Zelensky, P.K., White, B.H., and Holmes, T.C. (2006). Electrical hyperexcitation of lateral ventral pacemaker neurons desynchronizes downstream circadian oscillators in the fly circadian circuit and induces multiple behavioral periods. J. Neurosci. *26*, 479–489.

22. Baik, L.S., Recinos, Y., Chevez, J.A., and Holmes, T.C. (2018). Circadian modulation of light-evoked avoidance/attraction behavior in Drosophila. PLoS One *13*, e0201927. Available at: https://dx.plos.org/10.1371/journal.pone.0201927 [Accessed August 3, 2020].

23. Qiu, J., and Hardin, P.E. (1996). Developmental state and the circadian clock

interact to influence the timing of eclosion in Drosophila melanogaster. J. Biol. Rhythms *11*, 75–86.

24. Skopik, S.D., and Pittendrigh, C.S. (1967). Circadian systems, II. The oscillation in the individual Drosophila pupa; its independence of developmental stage. PNAS *58*, 1862–1869.

25. Veleri, S., Brandes, C., Helfrich-Förster, C., Hall, J.C., and Stanewsky, R. (2003). A Self-Sustaining, Light-Entrainable Circadian Oscillator in the Drosophila Brain. Curr. Biol. *13*, 1758–1767. Available at: https://www.sciencedirect.com/science/article/pii/S0960982203006997 [Accessed June 4, 2018].

26. Blanchardon, E., Grima, B., Klarsfeld, A., Chélot, E., Hardin, P.E., Préat, T., and Rouyer, F. (2001). Defining the role of Drosophila lateral neurons in the control of circadian rhythms in motor activity and eclosion by targeted genetic ablation and PERIOD protein overexpression. Eur. J. Neurosci. *13*, 871–888.

27. Emery, P., Stanewsky, R., Hall, J.C., and Rosbash, M. (2000). A unique circadian-rhythm photoreceptor. *404*, 456–457.

28. Myers, E.M., Jiujiu, Y., and Sehgal, A. (2003). Circadian Control of Eclosion: Interaction between a Central and Peripheral Clock in Drosophila melanogaster. Curr. Biol. *13*, 526–533.

29. Baik, L.S., Recinos, Y., Chevez, J.A., Au, D.D., and Holmes, T.C. (2019). Multiple Phototransduction Inputs Integrate to Mediate UV Light–evoked Avoidance/Attraction Behavior in Drosophila. J. Biol. Rhythms *34*, 391–400.

Available at: http://journals.sagepub.com/doi/10.1177/0748730419847339 [Accessed August 3, 2020].

30. Baik, L.S., Recinos, Y., Chevez, J.A., Au, D.D., and Holmes, T.C. (2019). Multiple Phototransduction Inputs Integrate to Mediate UV Light–evoked Avoidance/Attraction Behavior in Drosophila. J. Biol. Rhythms *34*, 391–400.

31. Kistenpfennig, C., Grebler, R., Ogueta, M., Hermann-Luibl, C., Schlichting, M., Stanewsky, R., Senthilan, P.R., and Helfrich-Förster, C. (2017). A New Rhodopsin Influences Light-dependent Daily Activity Patterns of Fruit Flies. J. Biol. Rhythms *32*, 406–422.

32. Renn, S.C.P., Park, J.H., Rosbash, M., Hall, J.C., and Taghert, P.H. (1999). A pdf neuropeptide gene mutation and ablation of PDF neurons each cause severe abnormalities of behavioral circadian rhythms in Drosophila. Cell *99*, 791–802.

33. Nitabach, M.N., Blau, J., and Holmes, T.C. (2002). Electrical Silencing of Drosophila Pacemaker Neurons Stops the Free-Running Circadian Clock An important area of circadian rhythm research is the relationship between the function of the molecular clock in pacemaker neurons and the central physiological. Cell *109*, 485–495. Available at: https://ac.els-cdn.com/S0092867402007377/1-s2.0-S0092867402007377-main.pdf?_tid=191a407f-2f36-4e51-b468-c0c04bc18151&acdnat=1520814518_8b6e01a8d692d51fc76ec3f96a9757e8.

34. Peschel, N., Chen, K.F., Szabo, G., and Stanewsky, R. (2009). Light-dependent interactions between the Drosophila circadian clock factors cryptochrome, jetlag,

and timeless. Curr. Biol. *19*, 241–7. Available at: http://www.sciencedirect.com/science/article/pii/S0960982208016977 [Accessed January 19, 2016].

35. Baik, L.S., Recinos, Y., Chevez, J.A., and Holmes, T.C. (2018). Circadian modulation of light-evoked avoidance/attraction behavior in Drosophila. PLoS One *13*, 1–14.

36. Fogle, K.J., Parson, K.G., Dahm, N.A., and Holmes, T.C. (2011). CRYPTOCHROME Is a Blue-Light Sensor That Regulates Neuronal Firing Rate. Science (80-.).

37. Collins, B., Mazzoni, E.O., Stanewsky, R., and Blau, J. (2006). Drosophila CRYPTOCHROME is a circadian transcriptional repressor. Curr. Biol. *16*, 441–449.

38. Sheeba, V., Fogle, K.J., Kaneko, M., Rashid, S., Chou, Y.-T., Sharma, V.K., and Holmes, T.C. (2008). Large ventral lateral neurons modulate arousal and sleep in Drosophila. Curr. Biol. *18*, 1537–45. Available at: http://www.pubmedcentral.nih.gov/articlerender.fcgi?artid=2597195&tool=pmcentrez&rendertype=abstract.

39. Konopka, R.J., and Benzer, S. (1971). Clock Mutants of Drosophila melanogaster. Proc. Natl. Acad. Sci. *68*, 2112–2116. Available at: https://www.pnas.org/content/68/9/2112 [Accessed August 3, 2020].

40. Agrawal, P., Houl, J.H., Gunawardhana, K.L., Liu, T., Zhou, J., Zoran, M.J., and Hardin, P.E. (2017). Drosophila CRY Entrains Clocks in Body Tissues to Light

and Maintains Passive Membrane Properties in a Non-clock Body Tissue Independent of Light. Curr. Biol. *27*, 2431-2441.e3. Available at: http://dx.doi.org/10.1016/j.cub.2017.06.064.

41. Myers, M.P., Wager-Smith, K., Wesley, C.S., Young, M.W., and Sehgal, A. (1995). Positional cloning and sequence analysis of the Drosophila clock gene, timeless. Science (80-.). *270*, 805–808. Available at: https://science.sciencemag.org/content/270/5237/805 [Accessed August 2, 2020].

42. Emery, P., Stanewsky, R., Helfrich-Förster, C., Emery-Le, M., Hall, J.C., and Rosbash, M. (2000). Drosophila CRY is a deep brain circadian photoreceptor. Neuron *26*, 493–504.

43. Allada, R., White, N.E., So, W.V., Hall, J.C., and Rosbash, M. (1998). A mutant Drosophila homolog of mammalian clock disrupts circadian rhythms and transcription of period and timeless. Cell *93*, 791–804.

44. Nitabach, M.N., Blau, J., and Holmes, T.C. (2002). Electrical silencing of Drosophila pacemaker neurons stops the free-running circadian clock. Cell *109*, 485–495.

45. Potdar, S., and Sheeba, V. (2018). Wakefulness is promoted during day time by PDFR signalling to dopaminergic neurons in Drosophila melanogaster. eNeuro *5*. Available at: /pmc/articles/PMC6102377/?report=abstract [Accessed August 2, 2020].

46. Park, J.H. (2000). Differential regulation of circadian pacemaker output by separate clock genes in Drosophila. Proc. Natl. Acad. Sci. *97*, 3608–3613.

Available at: http://www.pnas.org/cgi/doi/10.1073/pnas.070036197.

47. Im, S.H., Li, W., and Taghert, P.H. (2011). Pdfr and cry signaling converge in a subset of clock neurons to modulate the amplitude and phase of circadian behavior in Drosophila. PLoS One *6*.

48. Konopka, R.J., and Benzer, S. (1971). Clock mutants of Drosophila melanogaster. Proc. Natl. Acad. Sci. U. S. A. *68*, 2112–2116.

49. Hyun, S., Lee, Y., Hong, S.-T., Bang, S., Paik, D., Kang, J., Shin, J., Lee, J., Jeon, K., Hwang, S., *et al.* (2005). Drosophila GPCR Han Is a Receptor for the Circadian Clock Neuropeptide PDF. Neuron *48*, 267–278.

50. Baik, L.S., Fogle, K.J., Roberts, L., Galschiodt, A.M., Chevez, J.A., Recinos, Y., Nguy, V., and Holmes, T.C. (2017). CRYPTOCHROME mediates behavioral executive choice in response to UV light. Proc. Natl. Acad. Sci.

51. Grima, B., Chélot, E., Xia, R., and Rouyer, F. (2004). Morning and evening peaks of activity rely on different clock neurons of the Drosophila brain. Nature *431*, 869–873.

52. Im, S.H., and Taghert, P.H. (2010). PDF receptor expression reveals direct interactions between circadian oscillators in drosophila. J. Comp. Neurol. *518*, 1925–1945.

53. Helfrich-Förster, C. (2003). The neuroarchitecture of the circadian clock in the brain of Drosophila melanogaster. Microsc. Res. Tech. *62*, 94–102.

54. Myers, M.P., Wager-Smith, K., Rothenfluh-Hilfiker, A., Young, M.W., Myers, M.P.,

Wager-smith, K., Rothenfluh-hilfiker, A., and Young, M.W. (1996). Light-Induced Degradation of TIMELESS and Entrainment of the Drosophila Circadian Clock Published by : American Association for the Advancement of Science Stable URL : http://www.jstor.org/stable/2890841 JSTOR is a not-for-profit service that helps schola. Science (80-.). *271*, 1736–1740.

55. Murad, A., Emery-Le, M., and Emery, P. (2007). A Subset of Dorsal Neurons Modulates Circadian Behavior and Light Responses in Drosophila. Neuron *53*, 689–701.

56. Baik, L.S., Nave, C., Au, D.D., Guda, T., Chevez, J.A., Ray, A., and Holmes, T.C. (2020). Circadian Regulation of Light-Evoked Attraction and Avoidance Behaviors in Daytime- versus Nighttime-Biting Mosquitoes. Curr. Biol.

57. Kunst, M., Hughes, M.E., Raccuglia, D., Felix, M., Li, M., Barnett, G., Duah, J., and Nitabach, M.N. (2014). Calcitonin gene-related peptide neurons mediate sleep-specific circadian output in Drosophila. Curr. Biol. *24*, 2652–2664. Available at: http://dx.doi.org/10.1016/j.cub.2014.09.077.

58. Rhoades, S.D., Nayak, K., Zhang, S.L., Sehgal, A., and Weljie, A.M. (2018). Circadian- and Light-driven Metabolic Rhythms in Drosophila melanogaster. J. Biol. Rhythms *33*.

59. Guo, F., Yu, J., Jung, H.J., Abruzzi, K.C., Luo, W., Griffith, L.C., and Rosbash, M. (2016). Circadian neuron feedback controls the Drosophila sleep-activity profile. Nature *536*, 292–297. Available at: http://www.nature.com/articles/nature19097 [Accessed August 24, 2018].

60. Zhang, L., Chung, B.Y., Lear, B.C., Kilman, V.L., Liu, Y., Mahesh, G., Meissner, R.A., Hardin, P.E., and Allada, R. (2010). DN1p Circadian Neurons Coordinate Acute Light and PDF Inputs to Produce Robust Daily Behavior in Drosophila. Curr. Biol. *20*, 591–599. Available at: http://dx.doi.org/10.1016/j.cub.2010.02.056.

61. Vecsey, C.G., Pirez, N., and Griffith, L.C. (2014). The Drosophila neuropeptides PDF and sNPF have opposing electrophysiological and molecular effects on central neurons. J. Neurophysiol. *111*, 1033–1045. Available at: http://jn.physiology.org/cgi/doi/10.1152/jn.00712.2013.

62. Hall, J.C. (2005). Systems approaches to biological rhythms in Drosophila. Methods Enzymol. *393*, 61–185. Available at: http://www.sciencedirect.com/science/article/pii/S0076687905930048 [Accessed January 19, 2016].

63. Im, S.H., Li, W., and Taghert, P.H. (2011). PDFR and CRY Signaling Converge in a Subset of Clock Neurons to Modulate the Amplitude and Phase of Circadian Behavior in Drosophila. PLoS One *6*, e18974. Available at: https://dx.plos.org/10.1371/journal.pone.0018974 [Accessed August 2, 2020].

64. Harper, R.E.F., Ogueta, M., Dayan, P., Stanewsky, R., and Albert, J.T. (2017). Light Dominates Peripheral Circadian Oscillations in Drosophila melanogaster During Sensory Conflict. J. Biol. Rhythms *32*, 423–432. Available at: http://www.ncbi.nlm.nih.gov/pubmed/28903626 [Accessed July 21, 2020].

65. Rieger, D., Shafer, O.T., Tomioka, K., and Helfrich-Förster, C. (2006). Functional analysis of circadian pacemaker neurons in Drosophila melanogaster. J.

Neurosci. *26*, 2531–2543. Available at: http://rsb.info.nih.gov/ij/ [Accessed August 3, 2020].

66. Hyun, S., Lee, Y., Hong, S.T., Bang, S., Paik, D., Kang, J., Shin, J., Lee, J., Jeon, K., Hwang, S., *et al.* (2005). Drosophila GPCR han is a receptor for the circadian clock neuropeptide PDF. Neuron *48*, 267–278.

67. Mertens, I., Vandingenen, A., Johnson, E.C., Shafer, O.T., Li, W., Trigg, J.S., De Loof, A., Schoofs, L., and Taghert, P.H. (2005). PDF receptor signaling in Drosophila contributes to both circadian and geotactic behaviors. Neuron *48*, 213–219. Available at: https://www.sciencedirect.com/science/article/pii/S0896627305007762 [Accessed August 24, 2018].

68. Benito, J., Houl, J.H., Roman, G.W., and Hardin, P.E. (2008). The blue-light photoreceptor CRYPTOCHROME is expressed in a subset of circadian oscillator neurons in the Drosophila CNS. J. Biol. Rhythms *23*, 296–307. Available at: http://journals.sagepub.com/doi/10.1177/0748730408318588 [Accessed May 4, 2018].

69. Yoshii, T., Todo, T., Wülbeck, C., Stanewsky, R., and Helfrich-Förster, C. (2008). Cryptochrome is present in the compound eyes and a subset ofDrosophila's clock neurons. J. Comp. Neurol. *508*, 952–966. Available at: http://doi.wiley.com/10.1002/cne.21702 [Accessed June 4, 2018].

70. Moore-Ede, M.C., Czeisler, C.A., and Richardson, G.S. (1983). Circadian Timekeeping in Health and Disease. N. Engl. J. Med. *309*, 469–476. Available at:

http://www.nejm.org/doi/abs/10.1056/NEJM198308253090806 [Accessed May 4, 2018].

71. Hastings, M.H., Reddy, A.B., and Maywood, E.S. (2003). A clockwork web: circadian timing in brain and periphery, in health and disease. Nat. Rev. Neurosci. *4*, 649–661. Available at: http://www.nature.com/articles/nrn1177 [Accessed May 4, 2018].

72. Scheer, F.A.J.L., Hilton, M.F., Mantzoros, C.S., and Shea, S.A. (2009). Adverse metabolic and cardiovascular consequences of circadian misalignment. Proc. Natl. Acad. Sci. U. S. A. *106*, 4453–4458. Available at: http://www.pnas.org/content/106/11/4453.full.pdf?with-ds=yes [Accessed October 25, 2017].

73. Filipski, E., Delaunay, F., King, V.M., Wu, M.W., Claustrat, B., Gréchez-Cassiau, A., Guettier, C., Hastings, M.H., and Francis, L. (2004). Effects of chronic jet lag on tumor progression in mice. Cancer Res. *64*, 7879–7885. Available at: http://www.ncbi.nlm.nih.gov/pubmed/14612524 [Accessed October 25, 2017].

74. Aschoff, J. (1984). Circadian timing. Ann. N. Y. Acad. Sci. *423*, 442–68. Available at: http://www.ncbi.nlm.nih.gov/pubmed/6588808 [Accessed August 23, 2018].

75. Labrecque, N., and Cermakian, N. (2015). Circadian Clocks in the Immune System. J. Biol. Rhythms *30*, 277–290. Available at: http://journals.sagepub.com/doi/10.1177/0748730415577723 [Accessed August 23, 2018].

76. Hardin, P.E. The Circadian Timekeeping System of Drosophila. Available at:

https://ac.els-cdn.com/S0960982205009395/1-s2.0-S0960982205009395-main.pdf?_tid=c2ef38aa-bc1a-11e7-8466-00000aacb360&acdnat=1509221058_aa45ab1663c2fc7fea4d9e4432809336 [Accessed October 25, 2017].

77. Mimi Lee, W.-C., Yoshihara, M., and Troy Littleton, J. Cytoplasmic aggregates trap polyglutamine- containing proteins and block axonal transport in a Drosophila model of Huntington's disease. Available at: http://www.pnas.org/content/101/9/3224.full.pdf [Accessed September 12, 2017].

78. Morton, A.J. (2005). Disintegration of the Sleep-Wake Cycle and Circadian Timing in Huntington's Disease. J. Neurosci. *25*, 157–163. Available at: http://www.jneurosci.org/cgi/doi/10.1523/JNEUROSCI.3842-04.2005.

79. Askenasy, J.J.M. (2001). Approaching disturbed sleep in late Parkinson's disease: First step toward a proposal for a revised UPDRS. Park. Relat. Disord. *8*, 123–131.

80. Hatfield, C.F., Herbert, J., Van Someren, E.J.W., Hodges, J.R., and Hastings, M.H. (2004). Disrupted daily activity/rest cycles in relation to daily cortisol rhythms of home-dwelling patients with early Alzheimer's dementia. Brain *127*, 1061–1074.

81. Kaneko, M., Helfrich-Förster, C., and Hall, J.C. (1997). Spatial and temporal expression of the period and timeless genes in the developing nervous system of drosophila: Newly identified pacemaker candidates and novel features of clock gene product cycling. J. Neurosci. *17*, 6745–6760.

82. Kaneko, M., and Hall, J.C. (2000). Neuroanatomy of cells expressing clock genes in Drosophila: Transgenic manipulation of the period and timeless genes to mark the perikarya of circadian pacemaker neurons and their projections. J. Comp. Neurol. *422*, 66–94.

83. Beckwith, E.J., and Ceriani, M.F. (2015). Communication between circadian clusters: The key to a plastic network. FEBS Lett. *589*, 3336–3342. Available at: http://dx.doi.org/10.1016/j.febslet.2015.08.017.

84. Nitabach, M.N., and Taghert, P.H. (2008). Organization of the Drosophila Circadian Control Circuit. Curr. Biol. *18*, 84–93.

85. Ueda, H.R., Hayashi, S., Chen, W., Sano, M., Machida, M., Shigeyoshi, Y., Iino, M., and Hashimoto, S. (2005). System-level identification of transcriptional circuits underlying mammalian circadian clocks. Nat. Genet. *37*, 187–192.

86. Tei, H., Okamura, H., and Shigeyoshi, Y. (1997). Circadian oscillation of a mammalian homologue of the Drosophila period gene. *389*, 512–516.

87. Allada, R., Emery, P., Takahashi, J.S., and Rosbash, M. (2001). Stopping time: the genetics of fly and mouse circadian clocks. Annu. Rev. Neurosci. *24*, 1091–1119.

88. Duong, H.A., Robles, M.S., Knutti, D., and Weitz, C.J. (2011). A molecular mechanism for circadian clock negative feedback. Science (80-.). *332*, 1436–9.

89. Gonze, D., Bernard, S., Waltermann, C., Kramer, A., and Herzel, H. (2005). Spontaneous synchronization of coupled circadian oscillators. Biophys. J. *89*,

120–9.

90. Stanewsky, R., Kaneko, M., Emery, P., Beretta, B., Wager-Smith, K., Kay, S.A., Rosbash, M., and Hall, J.C. (1998). The cryb Mutation Identifies Cryptochrome as a Circadian Photoreceptor in Drosophila. Cell *95*, 681–692.

91. Hunter-Ensor, M., Ousley, A., and Sehgal, A. (1996). Regulation of the Drosophila protein timeless suggests a mechanism for resetting the circadian clock by light. Cell *84*, 677–685.

92. Zeng, H., Qian, Z., Myers, M.P., and Rosbash, M. (1996). A light-entrainment mechanism for the drosophila circadian clock. Nature *380*, 129–135. Available at: http://www.nature.com/doifinder/10.1038/380129a0 [Accessed August 24, 2018].

93. Sheeba, V. (2008). The Drosophila melanogaster circadian pacemaker circuit. J. Genet. *87*, 485–493.

94. Crowley, S.J., Acebo, C., and Carskadon, M.A. (2007). Sleep, circadian rhythms, and delayed phase in adolescence. Sleep Med. *8*, 602–612. Available at: http://www.ncbi.nlm.nih.gov/pubmed/17383934 [Accessed June 4, 2018].

95. Roberts, L., Leise, T.L.L., Noguchi, T., Galschiodt, A.M.M., Houl, J.H.H., Welsh, D.K.K., and Holmes, T.C.C. (2015). Light Evokes Rapid Circadian Network Oscillator Desynchrony Followed by Gradual Phase Retuning of Synchrony. Curr. Biol. *25*, 858–867. Available at: http://www.ncbi.nlm.nih.gov/pubmed/25754644 [Accessed May 4, 2018].

96. Papagiannakopoulos, T., Bauer, M.R., Davidson, S.M., Heimann, M., Subbaraj,

L., Bhutkar, A., Bartlebaugh, J., Vander Heiden, M.G., and Jacks, T. (2016). Circadian Rhythm Disruption Promotes Lung Tumorigenesis. Cell Metab. *24*, 324–331. Available at: http://dx.doi.org/10.1016/j.cmet.2016.07.001 [Accessed September 12, 2017].

97. Hamada, T., LeSauter, J., Venuti, J.M., and Silver, R. (2001). Expression of period genes: Rhythmic and nonrhythmic compartments of the suprachiasmatic nucleus pacemaker. J. Neurosci. *21*, 7742–7750.

98. Yamaguchi, S., Isejima, H., Matsuo, T., Okura, R., Yagita, K., Kobayashi, M., and Okamura, H. (2003). Synchronization of Cellular Clocks in the Suprachiasmatic Nucleus. Science (80-.). *302*, 1408–1412.

99. Azzi, A., Evans, J.A., Leise, T., Myung, J., Takumi, T., Davidson, A.J., and Brown, S.A. (2017). Network Dynamics Mediate Circadian Clock Plasticity. Neuron *93*, 441–450. Available at: http://dx.doi.org/10.1016/j.neuron.2016.12.022 [Accessed December 28, 2019].

100. Evans, J.A., Leise, T.L., Castanon-Cervantes, O., and Davidson, A.J. (2013). Dynamic Interactions Mediated by Nonredundant Signaling Mechanisms Couple Circadian Clock Neurons. Neuron *80*, 973–983.

101. Quintero, J.E., Kuhlman, S.J., and McMahon, D.G. (2003). The biological clock nucleus: A multiphasic oscillator network regulated by light. J. Neurosci. *23*, 8070–8076.

102. Schaap, J., Pennartz, C.M.A., and Meijer, J.H. (2003). Electrophysiology of the circadian pacemaker in mammals. Chronobiol. Int. *20*, 171–188.

103. Moga, M.M., and Moore, R.Y. (1997). Organization of neural inputs to the suprachiasmatic nucleus in the rat. J. Comp. Neurol. *389*, 508–534.

104. Fogle, K.J., Parson, K.G., Dahm, N.A., and Holmes, T.C. (2011). Cryptochrome is a blue-light sensor that regulates neuronal firing rate. Science (80-.). *331*, 1409–1413. Available at: http://www.ncbi.nlm.nih.gov/pubmed/21385718 [Accessed May 4, 2018].

105. Sakai, K., Tsutsui, K., Yamashita, T., Iwabe, N., Takahashi, K., Wada, A., and Shichida, Y. (2017). Drosophila melanogaster rhodopsin Rh7 is a UV-to-visible light sensor with an extraordinarily broad absorption spectrum. Sci. Rep. *7*, 7349.

106. Helfrich-Förster, C., Winter, C., Hofbauer, A., Hall, J.C., and Stanewsky, R. (2001). The circadian clock of fruit flies is blind after elimination of all known photoreceptors. Neuron *30*, 249–261.

107. Li, M.-T.T., Cao, L.-H.H., Xiao, N., Tang, M., Deng, B., Yang, T., Yoshii, T., and Luo, D.-G.G. (2018). Hub-organized parallel circuits of central circadian pacemaker neurons for visual photoentrainment in Drosophila. Nat. Commun. *9*, 4247.

108. Roberts, L., Leise, T.L., Welsh, D.K., and Holmes, T.C. (2016). Functional Contributions of Strong and Weak Cellular Oscillators to Synchrony and Light-shifted Phase Dynamics. J. Biol. Rhythms *XX*, 1–15.

109. Hege, D.M., Stanewsky, R., Hall, J.C., and Giebultowicz, J.M. (1997). Rhythmic Expression of a PER-Reporter in the Malpighian Tubules of Decapitated Drosophila: Evidence for a Brain-Independent Circadian Clock. J. Biol. Rhythms

12, 300–308.

110. Zerr, D.M., Hall, J.C., Rosbash, M., and Siwicki, K.K. (1990). Circadian fluctuations of period protein immunoreactivity in the CNS and the visual system of drosophila. J. Neurosci. *10*, 2749–2762.

111. Maywood, E.S., Reddy, A.B., Wong, G.K.Y., O'Neill, J.S., O'Brien, J.A., McMahon, D.G., Harmar, A.J., Okamura, H., and Hastings, M.H. (2006). Synchronization and maintenance of timekeeping in suprachiasmatic circadian clock cells by neuropeptidergic signaling. Curr. Biol. *16*, 599–605.

112. Johard, H.A.D., Yoishii, T., Dircksen, H., Cusumano, P., Rouyer, F., Helfrich-Förster, C., and Nässel, D.R. (2009). Peptidergic clock neurons in Drosophila: Ion transport peptide and short neuropeptide F in subsets of dorsal and ventral lateral neurons. J. Comp. Neurol. *516*, 59–73.

113. Shafer, O.T., and Yao, Z. (2014). Pigment-dispersing factor signaling and circadian rhythms in insect locomotor activity. Curr. Opin. Insect Sci. *1*, 73–80. Available at: https://www.sciencedirect.com/science/article/pii/S2214574514000108 [Accessed August 24, 2018].

114. Jones, J.R., Simon, T., Lones, L., and Herzog, E.D. (2018). SCN VIP neurons are essential for normal light-mediated resetting of the circadian system. J. Neurosci. *38*, 7986–7995.

115. Seugnet, L., Suzuki, Y., Stidd, R., and Shaw, P.J. (2009). Aversive phototaxic suppression: evaluation of a short-term memory assay in *Drosophila*

melanogaster. Genes, Brain Behav. *8*, 377–389. Available at: http://doi.wiley.com/10.1111/j.1601-183X.2009.00483.x [Accessed May 4, 2018].

116. Emery, P., So, W.V., Kaneko, M., Hall, J.C., and Rosbash, M. (1998). Cry, a Drosophila clock and light-regulated cryptochrome, is a major contributor to circadian rhythm resetting and photosensitivity. Cell *95*, 669–679.

117. Dolezelova, E., Dolezel, D., and Hall, J.C. Rhythm Defects Caused by Newly Engineered Null Mutations in Drosophila's cryptochrome Gene.

118. Hendricks, J.C., Finn, S.M., Panckeri, K.A., Chavkin, J., Williams, J.A., Sehgal, A., and Pack, A.I. (2000). Rest in Drosophila is a sleep-like state. Neuron *25*, 129–138.

119. Tononi, G. (2000). Correlates of sleep and waking in Drosophila melanogaster. Science (80-.). *287*, 1834–1837.

120. Stickgold, R., Hobson, J.A., Fosse, R., and Fosse, M. (2001). Sleep, learning, and dreams: Off-line memory reprocessing. Science (80-.). *294*, 1052–1057.

121. Donlea, J.M., Thimgan, M.S., Suzuki, Y., Gottschalk, L., and Shaw, P.J. (2011). Inducing sleep by remote control facilitates memory consolidation in Drosophila. Science (80-.). *332*, 1571–1576.

122. Shafer, O.T., Rosbash, M., and Truman, J.W. (2002). Sequential nuclear accumulation of the clock proteins period and timeless in the pacemaker neurons of Drosophila melanogaster. J. Neurosci. *22*, 5946–5954.

123. Baik, L.S., Nave, C., Au, D.D., Guda, T., Chevez, J.A., Ray, A., and Holmes, T.C.

(2020). Circadian Regulation of Light-Evoked Attraction and Avoidance Behaviors in Daytime- versus Nighttime-Biting Mosquitoes. Curr. Biol., 1–8. Available at: https://doi.org/10.1016/j.cub.2020.06.010.

124. Baik, L.S., Au, D.D., Nave, C., Foden, A.J., Enrriquez-Villalva, W.K., and Holmes, T.C. (2019). Distinct mechanisms of Drosophila CRYPTOCHROME-mediated light-evoked membrane depolarization and in vivo clock resetting. Proc. Natl. Acad. Sci. U. S. A. *116*, 23339–23344.

125. Barber, A.F., Erion, R., Holmes, T.C., and Sehgal, A. (2016). Circadian and feeding cues integrate to drive rhythms of physiology in Drosophila insulin-producing cells. Genes Dev. *30*, 2596–2606.

126. Cavanaugh, D.J., Geratowski, J.D., Wooltorton, J.R.A., Spaethling, J.M., Hector, C.E., Zheng, X., Johnson, E.C., Eberwine, J.H., and Sehgal, A. (2014). Identification of a circadian output circuit for rest: Activity rhythms in drosophila. Cell *157*, 689–701.

127. Parisky, K.M., Agosto, J., Pulver, S.R., Shang, Y., Kuklin, E., Hodge, J.J.L., Kang, K., Kang, K., Liu, X., Garrity, P.A., *et al.* (2008). PDF cells are a GABA-responsive wake-promoting component of the Drosophila sleep circuit. Neuron *60*, 672–82.

128. Guo, F., Chen, X., and Rosbash, M. (2017). Temporal calcium profiling of specific circadian neurons in freely moving flies. Proc. Natl. Acad. Sci. U. S. A. *114*, E8780–E8787.

129. Czeisler, C.A., Duffy, J.F., Shanahan, T.L., Brown, E.N., Jude, F., Rimmer, D.W., Ronda, J.M., Silva, E.J., Allan, J.S., Jonathan, S., *et al.* (1999). Stability,

precision, and near-24-hour period of the human circadian pacemaker. Science (80-.). *284*, 2177–2181.

130. Stothard, E.R., McHill, A.W., Depner, C.M., Birks, B.R., Moehlman, T.M., Ritchie, H.K., Guzzetti, J.R., Chinoy, E.D., LeBourgeois, M.K., Axelsson, J., *et al.* (2017). Circadian Entrainment to the Natural Light-Dark Cycle across Seasons and the Weekend. Curr. Biol. *27*, 508–513.

CHAPTER 3

Characterizing the Role of MILES-TO-GO in Circadian-Modulated Outputs

(Nave, et al.)

Abstract

MILES-TO-GO (MTGO) is the *Drosophila* ortholog of mammalian Fibronectin type-III domain-containing protein 3 (FNDC3). Recent work has shown that MTGO heterozygote larval mutants show abnormal terminal axonal arborization of neuromuscular junctions. Furthermore, MTGO$^{-/-}$ homozygote mutants display reduced lifespan, and late pupal lethality due to failure in eclosion. Because pupal eclosion is modulated by a subset of circadian neurons (LNv), we hypothesize that MTGO may mediate or be mediated by the molecular clock. Immunocytochemical data indicate that in adult brains, MTGO is expressed in subsets of circadian neurons along with newly identified cell subgroups distributed across the fly brain. Additionally, we identified defects in clock protein cycling, and circadian-modulated locomotor behaviors in flies heterozygous for MTGO mutations. Lastly, we show that the MTGO protein oscillates in a circadian-dependent manner. These results suggest that MTGO may modulate important developmental stages in a circadian-dependent manner.

3.1 Introduction

MILES-TO-GO (MTGO) is the *Drosophila* ortholog of the mammalian Fibronectin Type-III Domain-Containing-3 (FNDC3) protein [6]. Work on FNDC3 has shown its importance on cell adhesion, formation of intracellular bridges in spermatid, cranio-facial, skeletal, and lung development, and adipogenesis. Defects to FNDC3 is shown to lead to the cancer progression in glioma, glioblastoma (brain tumors), and hepatocellular carcinoma [3,4,7]. Recent work on *Drosophila* show that MTGO (CG42389) is important for the development of larval neuromuscular junctions (NMJs) and allelic mutations to MTGO exhibit lower numbers of synaptic boutons with reduced branching within NMJs [6]. High mortality in MTGO homozygous mutants in *Drosophila* is prevalent due to late pupal lethality caused by failure of eclosion. Additionally, wandering 3$_{rd}$-instar larvae exhibit defects in sweeping/pausing behavior associated with foraging suggesting defects in olfactory physiology [6].

Biochemical studies revealed that MTGO forms a complex with TRiC/CCT3 (Group II Chaperonins, TCP-1 Ring Complex/Complex-Containing TCP-1) for proper *in vivo* function. Furthermore, the TRiC/CCT complex interacts with numerous unknown cytosolic proteins, and mediates protein folding for actin and tubulin [6,9,11,13,15,17]. Furthermore, the TRiC/CCT complex is shown to play a key role in circadian-mediated autophagy associated with Alzheimer's and Huntington's Disease [9,19,21], suggesting a that mutations to MTGO may lead to certain disruptions to circadian rhythmicity. In addition to mediating circadian-modulated autophagy, clues from work by Syed, et al, 2018, reveal how MTGO potentially interacts with other circadian-modulated functions. MTGO mutants reveal pupal lethality, indicating issues with eclosion, a process mediated

by the circadian clock [23,24,26,28]. Although recent work has shown that mutations to MTGO lead to defects attributed to circadian rhythm disruption, how MTGO interacts with the molecular clock and its *downstream* outputs are yet to be elucidated.

Here, we show that mutations to *mtgo* lead to circadian disruption at the behavioral and molecular level. Our studies show disruptions to circadian-modulated activity in *mtgo* mutants, and additionally, changes in daily clock protein expression. Taken together, this body of work characterized importance of *mtgo* on important circadian hallmarks and how *mtgo* could potentially provide input into the molecular clock.

3.2 Materials and Methods

Fly stocks and maintenance

Fly stocks are maintained in 23º C on standard cornmeal-sucrose-agarose medium. Flies were entrained under a standard 12-hrs lights on:12-hrs lights off schedule (12.57 W/m2 (2,000 lux)). Wildtype control files used were Canton-S flies. Flies used for secondary control and label MTGO-expressing cells were $MTGO_{EYFP}$ where a protein-trap sequence is inserted within the MTGO-RF transcript becoming an in-frame combination. This results in a MTGO and EYFP fusion protein while retaining MTGO *in vivo* function [6]. MTGO heterozygous mutants used for all experiments ($MTGO^{+/-}$) were chr. II allelic mutations of $mtgo_{e02963}$ held over a *CyO-GFP* balancer [6].

Behavioral analysis and entrainment

Activity under standard LD and DD were obtained using the TriKinetics *Drosophila* Activity Monitors (DAM). Activity is measured when flies cross infrared beams recorded by the DAM acquisition program at every 1-min bins. Prior to experimentation, ~3-7day old adult male flies are entrained in 12-hrs light:12hr dark (12.57 W/m2 (2,000 lux)) for ≥3 days. To avoid confounding factors between entrainment and recorded entrainment, we retained the same parameters between entrainment and data collection (i.e. temperature, ZT, and light intensity). Data analyses and plots were performed and created using FaasX (Dr. Francois Royer, Paris-Saclay Institute of Neuroscience).

Multibeam and spatial preference assay

We employed the TriKinetics Multibeam Monitors to determine fly spatial preference under 12-hr light:12hr dark and constant darkness (DD) entrainment

employed in [30]. Individual ~3-7day old adult male flies were loaded into tubes with food and a cotton plug on each end. Each monitor measures fly activity and spatial preference using 17 infrared beams spaced every 3mm to ensure proper coverage of fly movement to determine activity or lack thereof. Heat maps were generated using Microsoft Excel to indicate spatial positioning percentile of flies within the tube per 1-hr bins across a 24-hour period. Spatial preference of flies under standard LD and DD conditions were averages of 5-day runs for each LD or DD entrainment.

Antibodies

Antibodies for *Drosophila* PIGMENT DISPERSING FACTOR (mouse anti-PDF-C7) were obtained from the Developmental Studies Hybridoma Bank deposited by Dr. Justin Blau (Department of Biology, New York University). Antibodies to EYFP were goat polyclonal anti-GFP (VWR International, cat. no. GTX26673). Antibodies for the clock protein, PERIOD, were rabbit anti-PER provided by Dr. Amita Sehgal (UPenn Perelman School of Medicine). Secondary antibodies used were obtained from Life Technologies and are as follows: anti-mouse 647nm (ref. no. A21235), anti-rabbit 488nm (ref. no. A11008), anti-guinea pig 555nm (ref. no. A21435).

Immunocytochemistry and imaging

Prior to immunostaining, adult male flies are entrained to ≥3 days 12-hr lights on:12-hr lights off schedule (12.57 W/m2 (2,000 lux)) white light. Flies were dissected in room temperature (RT) ~1-hr prior to fix based on the ZT timepoints indicated. For ZT 17 and 23, dissections were performed in a light-tight room under dim orange light to prevent light-activation of clock resetting and degradation of PER. Flies were dissected in RT 1x

PBS prior to fixing using 4% paraformaldehyde at ZT5, ZT11, ZT17 and ZT23 for 30 minutes and washed 3x with 1% Triton-X/1x PBS 10 min. each (RT). Brains were incubated in blocking buffer (10% horse serum in 0.5% TX/1x PBS) for 1.5-hrs then incubated overnight with primary antibodies (mouse anti-PDF (1:10,000), rabbit, anti-GFP (1:2000), and/or guinea pig anti-PER (1:3000)) in 4ºC. On the following day, brains are washed 5x with 0.5%TX/1x PBS for 10 minutes each (RT), then incubated overnight with secondary Alexa Fluor antibodies (mouse Alexa 647nm (1:1000), rabbit Alexa 488nm (1:1000), and guinea pig Alexa 555nm (1:1000)) in 4ºC. On the final day, secondary antibodies are washed using 0.5% TX/1x PBS 5x 15-mins each and then mounted on a glass slide and coverslip in VectaShield Mounting Media (Fisher Scientific, cat. no. NC9265087). Prepared slides with brains were stored in 4ºC prior to imaging. Imaging of brains were performed using a Leica SP8 Confocal Microscope, settings for laser power and gain were standardized across all brain images to control normalization in quantifying fluorescence intensity. Brains were imaged using a 20x immersion objective (Plan-Apochromat 20x/0.75 NA Immersion).

Quantification of mean fluorescence intensity

Quantitative analysis of PDF, PER, and EYFP mean fluorescence intensity was performed using ImageJ (imagej.nih.gov/ij/). ROIs were drawn on target cells and the background of the image, and mean fluorescence intensity was measured by the program for all genotypes and timepoints. MFI values for each measured cell were analyzed in Microsoft Excel, where average MFI, and SEM was calculated for all cell groups and MFI for all cells by ZT. Background was subtracted for all cells per respective image for

normalization purposes. Data points were imported into GraphPad Prism 8 to create plots used for figures.

3.3 Results

3.3.1 *Circadian locomotor activity is disrupted in adult MTGO$^{+/-}$ mutant flies*

Initial studies to determine the role of MTGO in *Drosophila* development are performed at the larval stage. Work on MTGO defects indicate that homozygous (-/-) mutations to the MTGO protein indicate disruptions to circadian-modulated behaviors such as locomotor activity, and late pupal lethality due to failure to escape the pupa [6]. Due to our limitations on studying homozygous allelic mutants, we sought to determine disruptions in locomotor behavior using heterozygotes (MTGO$^{+/-}$) due to their ability for proper eclosion and survivability into adulthood. Preliminary immunocytochemical studies revealed defects in the development of lateral-ventral neurons (LNv) in adult MTGO$^{+/-}$ brains suggesting that locomotor activity will be disrupted (data not included). In the absence of s-LNvs, circadian locomotion is disrupted leading to arrhythmic activity [26,32,33,35]. We investigated locomotor activity in adult MTGO$^{+/-}$ flies and compared them to two control background groups: Canton-S (CS) and MTGO^{EYFP} (Figure 1). MTGO mutant fly lines were created under the CS background, and MTGO^{EYFP} was used as a means to identify MTGO localization in larval CNS under non-mutant conditions [6].

Control and experimental flies were placed in five days of 12-hr light:12-hr dark (control LD) entrainment to determine locomotor behavior under control standard light conditions. We relied on CS (Figure 1A, top panel) and MTGO^{EYFP} (Figure 1B, top panel) to serve as baseline behavior under control conditions and compared them to MTGO$^{+/-}$ mutants (Figure 1C). Because our overall goal is to connect how MTGO connects to the circadian clock, we placed the same flies in constant darkness (DD) to monitor free-running clock behaviors, free of environmental light cues (Figure 1, lower panels). Under

control LD, we immediately find disruptions to locomotor behavior in MTGO$^{+/-}$ mutants, where adults exhibit defects in morning and evening anticipatory behavior (Figure 1C, top panel) [26,32,33]. Compared to CS and MTGO$_{EYFP}$ controls, MTGO$^{+/-}$ locomotor behavior remains dampened across entrainment suggesting possible developmental defects in light perception or due to the absence of LNvs initially observed in preliminary immunocytochemical studies leading to[37] disruptions to clock-mediated anticipatory behaviors. Furthermore, we investigated how the free running clock controls locomotor behavior in MTGO$^{+/-}$ flies. Under DD conditions, we see the persistence of circadian clock disruption in that locomotor behavior remains virtually absent in MTGO mutants (Figure 1C, lower panel) compared to controls flies (Figure 1A, and B, lower panels). Together, we find that *mtgo* mutations may contribute to circadian-modulated locomotor activity suggesting that *mtgo*, itself, may play a further, and intrinsic role in modulating the molecular mechanisms controlling the biological clock.

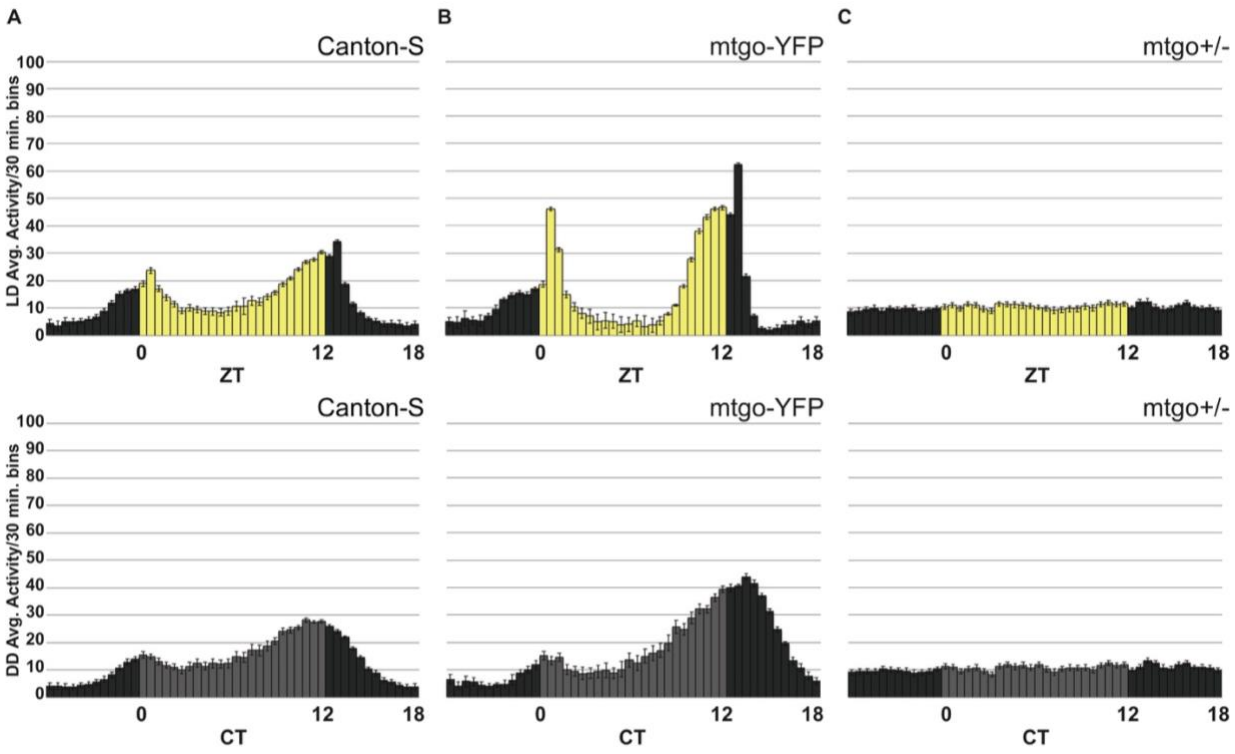

Figure 1. Heterozygous *mtgo* mutant adults exhibit defects in circadian-modulated locomotor activity. **(A)** Activity plots for averaged behavior using control, adult Canton-S male flies for a total of 8 days of standard 12-hrs light: 12-hrs dark (top panel) followed by 5 days under constant darkness (bottom panel). Activity is averaged in 30-min bins for a 24-hr period. During LD entrainment, black bars indicate 30-min bins of dark, yellow bars indicate 30-min bins of light (top panels). During DD entrainment, black bars indicate 30-min bins of dark, gray bars indicate 30-mins of dark during subjective daytime (bottom panel) based on previous LD entrainment (Canton-S n=96 adult male flies). **(B)** Activity plots for averaged behavior using control, adult MTGO$_{EYFP}$ male flies for a total of 8 days of standard 12-hrs light: 12-hrs dark (top panel) followed by 5 days under constant darkness (bottom panel). Activity is averaged in 30-min bins for a 24-hr period. During LD

entrainment, black bars indicate 30-min bins of dark, yellow bars indicate 30-min bins of light (top panels). During DD entrainment, black bars indicate 30-min bins of dark, gray bars indicate 30-mins of dark during subjective daytime (bottom panel) based on previous LD entrainment ($MTGO_{EYFP}$ n=47 adult male flies). **(C)** Activity plots for averaged behavior using control, adult *mtgo*$^{+/-}$ male flies for a total of 8 days of standard 12-hrs light: 12-hrs dark (top panel) followed by 5 days under constant darkness (bottom panel). Activity is averaged in 30-min bins for a 24-hr period. During LD entrainment, black bars indicate 30-min bins of dark, yellow bars indicate 30-min bins of light (top panels). During DD entrainment, black bars indicate 30-min bins of dark, gray bars indicate 30-mins of dark during subjective daytime (bottom panel) based on previous LD entrainment (*mtgo*$^{+/-}$ n=64 adult male flies). Error bars indicate $\pm$SEM.

3.3.2 *PERIOD expression in circadian neurons is disrupted in MTGO+/- mutants*

Locomotor behaviors exhibited by MTGO+/- under standard LD entrainment (Figure 1C) reveal potential underlying disruptions to the molecular clock exhibited by inability to perceive light/dark entrainment. We speculated that shortcomings in locomotor behavior may be due to MTGO+/- mutation's influence on the molecular clock. The precise timing and oscillations of circadian protein expression is crucial to the maintenance of circadian rhythmicity. Disruptions to the molecular clock lead to disturbance in locomotor activity, and significant changes to the organism's daily physiology [39,41,43]. We utilized an immunocytochemical approach to investigate clock protein behaviors of PERIOD (PER) in a MTGO+/- mutant background. Whole adult brains were fixed in 4% paraformaldehyde at four different circadian timepoints after the onset of lights on, under a 12-hr light:12-hr dark entrainment schedule (ZT): ZT5, ZT11, ZT17, and ZT23. We analyzed PER fluorescence intensity in canonical circadian neurons during the four ZT timepoints to determine any changes caused by *mtgo* mutations (Figure 2A, rows represent neuron type, columns indicate time fixed). Qualitative assessment of PER fluorescence among the individual neuron subgroups indicated gradual changes in fluorescence intensity between the four ZT timepoints across a 24-hr day.

Quantitative analysis of mean fluorescence intensity of PER signal in canonical circadian neurons revealed surprising oscillatory behaviors of the clock protein in *mtgo+/-* mutants. We found that quantified circuit-wide PER expression from mtgo+/- (Figure 2B, top left panel, dotted trace) ran antiphase to PER oscillations seen in control CS flies (Figure S2). Overall, we found that individual subsets of PER-expressing circadian neurons in *mtgo+/-* oscillate in an anti-phasic manner opposite to the PER expression of

circadian neuron subsets in control CS fly brains (Figure 2B: s-LNv, top right panel; l-LNv, middle left panel, LNd, middle right panel; DN1, bottom left panel; DN3, bottom right panel). The dramatic change in PER oscillatory behaviors in a *mtgo*$^{+/-}$ background further supports our speculation that *mtgo* not only plays a role in in regulating circadian-modulated behaviors (Figure 1C) but is also a crucial component in mediating the molecular clock (Figure 2). These findings served as motivation in studying the behaviors of the MTGO protein itself.

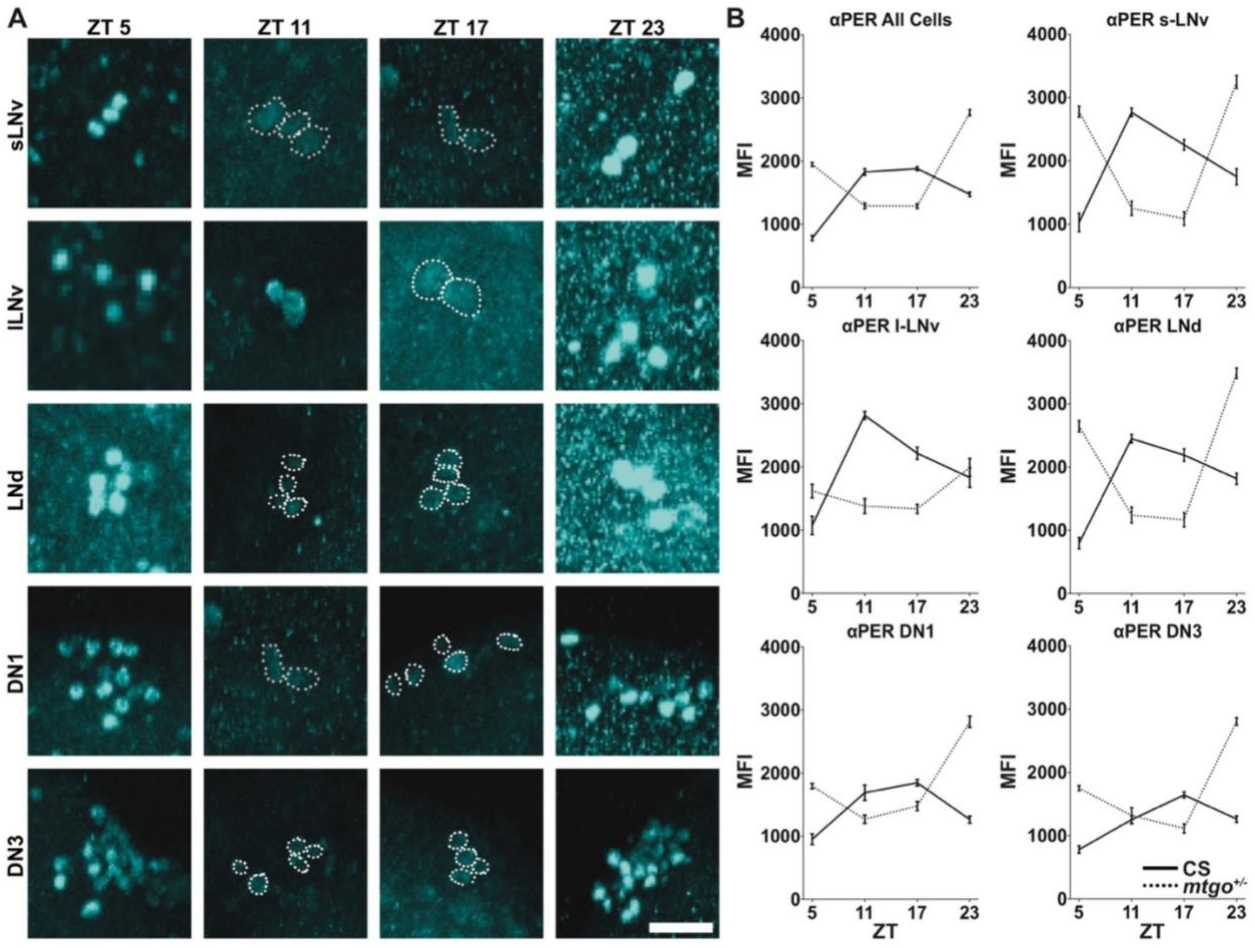

Figure 2. PERIOD clock protein oscillates in an anti-phasic manner in *mtgo*$^{+/-}$ mutants. Whole-brain immunocytochemical analysis of PERIOD clock protein in canonical circadian neurons in adult male *mtgo*$^{+/-}$ flies. Adult *mtgo*$^{+/-}$ were fixed in 4% paraformaldehyde during four circadian timepoints: ZT5, ZT11, ZT17, and ZT 23. Fluorescence intensity of individual circadian neurons were identified and measured using ImageJ. Neurons that are difficult to distinguish from background are traced using Adobe Photoshop. Circadian neuron subsets of *mtgo*$^{+/-}$ brains are as follows: ZT 5 (9 brains; s-LNv n=44, l-LNv n=46, LNd n=75, DN1 n=191, DN3 n=228), ZT 11 (10 brains, s-LNv n=,21 l-LNv n=40, LNd n=44, DN1 n=,98 DN3 n=47), ZT 17 (10 brains; s-LNv n=16,

l-LNv n=53, LNd n=29, DN1 n=74, DN3 n=55), ZT 23 (10 brains; s-LNv n=26, l-LNv n=51, LNd n=26, DN1 n=67, DN3 n=119, scale bar = 25 µm). **(B)** PER oscillations from control Canton-S circadian neurons (dotted) were compared with *mtgo*$^{+/-}$ mutants (solid). Comparisons between CS and *mtgo*$^{+/-}$ are for the overall circuit, as well as comparisons in PER oscillations within circadian subgroups. mtgo (-/+): ZT 5 (9 brains; s-LNv n=44, l-LNv n=46, LNd n=75, DN1 n=191, DN3 n=228), ZT 11 (10 brains, s-LNv n=,21 l-LNv n=40, LNd n=44, DN1 n=,98 DN3 n=47), ZT 17 (10 brains; s-LNv n=16, l-LNv n=53, LNd n=29, DN1 n=74, DN3 n=55), ZT 23 (10 brains; s-LNv n=26, l-LNv n=51, LNd n=26, DN1 n=67, DN3 n=119). Canton-S: ZT 5 (16 brains; s-LNv n=84, l-LNv n=79, LNd n=142, DN1 n=161, DN3 n=232), ZT 11 (9 brains; s-LNv n=44 l-LNv n=51, LNd n=61, DN1 n=43, DN3 n=69), ZT 17 (11 brains; s-LNv n=50, l-LNv n=63, LNd n=50, DN1 n=180, DN3 n=208), ZT 23 (9 brains; s-LNv n=58, l-LNv n=37, LNd n=90, DN1 n=125, DN3 n=162). Error bars indicate $\pm$SEM.

3.3.3 *MILES-TO-GO is expressed in circadian neurons and distinct neuronal subgroups in Drosophila*

The disruption in daily oscillations of PER expression caused by the mtgo+/- mutation led to speculation that MTGO plays a larger role in the mechanism controlling the molecular clock. To further our studies, we sought to determine if the clock itself also modulates the expression of MTGO throughout a 24-hr period. We performed immunocytochemical analyses on adult $MTGO_{EYFP}$ brains fixed in 4% paraformaldehyde at four different time points (ZT5, ZT11, ZT17, and ZT23) to determine if the levels of MTGO protein expression oscillations throughout the 24-hr time period (Figure 3). To track the relative expression of MTGO, and to determine protein localization within the fly brain, we performed antibody staining on $MTGO_{EYFP}$ flies using rabbit anti-YFP/GFP (see methods). Surprisingly, based on EYFP expression, we found that MTGO is expressed in numerous cell subgroups distributed across the fly brain.

Qualitative assessment shows that MTGO expression in these cells peak at ~ZT11, then diminishes near the end of the 24-hr day at ~ZT23. In addition to the YFP/GFP antibody staining, we performed immunocytochemical staining with mouse anti-PIGMENT DISPERSING FACTOR (anti-PDF, Figure 3A, middle row) and anti-PERIOD (not shown due to noise). *Drosophila* PDF is a neuropeptide produced and released by the LNvs that allows for circadian-circuit connectivity and communication via the PDF receptor, PDFr [45,47,49]. Additionally, we also used anti-PER to determine whether cells expressing MTGO co-localized with non-PDF-expressing circadian neurons (i.e. LNd, DN1 and DN3 subgroups).

Immunocytochemical data of $MTGO_{EYFP}$ revealed MTGO distribution in distinct cell subgroups. To distinguish these cellular subsets, we named clusters of cells based on the following: [1] established anatomical positioning along with fly brain, [2] expression of PDF, and [3] expression of PER. We, then, generated a diagram of the fly brain mapping the different MTGO-expressing cells (Figure 3B). Most MTGO-expressing cells that were identified were grouped based on their anatomical position, however, some cells were grouped due to expression of the PER clock protein (LNd) or both PER and PDF (s-LNv and l-LNv) (Figure 3B, indicated by black dots). Lastly, we quantified the overall mean fluorescence intensity (MFI) emitted by all MTGO-expressing cells for each ZT timepoint. We found varying changes to MFI for each ZT. The global average of MTGO expression peaks at ZT11, the end of the subjective lights-on, and MFI is at its lowest prior to the onset of the next light regime, at ZT23 (Figure 3C). The varying levels of MTGO expression throughout the 24-hour day suggests MTGO may be mediated by the circadian clock via direct or indirect interaction. Our ability to characterize MTGO-expressing cells in the *Drosophila* brain motivated our interest in elucidating MTGO expression behavior among each of the novel cell groups that were identified.

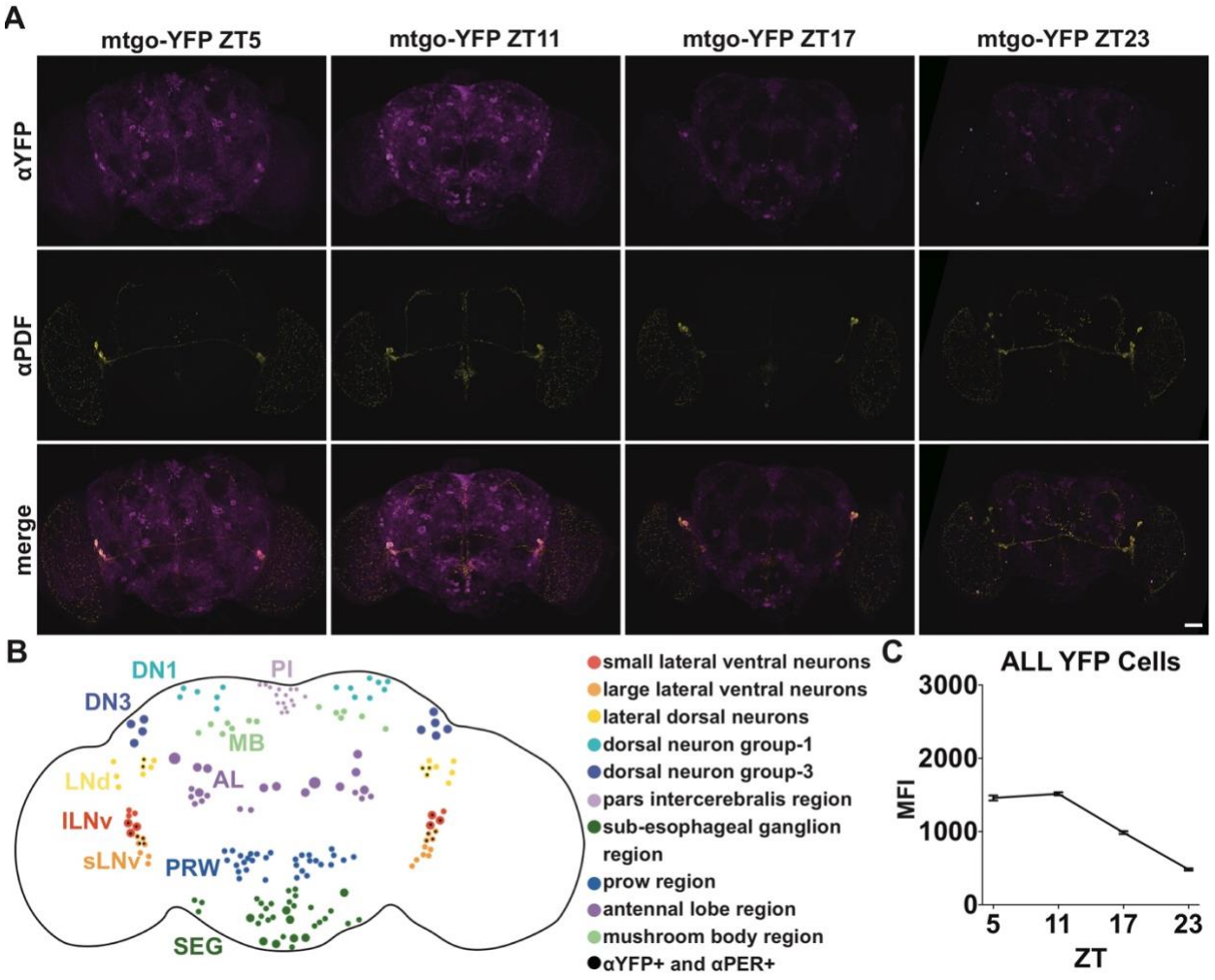

Figure 3. MTGO expression oscillates throughout the 24-hr day. (A) Qualitative fluorescence imaging of adult male *MTGO*$_{EYFP}$ brains fixed in 4% paraformaldehyde at four different circadian timepoints: ZT5, ZT11, ZT17, and ZT23 (first through fourth columns, respectively). *MTGO*$_{EYFP}$ adult male fly brains were immunostained with rabbit anti-GFP/YFP (top panels) and antibodies for PIGMENT DISPERSION FACTOR (mouse anti-PDF, middle panels). Merged channels indicate co-localization of fluorescence signals from the two antibodies (bottom panel). Scale bars = 25μm. **(B)** Diagram depicting identified neurons from *MTGO*$_{EYFP}$ brains. Neuron labeling is based on their anatomical

position in the fly brain or named based on adjacent structures. Cells that express both *MTGO$_{EYFP}$* and PER are indicated with a black dot (s-LNv, l-LNv, and ~2-3 LNds). **(C)** Quantified MFI for MTGO$_{EYFP}$ expression throughout four different time points within a 24-hr day. Fluorescence intensity is obtained using ImageJ where background from each individual image was subtracted from the background for normalization. ZT5 (7 brains, n=600 EYFP-expressing cells); ZT11 (8 brains, n=1213 EYFP-expressing cells); ZT17 (10 brains, n=673 EYFP-expressing cells); ZT23 (8 brains, n=483 EYFP-expressing cells). Error bars indicate $\pm$SEM.

3.3.4 *MILES-TO-GO expression in MTGO-positive cell subgroups oscillates throughout a 24-hr day*

MTGO is expressed in an organized, and group cell subsets in the fly brain, and that the global MTGO expression in the brain appears to oscillate across a 24-hour period (Figure 3). Given this, we sought to establish whether MTGO oscillation occurs within all cell subtypes and whether they oscillate in distinct patterns. Utilizing the immunocytochemical approach used to identify subgroups, we quantified MFI of each of the cell subtypes to determine individual oscillatory behaviors (Figure 4). MTGO-expressing cell subgroups were categorized into three types: [1] PER- and PDF-expressing circadian neurons (Figure 4A; s-LNv, l-LNv, LNd, DN1, and DN3), [2] MTGO-expressing cells adjacent to circadian neurons (Figure 4B: non-LNv, non-LNd, non-DN1, and non-DN3), and [3] cell subgroups identified based on anatomical position and proximity to known brain structures (Figure 4C: pars intercerebralis (PI) region, sub-esophageal ganglion (SEG), prow (PRW), antennal lobe (AL), and mushroom body (MB) region).

We report that MTGO expression in circadian neurons indicate the highest MFI peaks in the s-LNv and l-LNv subgroup during ZT11, before the onset of lights-off (Figure 4, first and second panel, respectively). Similarly, but not quite, the reported MFI in the LNd subgroup peak at ZT5 and continues to decrease throughout the 24-hr day. In contrast, the DN1 and DN3 subgroups have peak MFI at ZT5 but yielded virtually no presence of MTGO expression during ZT11 and ZT23. For cells expressing MTGO that lie in proximity to circadian neurons, we report a lower overall MFI compared to that seen in canonical circadian neurons. We utilized anti-PER immunocytochemical data to

determine whether MTGO-expressing cells were either canonical circadian neurons, or cells adjacent to them. Non-circadian cells closest to the lateral neurons showed highest peak MFI at ZT5 (Figure 4B, first and second panels). Similarly, those closest to the DN1 subgroup showed peak MTGO expression at ZT5 (Figure 4B, third panel). The MTGO-expressing cells closest to the DN3s showed highest peaks at ZT5 but changes in MTGO expression throughout the day appear to plateau, and indistinguishable from the other ZTs (Figure 4B, fourth panel). Lastly, we tracked the MFI for MTGO expressing cells that were identified based on anatomical position within the fly brain. Cells found in the PI region, SEG, and PRW (Figure 4C, first, second and third panels, respectively) followed similar patterns of MTGO expression as the circadian lateral ventral neurons (LNvs). The MFI in cells in the AL show a peak of expression at ZT5 (Figure 4C, fourth panel). Lastly, the MFI in the MB area showed the only MFI that peaks at ZT17 (Figure 4C, fifth panel). These findings indicate that expression of MTGO in numerous subsets of cells across the *Drosophila* brain yield different expression levels throughout different time points of the 24-hr day. This suggests that MTGO abundance in different cell subsets, at different times of the day, may play a role in promoting physiological outputs that these MTGO-expressing cells may govern.

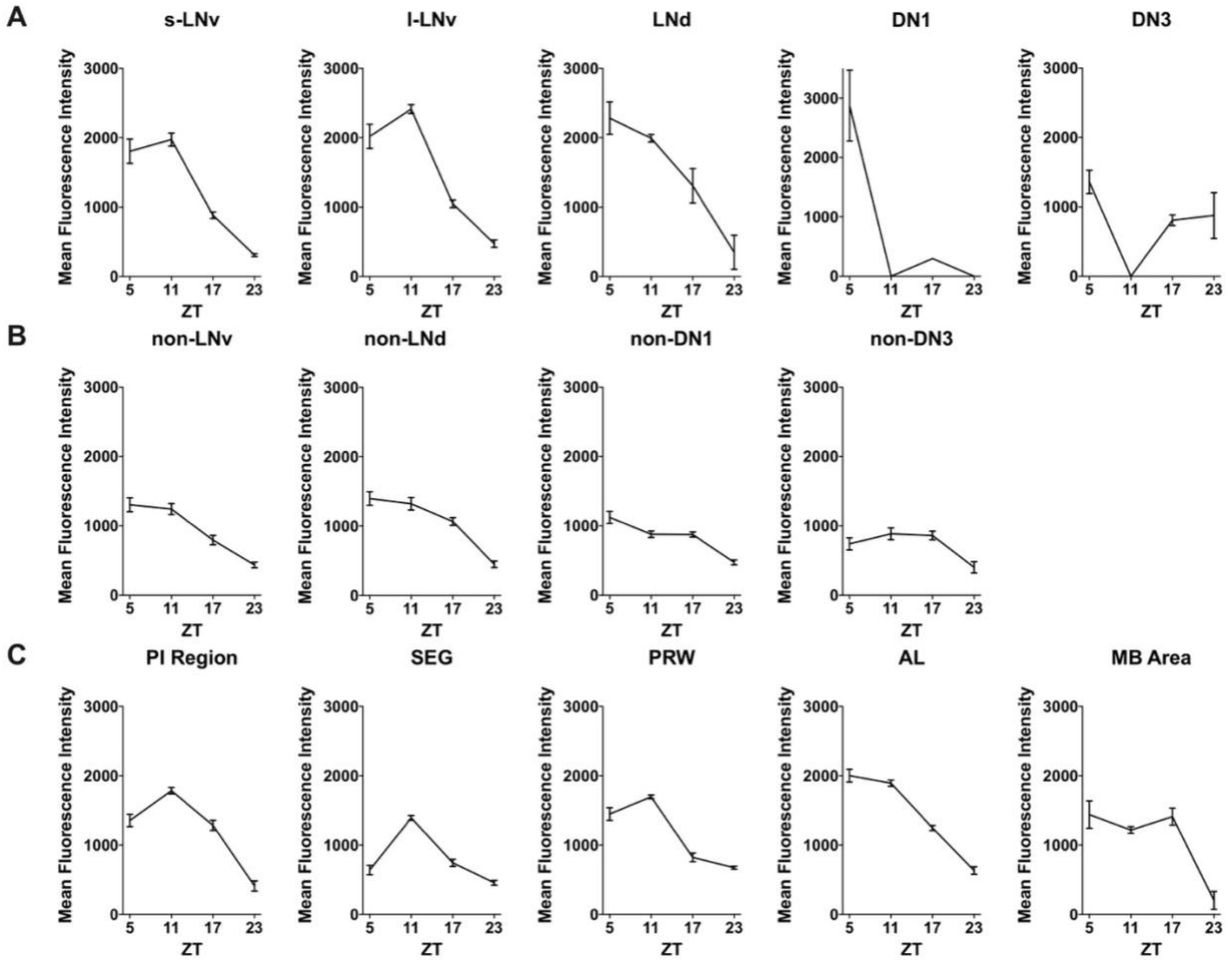

Figure 4. Distinct patterns of MTGO oscillations in newly identified neuronal subgroups cycle throughout a 24-hr period. Mean fluorescence intensity (MFI) of yellow fluorescence protein (YFP) signal from distinct neuronal subgroups expressing MTGO across four different circadian timepoints (ZT5, ZT11, ZT17, ZT23). Fluorescence intensity is obtained using ImageJ where background from each individual image was subtracted from the background for normalization**.** Refer to Figure 3B for neuron distribution throughout the fly brain. **(A)** YFP MFI for canonical circadian neurons throughout a 24-hour period. **(B)** YFP MFI for $MTGO_{EYFP}$ -positive neurons localized in

the vicinity of their respective circadian neuron subgroup and are reported to not express PER. **(C)** YFP MFI for MTGO$_{EYFP}$ -positive neurons labeled based on their anatomical position within the fly brain, or based on their close proximity to known brain structures (ZT5 (7 brains, n=600 EYFP-expressing cells, s-LNv=*37*, l-LNv=28, LNd=11, DN1=4, DN3=17, SEG=55, PRW=70, AL=115, MB=8, PI region=65, non-LNv=47, non-LNd=48, non-DN3=68, non-DN1=27); ZT11 (8 brains, n=1213 EYFP-expressing cells, s-LNv=38, l-LNv=47, LNd=41, DN1=0, DN3=0, SEG=197, PRW=215, AL=197, MB=67, PI region=100, non-LNv=105, non-LNd=18, non-DN3=113, non-DN1=75); ZT17 (10 brains, n=673 EYFP-expressing cells, s-LNv=53, l-LNv=48, LNd=7, DN1=1, DN3=10, SEG=96, PRW=41, AL=84, MB=34, PI region=67, non-LNv=41, non-LNd=49, non-DN3=86, non-DN1=56); ZT23 (8 brains, n=483 EYFP-expressing cells, s-LNv=39, l-LNv=40, LNd=3, DN1=0, DN3=5, SEG=70, PRW=59, AL=44, MB=8, PI region=29, non-LNv=38, non-LNd=49, non-DN3=67, non-DN1=32)). Error bars indicate $\pm$SEM.

3.4 Discussion

This body of work sought to characterize the role of miles-to-go on the modulation of circadian-controlled behaviors in *Drosophila.* Based on initial studies by Syed, et al, many clues suggested a relationship between CG42389 (*miles-to-go*) and the molecular clock. *Drosophila* larvae studies show that mutations in MTGO led to disruptions in the neuromuscular junction formation, leading to issues in locomotion (i.e. head sweeping motion). Additionally, complete allelic absence of *Drosophila* MTGO prevents pharate ability to exit the pupa via eclosion, a circadian-modulated behavior that requires precise timing of the molecular clock and the animal's external environment [6,23,48]. Furthermore, our initial studies investigating *mtgo* suggest developmental defects preventing the formation of circadian-specific neurons (LNvs) that modulate the affected behaviors seen in *mtgo* mutants. Here we found additional evidence suggesting the interplay between *mtgo* and the *Drosophila* circadian clock.

Based on initial studies, we found that in adult mtgo heterozygous mutants, circadian neurons, small-LNvs and large-LNvs, are expressed in lower numbers (<4 s-LNv; <4 l-LNv). Issues in the development of core circadian neurons are not directly modulated by the biological clock, the absence of either small- and/or large-lateral ventral neurons significantly impact circadian-modulated physiological and behavioral outputs. The LNv circadian subgroup are located in a region that borders the *Drosophila* cerebrum and optic lobe serving as the initial light input into the circadian neural circuit [19,50,52]. We found that in the presence of a heterozygous allelic mutation to *mtgo*, led to disruption in the formation of key circadian neurons leading to defects in locomotor behavior (described below), which are also described by Syed et al. while investigating larval locomotion and directionality in a *mtgo* mutant background. Though we see the reduction of LNvs in adult immunohistochemical studies (Fig. 2, S2), we speculate that these neurons are present prior to eclosion. Due to the presence of the dorsal-projecting PDF signal seen in heterozygous mutants (data not shown), the loss in lateral ventral neuron numbers occur

between the third instar larvae stage and pharate eclosion in heterozygous mutants. Further studies are needed to verify that the loss of important circadian neurons is due to mutations in *mtgo*. In fact, our inability to locate certain clock neurons in *mtgo*$^{+/-}$ may not be due to the absence of the cells, but merely the inability for these cells to properly express our fluorescent markers, PDF and PER [49,53,56]. Because of this, we speculate that tracking the expression of non-circadian-modulated markers may confirm whether there is an absence of neurons, or a defect in expression of clock proteins, and clock-mediated neurotransmitters.

We find that in a *mtgo* mutant background, circadian-modulated locomotor behavior is severely disrupted. Mutants exhibit the complete absence of morning and evening anticipatory behavior under both control LD and constant darkness (DD) conditions (Fig.1). The inability for *mtgo*$^{+/-}$ flies to entrain to the LD cycle, as exhibited by absence of anticipatory locomotion before lights on and lights off, suggests a deeper obstruction to the molecular clock caused by the *mtgo* mutation [56,58,60]. We hypothesize that in a *mtgo* mutant background, circadian rhythms are disrupted. This is reinforced by our observations of locomotor activity utilizing the TriKinetics Multibeam Activity Monitor, indicating severely dampened, but not absent, locomotor activity (Fig. S1). This indicates that *mtgo*$^{+/-}$ flies were not completely inactive (Fig. 1), but were incapable of LD entrainment, suggesting underlying circadian rhythm disruptions.

To further investigate the role of *mtgo* with the molecular clock, we performed immunohistochemical analysis on *mtgo*$^{+/-}$ mutants probing for the clock protein, PERIOD. We found that the expression of the PER protein oscillates in antiphase of PER found in control CS flies [62,64,65]. The overall behavior of PER in *mtgo*$^{+/-}$ mutants are consistent in the oscillations found in individual circadian neuronal subgroups of mutants flies as well (Fig. 2). The oscillatory behaviors exhibited by circadian neuron subgroups in a *mtgo*$^{+/-}$ mutant background corroborate the behaviors exhibited by whole, adult, intact flies. Due to the significant changes done to the molecular clock in *mtgo* mutants, this opens the suggestion that MTGO may be directly mediating

components of the molecular clock. However, further studies are needed to clarify exactly which clock components are being acted upon by MTGO. Additionally, studies done by Syed, et al., indicate that *mtgo* mutants lead to disruptions in circadian-modulated behaviors such as failure in eclosion. Moreover, our findings with locomotor disruption in *mtgo*$^{+/-}$ mutants suggest that the inversion in oscillation of the PER clock protein may contribute to the absence of circadian-modulated anticipatory behaviors.

The abnormal oscillation of PER in a *mtgo* mutant background suggest that MTGO may play a direct or indirect role in mediating the molecular clock. However, we sought to determine if MTGO itself varies in oscillation throughout a 24-hour day. Using immunohistochemical data, we determined that MTGO oscillates throughout the day, and that it is expressed in the circadian neuron subgroups, LNvs and LNds. Additionally, they are found dispersed throughout the fly brain, which they are labeled based on their anatomical positioning. Quantification of MTGOEYFP mean fluorescence intensity, we find that MTGO oscillates in distinct patterns among the identified cell subgroups (Fig. 3 and 4). The behaviors of MTGO throughout the 24 day suggests that if it is mediating the molecular clock, it is doing so in a time-dependent manner. The disruption in PER oscillation is supported by the disruption in MTGO expression. We set our goal to characterize how *mtgo* plays a role in circadian modulated behaviors. Here, we found that *mtgo* is essential for the proper modulation and expression of the clock protein, PER. Thus, providing explanation in the defects we observed in locomotor activity and the general expression of the PER protein in adult flies. If the behaviors exhibited by the molecular clock observed in adults carry over in the larval stage, this provides a potential explanation in the circadian defects observed by Syed, et al. (eclosion and locomotor behavior). Additionally, we can conclude that due to the fact that MTGO oscillates, if it is mediating the circadian rhythms, its absence would pose disruptions to the molecular clock, thus leading to our observed circadian-modulated defects.

3.5 Supplementary Figures

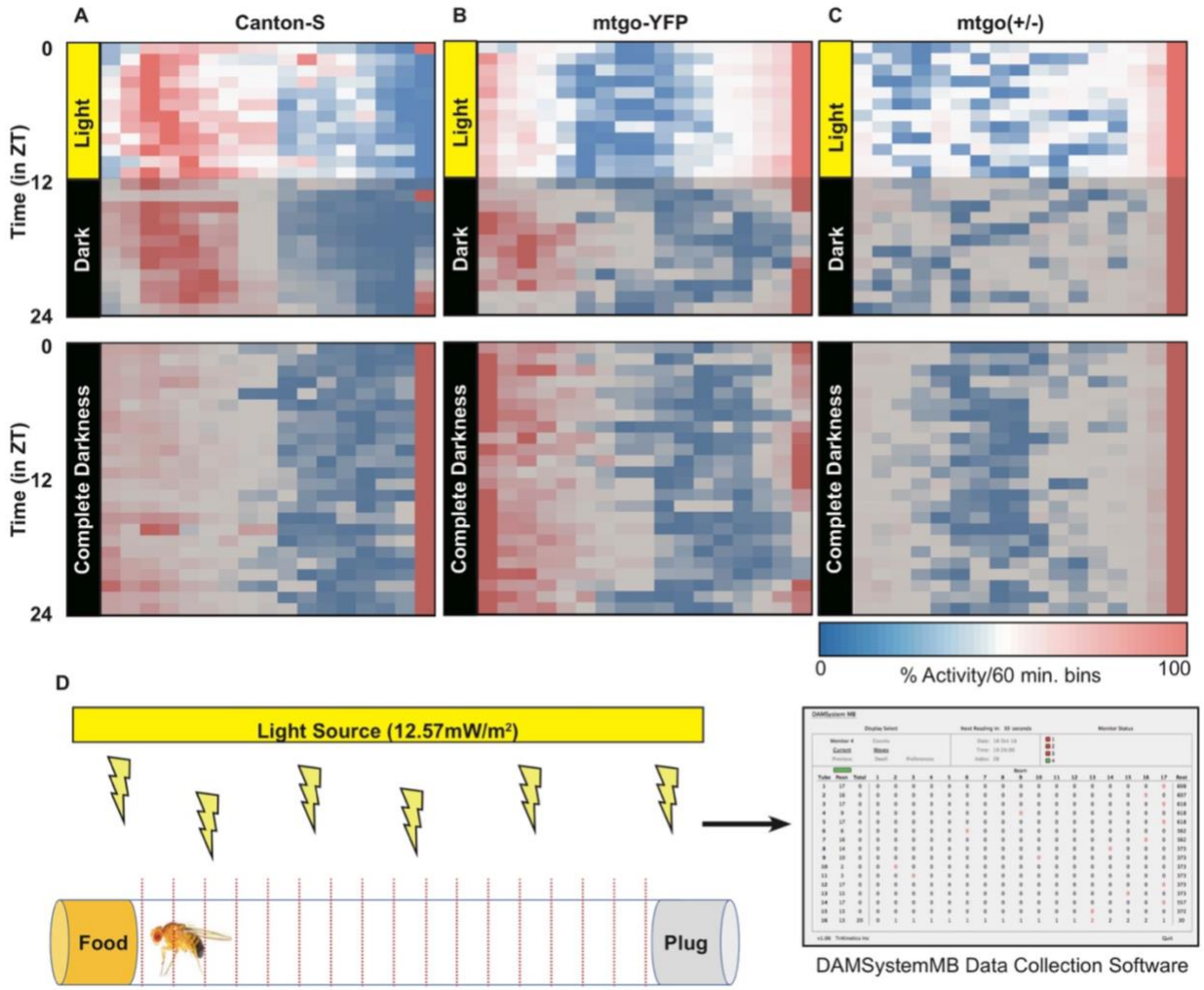

Supp. Figure 1. *Mtgo*$^{+/-}$ mutants have no spatial preference in activity tube. We utilized the DAM System Multi-beam system to determine 1-hr bins of spatial preference in adult male flies *in vivo.* We tracked three genotypes of adult male flies: **(A)** Canton-S, **(B)** *MTGO-EYFP*, **(C)** *mtgo*$^{+/-}$ for five days of 12L:12D entrainment (top panels, yellow indicates subjective daytime, black for subjective nighttime) followed by five days of constant darkness (bottom panels). Spatial preference heat maps indicate the average

percentage of preference for all flies at a given ZT/row. Each column represents one potential region of activity (total of 17) as flies break and cross beams in each tube on the activity monitor. The % activity of each fly is averaged at 1-hour bins where the absence of activity/1-hr bins (0% Activity/1hr-bin) is in blue, and complete activity (100% Activity/1hr-bin) is marked as red. **(D)** Schematic of multibeam tracking of individual flies to indicate spatial preference. Light sources are provided to simulate daytime and nighttime entrainment. Flies are house in glass tubes with food or cotton plug on each side. 17 infrared beams are used to track fly preference within the glass tube. DAM System Multibeam collection software is used for data acquisition. Custom excel templates were employed to generate heatmaps for spatial preference for each 1-hr bin.

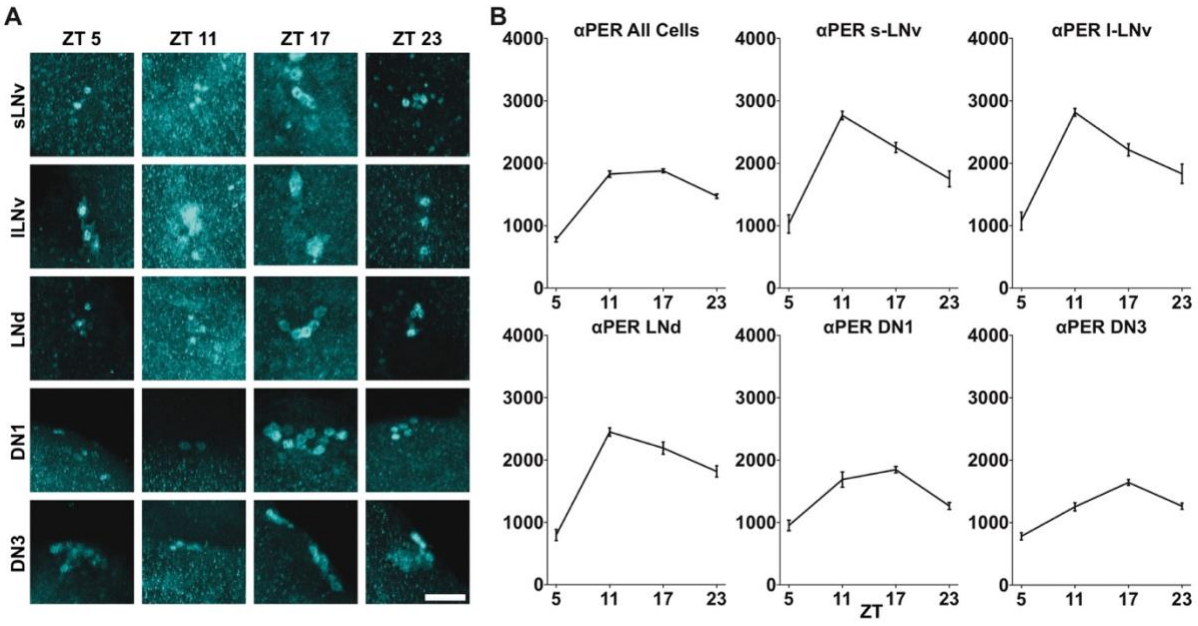

Supp. Figure 2. PER oscillations in control Canton-S adult male fly brains. Whole brain immunocytochemical analysis of PERIOD clock protein in canonical circadian neurons in adult male CS flies. Adult CS flies were fixed in 4% paraformaldehyde during four circadian timepoints: ZT5, ZT11, ZT17, and ZT 23. Fluorescence intensity of individual circadian neurons were identified and measured using ImageJ. **(B)** PER oscillations from control Canton-S circadian neurons. ZT 5 (16 brains; s-LNv n=84, l-LNv n=79, LNd n=142, DN1 n=161, DN3 n=232), ZT 11 (9 brains; s-LNv n=44 l-LNv n=51, LNd n=61, DN1 n=43, DN3 n=69), ZT 17 (11 brains; s-LNv n=50, l-LNv n=63, LNd n=50, DN1 n=180, DN3 n=208), ZT 23 (9 brains; s-LNv n=58, l-LNv n=37, LNd n=90, DN1 n=125, DN3 n=162). Error bars indicate ±SEM.

3.6 References

1. Pittendrigh, C.S., and Minis, D. (1964). The Entrainment of Circadian Oscillations by Light and Their Role as Photoperiodic Clocks Colin. Am. Nat. *98*, 261–294.
2. Pittendrigh, C.S., and Daan, S. (1976). A functional analysis of circadian pacemakers in nocturnal rodents. J. Comp. Physiol. A *106*, 223–252. Available at: http://link.springer.com/article/10.1007/BF01417860%5Cnhttp://link.springer.com/content/pdf/10.1007/BF01417860.pdf%5Cnhttp://link.springer.com/10.1007/BF01417860 [Accessed May 4, 2018].
3. Obholz, K.L., Akopyan, A., Waymire, K.G., and MacGregor, G.R. (2006). FNDC3A is required for adhesion between spermatids and Sertoli cells. Dev. Biol. *298*, 498–513.
4. Carrouel, F., Couble, M.-L., Vanbelle, C., Staquet, M.-J., Magloire, H., and Bleicher, F. (2008). HUGO (FNDC3A): a new gene overexpressed in human odontoblasts. J. Dent. Res. *87*, 131–6. Available at: http://www.ncbi.nlm.nih.gov/pubmed/18218838 [Accessed February 6, 2020].
5. Rivas, G.B.S., Teles-de-Freitas, R., Pavan, M.G., Lima, J.B.P., Peixoto, A.A., and Bruno, R.V. (2018). Effects of Light and Temperature on Daily Activity and Clock Gene Expression in Two Mosquito Disease Vectors. J. Biol. Rhythms *33*, 272–288. Available at: http://www.ncbi.nlm.nih.gov/pubmed/29761749 [Accessed August 3, 2020].
6. Syed, A., Lukacsovich, T., Pomeroy, M., Bardwell, A.J., Decker, G.T., Waymire, K.G., Purcell, J., Huang, W., Gui, J., Padilla, E.M., *et al.* (2019). Miles to go (mtgo) encodes FNDC3 proteins that interact with the chaperonin subunit CCT3 and are

required for NMJ branching and growth in Drosophila. Dev. Biol. *445*, 37–53. Available at: https://linkinghub.elsevier.com/retrieve/pii/S0012160618303178 [Accessed December 16, 2018].

7. Ke, J., Zhao, Z., Hong, S.H., Bai, S., He, Z., Malik, F., Xu, J., Zhou, L., Chen, W., Martin-Trevino, R., *et al.* (2015). Role of microRNA221 in regulating normal mammary epithelial hierarchy and breast cancer stem-like cells. Oncotarget *6*, 3709–3721.
8. Yoshii, T., Hermann-Luibl, C., and Helfrich-Föorster, C. (2016). Circadian light-input pathways in Drosophila. Commun. Integr. Biol. *9*.
9. Pavel, M., Imarisio, S., Menzies, F.M., Jimenez-Sanchez, M., Siddiqi, F.H., Wu, X., Renna, M., O'Kane, C.J., Crowther, D.C., and Rubinsztein, D.C. (2016). CCT complex restricts neuropathogenic protein aggregation via autophagy. Nat. Commun. *7*, 1–18.
10. Welsh, D.K., Logothetis, D.E., Meister, M., and Reppert, S.M. (1995). Individual neurons dissociated from rat suprachiasmatic nucleus express independently phased circadian firing rhythms. Neuron *14*, 697–706. Available at: http://journals.sagepub.com/doi/10.1177/0748730419877315 [Accessed October 16, 2019].
11. Yam, A.Y., Xia, Y., Lin, H.T.J., Burlingame, A., Gerstein, M., and Frydman, J. (2008). Defining the TRiC/CCT interactome links chaperonin function to stabilization of newly made proteins with complex topologies. Nat. Struct. Mol. Biol. *15*, 1255–1262.
12. Roenneberg, T., Allebrandt, K. V, Merrow, M., Line Vetter, C., and Vetter, C.

(2012). Social jetlag and obesity. Curr. Biol. *22*, 939–43. Available at: http://www.ncbi.nlm.nih.gov/pubmed/22578422 [Accessed October 25, 2017].

13. Gao, Y., Thomas, J.O., Chow, R.L., Lee, G.H., and Cowan, N.J. (1992). A cytoplasmic chaperonin that catalyzes β-actin folding. Cell *69*, 1043–1050. Available at: https://linkinghub.elsevier.com/retrieve/pii/009286749290622J [Accessed February 21, 2020].
14. Shang, Y., Griffith, L.C., and Rosbash, M. (2008). Light-arousal and circadian photoreception circuits intersect at the large PDF cells of the Drosophila brain. Proc. Natl. Acad. Sci. *105*, 19587–19594. Available at: http://www.pnas.org/content/105/50/19587%5Cnhttp://www.ncbi.nlm.nih.gov/pubmed/19060186%5Cnhttp://www.pnas.org/content/105/50/19587.full.pdf%5Cnhttp://www.pnas.org/content/105/50/19587.short.
15. Hartl, F.U., and Hayer-Hartl, M. (2002). Protein folding. Molecular chaperones in the cytosol: From nascent chain to folded protein. Science (80-.). *295*, 1852–1858.
16. Renn, S.C.P., Park, J.H., Rosbash, M., Hall, J.C., and Taghert, P.H. (1999). A pdf neuropeptide gene mutation and ablation of PDF neurons each cause severe abnormalities of behavioral circadian rhythms in Drosophila. Cell *99*, 791–802.
17. Joachimiak, L.A., Walzthoeni, T., Liu, C.W., Aebersold, R., and Frydman, J. (2014). The structural basis of substrate recognition by the eukaryotic chaperonin TRiC/CCT. Cell *159*, 1042–1055.
18. Fogle, K.J., Baik, L.S., Houl, J.H., Tran, T.T., Roberts, L., Dahm, N.A., Cao, Y., Zhou, M., and Holmes, T.C. (2015). CRYPTOCHROME-mediated

phototransduction by modulation of the potassium ion channel β-subunit redox sensor. Proc. Natl. Acad. Sci.

19. Sheeba, V., Sharma, V.K., Gu, H., Chou, Y.T., O'Dowd, D.K., and Holmes, T.C. (2008). Pigment dispersing factor-dependent and -independent circadian locomotor behavioral rhythms. J. Neurosci. *28*, 217–227.

20. Ni, J.D., Baik, L.S., Holmes, T.C., and Montell, C. (2017). A rhodopsin in the brain functions in circadian photoentrainment in Drosophila. Nature *545*, 340–344. Available at: http://www.nature.com/doifinder/10.1038/nature22325 [Accessed May 4, 2018].

21. Nitabach, M.N., Wu, Y., Sheeba, V., Lemon, W.C., Strumbos, J., Zelensky, P.K., White, B.H., and Holmes, T.C. (2006). Electrical hyperexcitation of lateral ventral pacemaker neurons desynchronizes downstream circadian oscillators in the fly circadian circuit and induces multiple behavioral periods. J. Neurosci. *26*, 479–489.

22. Baik, L.S., Recinos, Y., Chevez, J.A., and Holmes, T.C. (2018). Circadian modulation of light-evoked avoidance/attraction behavior in Drosophila. PLoS One *13*, e0201927. Available at: https://dx.plos.org/10.1371/journal.pone.0201927 [Accessed August 3, 2020].

23. Qiu, J., and Hardin, P.E. (1996). Developmental state and the circadian clock interact to influence the timing of eclosion in Drosophila melanogaster. J. Biol. Rhythms *11*, 75–86.

24. Skopik, S.D., and Pittendrigh, C.S. (1967). Circadian systems, II. The oscillation in the individual Drosophila pupa; its independence of developmental stage. PNAS

58, 1862–1869.

25. Veleri, S., Brandes, C., Helfrich-Förster, C., Hall, J.C., and Stanewsky, R. (2003). A Self-Sustaining, Light-Entrainable Circadian Oscillator in the Drosophila Brain. Curr. Biol. *13*, 1758–1767. Available at: https://www.sciencedirect.com/science/article/pii/S0960982203006997 [Accessed June 4, 2018].
26. Blanchardon, E., Grima, B., Klarsfeld, A., Chélot, E., Hardin, P.E., Préat, T., and Rouyer, F. (2001). Defining the role of Drosophila lateral neurons in the control of circadian rhythms in motor activity and eclosion by targeted genetic ablation and PERIOD protein overexpression. Eur. J. Neurosci. *13*, 871–888.
27. Emery, P., Stanewsky, R., Hall, J.C., and Rosbash, M. (2000). A unique circadian-rhythm photoreceptor. *404*, 456–457.
28. Myers, E.M., Jiujiu, Y., and Sehgal, A. (2003). Circadian Control of Eclosion: Interaction between a Central and Peripheral Clock in Drosophila melanogaster. Curr. Biol. *13*, 526–533.
29. Baik, L.S., Recinos, Y., Chevez, J.A., Au, D.D., and Holmes, T.C. (2019). Multiple Phototransduction Inputs Integrate to Mediate UV Light–evoked Avoidance/Attraction Behavior in Drosophila. J. Biol. Rhythms *34*, 391–400. Available at: http://journals.sagepub.com/doi/10.1177/0748730419847339 [Accessed August 3, 2020].
30. Baik, L.S., Recinos, Y., Chevez, J.A., Au, D.D., and Holmes, T.C. (2019). Multiple Phototransduction Inputs Integrate to Mediate UV Light–evoked Avoidance/Attraction Behavior in Drosophila. J. Biol. Rhythms *34*, 391–400.

31. Kistenpfennig, C., Grebler, R., Ogueta, M., Hermann-Luibl, C., Schlichting, M., Stanewsky, R., Senthilan, P.R., and Helfrich-Förster, C. (2017). A New Rhodopsin Influences Light-dependent Daily Activity Patterns of Fruit Flies. J. Biol. Rhythms *32*, 406–422.

32. Renn, S.C.P., Park, J.H., Rosbash, M., Hall, J.C., and Taghert, P.H. (1999). A pdf neuropeptide gene mutation and ablation of PDF neurons each cause severe abnormalities of behavioral circadian rhythms in Drosophila. Cell *99*, 791–802.

33. Nitabach, M.N., Blau, J., and Holmes, T.C. (2002). Electrical Silencing of Drosophila Pacemaker Neurons Stops the Free-Running Circadian Clock An important area of circadian rhythm research is the relationship between the function of the molecular clock in pacemaker neurons and the central physiological. Cell *109*, 485–495. Available at: https://ac.els-cdn.com/S0092867402007377/1-s2.0-S0092867402007377-main.pdf?_tid=191a407f-2f36-4e51-b468-c0c04bc18151&acdnat=1520814518_8b6e01a8d692d51fc76ec3f96a9757e8.

34. Peschel, N., Chen, K.F., Szabo, G., and Stanewsky, R. (2009). Light-dependent interactions between the Drosophila circadian clock factors cryptochrome, jetlag, and timeless. Curr. Biol. *19*, 241–7. Available at: http://www.sciencedirect.com/science/article/pii/S0960982208016977 [Accessed January 19, 2016].

35. Baik, L.S., Recinos, Y., Chevez, J.A., and Holmes, T.C. (2018). Circadian modulation of light-evoked avoidance/attraction behavior in Drosophila. PLoS One *13*, 1–14.

36. Fogle, K.J., Parson, K.G., Dahm, N.A., and Holmes, T.C. (2011). CRYPTOCHROME Is a Blue-Light Sensor That Regulates Neuronal Firing Rate. Science (80-.).

37. Collins, B., Mazzoni, E.O., Stanewsky, R., and Blau, J. (2006). Drosophila CRYPTOCHROME is a circadian transcriptional repressor. Curr. Biol. *16*, 441–449.

38. Sheeba, V., Fogle, K.J., Kaneko, M., Rashid, S., Chou, Y.-T., Sharma, V.K., and Holmes, T.C. (2008). Large ventral lateral neurons modulate arousal and sleep in Drosophila. Curr. Biol. *18*, 1537–45. Available at: http://www.pubmedcentral.nih.gov/articlerender.fcgi?artid=2597195&tool=pmcentrez&rendertype=abstract.

39. Konopka, R.J., and Benzer, S. (1971). Clock Mutants of Drosophila melanogaster. Proc. Natl. Acad. Sci. *68*, 2112–2116. Available at: https://www.pnas.org/content/68/9/2112 [Accessed August 3, 2020].

40. Agrawal, P., Houl, J.H., Gunawardhana, K.L., Liu, T., Zhou, J., Zoran, M.J., and Hardin, P.E. (2017). Drosophila CRY Entrains Clocks in Body Tissues to Light and Maintains Passive Membrane Properties in a Non-clock Body Tissue Independent of Light. Curr. Biol. *27*, 2431-2441.e3. Available at: http://dx.doi.org/10.1016/j.cub.2017.06.064.

41. Myers, M.P., Wager-Smith, K., Wesley, C.S., Young, M.W., and Sehgal, A. (1995). Positional cloning and sequence analysis of the Drosophila clock gene, timeless. Science (80-.). *270*, 805–808. Available at: https://science.sciencemag.org/content/270/5237/805 [Accessed August 2, 2020].

42. Emery, P., Stanewsky, R., Helfrich-Förster, C., Emery-Le, M., Hall, J.C., and Rosbash, M. (2000). Drosophila CRY is a deep brain circadian photoreceptor. Neuron *26*, 493–504.

43. Allada, R., White, N.E., So, W.V., Hall, J.C., and Rosbash, M. (1998). A mutant Drosophila homolog of mammalian clock disrupts circadian rhythms and transcription of period and timeless. Cell *93*, 791–804.

44. Nitabach, M.N., Blau, J., and Holmes, T.C. (2002). Electrical silencing of Drosophila pacemaker neurons stops the free-running circadian clock. Cell *109*, 485–495.

45. Potdar, S., and Sheeba, V. (2018). Wakefulness is promoted during day time by PDFR signalling to dopaminergic neurons in Drosophila melanogaster. eNeuro *5*. Available at: /pmc/articles/PMC6102377/?report=abstract [Accessed August 2, 2020].

46. Park, J.H. (2000). Differential regulation of circadian pacemaker output by separate clock genes in Drosophila. Proc. Natl. Acad. Sci. *97*, 3608–3613. Available at: http://www.pnas.org/cgi/doi/10.1073/pnas.070036197.

47. Im, S.H., Li, W., and Taghert, P.H. (2011). Pdfr and cry signaling converge in a subset of clock neurons to modulate the amplitude and phase of circadian behavior in Drosophila. PLoS One *6*.

48. Konopka, R.J., and Benzer, S. (1971). Clock mutants of Drosophila melanogaster. Proc. Natl. Acad. Sci. U. S. A. *68*, 2112–2116.

49. Hyun, S., Lee, Y., Hong, S.-T., Bang, S., Paik, D., Kang, J., Shin, J., Lee, J., Jeon, K., Hwang, S., *et al.* (2005). Drosophila GPCR Han Is a Receptor for the

Circadian Clock Neuropeptide PDF. Neuron *48*, 267–278.

50. Baik, L.S., Fogle, K.J., Roberts, L., Galschiodt, A.M., Chevez, J.A., Recinos, Y., Nguy, V., and Holmes, T.C. (2017). CRYPTOCHROME mediates behavioral executive choice in response to UV light. Proc. Natl. Acad. Sci.

51. Grima, B., Chélot, E., Xia, R., and Rouyer, F. (2004). Morning and evening peaks of activity rely on different clock neurons of the Drosophila brain. Nature *431*, 869–873.

52. Im, S.H., and Taghert, P.H. (2010). PDF receptor expression reveals direct interactions between circadian oscillators in drosophila. J. Comp. Neurol. *518*, 1925–1945.

53. Helfrich-Förster, C. (2003). The neuroarchitecture of the circadian clock in the brain of Drosophila melanogaster. Microsc. Res. Tech. *62*, 94–102.

54. Myers, M.P., Wager-Smith, K., Rothenfluh-Hilfiker, A., Young, M.W., Myers, M.P., Wager-smith, K., Rothenfluh-hilfiker, A., and Young, M.W. (1996). Light-Induced Degradation of TIMELESS and Entrainment of the Drosophila Circadian Clock Published by : American Association for the Advancement of Science Stable URL : http://www.jstor.org/stable/2890841 JSTOR is a not-for-profit service that helps schola. Science (80-.). *271*, 1736–1740.

55. Murad, A., Emery-Le, M., and Emery, P. (2007). A Subset of Dorsal Neurons Modulates Circadian Behavior and Light Responses in Drosophila. Neuron *53*, 689–701.

56. Baik, L.S., Nave, C., Au, D.D., Guda, T., Chevez, J.A., Ray, A., and Holmes, T.C. (2020). Circadian Regulation of Light-Evoked Attraction and Avoidance Behaviors

in Daytime- versus Nighttime-Biting Mosquitoes. Curr. Biol.

57. Kunst, M., Hughes, M.E., Raccuglia, D., Felix, M., Li, M., Barnett, G., Duah, J., and Nitabach, M.N. (2014). Calcitonin gene-related peptide neurons mediate sleep-specific circadian output in Drosophila. Curr. Biol. *24*, 2652–2664. Available at: http://dx.doi.org/10.1016/j.cub.2014.09.077.

58. Rhoades, S.D., Nayak, K., Zhang, S.L., Sehgal, A., and Weljie, A.M. (2018). Circadian- and Light-driven Metabolic Rhythms in Drosophila melanogaster. J. Biol. Rhythms *33*.

59. Guo, F., Yu, J., Jung, H.J., Abruzzi, K.C., Luo, W., Griffith, L.C., and Rosbash, M. (2016). Circadian neuron feedback controls the Drosophila sleep-activity profile. Nature *536*, 292–297. Available at: http://www.nature.com/articles/nature19097 [Accessed August 24, 2018].

60. Zhang, L., Chung, B.Y., Lear, B.C., Kilman, V.L., Liu, Y., Mahesh, G., Meissner, R.A., Hardin, P.E., and Allada, R. (2010). DN1p Circadian Neurons Coordinate Acute Light and PDF Inputs to Produce Robust Daily Behavior in Drosophila. Curr. Biol. *20*, 591–599. Available at: http://dx.doi.org/10.1016/j.cub.2010.02.056.

61. Vecsey, C.G., Pirez, N., and Griffith, L.C. (2014). The Drosophila neuropeptides PDF and sNPF have opposing electrophysiological and molecular effects on central neurons. J. Neurophysiol. *111*, 1033–1045. Available at: http://jn.physiology.org/cgi/doi/10.1152/jn.00712.2013.

62. Hall, J.C. (2005). Systems approaches to biological rhythms in Drosophila. Methods Enzymol. *393*, 61–185. Available at: http://www.sciencedirect.com/science/article/pii/S0076687905930048 [Accessed

January 19, 2016].

63. Im, S.H., Li, W., and Taghert, P.H. (2011). PDFR and CRY Signaling Converge in a Subset of Clock Neurons to Modulate the Amplitude and Phase of Circadian Behavior in Drosophila. PLoS One *6*, e18974. Available at: https://dx.plos.org/10.1371/journal.pone.0018974 [Accessed August 2, 2020].

64. Harper, R.E.F., Ogueta, M., Dayan, P., Stanewsky, R., and Albert, J.T. (2017). Light Dominates Peripheral Circadian Oscillations in Drosophila melanogaster During Sensory Conflict. J. Biol. Rhythms *32*, 423–432. Available at: http://www.ncbi.nlm.nih.gov/pubmed/28903626 [Accessed July 21, 2020].

65. Rieger, D., Shafer, O.T., Tomioka, K., and Helfrich-Förster, C. (2006). Functional analysis of circadian pacemaker neurons in Drosophila melanogaster. J. Neurosci. *26*, 2531–2543. Available at: http://rsb.info.nih.gov/ij/ [Accessed August 3, 2020].

66. Hyun, S., Lee, Y., Hong, S.T., Bang, S., Paik, D., Kang, J., Shin, J., Lee, J., Jeon, K., Hwang, S., *et al.* (2005). Drosophila GPCR han is a receptor for the circadian clock neuropeptide PDF. Neuron *48*, 267–278.

67. Mertens, I., Vandingenen, A., Johnson, E.C., Shafer, O.T., Li, W., Trigg, J.S., De Loof, A., Schoofs, L., and Taghert, P.H. (2005). PDF receptor signaling in Drosophila contributes to both circadian and geotactic behaviors. Neuron *48*, 213–219. Available at: https://www.sciencedirect.com/science/article/pii/S0896627305007762 [Accessed August 24, 2018].

68. Benito, J., Houl, J.H., Roman, G.W., and Hardin, P.E. (2008). The blue-light

photoreceptor CRYPTOCHROME is expressed in a subset of circadian oscillator neurons in the Drosophila CNS. J. Biol. Rhythms *23*, 296–307. Available at: http://journals.sagepub.com/doi/10.1177/0748730408318588 [Accessed May 4, 2018].

69. Yoshii, T., Todo, T., Wülbeck, C., Stanewsky, R., and Helfrich-Förster, C. (2008). Cryptochrome is present in the compound eyes and a subset ofDrosophila's clock neurons. J. Comp. Neurol. *508*, 952–966. Available at: http://doi.wiley.com/10.1002/cne.21702 [Accessed June 4, 2018].

70. Moore-Ede, M.C., Czeisler, C.A., and Richardson, G.S. (1983). Circadian Timekeeping in Health and Disease. N. Engl. J. Med. *309*, 469–476. Available at: http://www.nejm.org/doi/abs/10.1056/NEJM198308253090806 [Accessed May 4, 2018].

71. Hastings, M.H., Reddy, A.B., and Maywood, E.S. (2003). A clockwork web: circadian timing in brain and periphery, in health and disease. Nat. Rev. Neurosci. *4*, 649–661. Available at: http://www.nature.com/articles/nrn1177 [Accessed May 4, 2018].

72. Scheer, F.A.J.L., Hilton, M.F., Mantzoros, C.S., and Shea, S.A. (2009). Adverse metabolic and cardiovascular consequences of circadian misalignment. Proc. Natl. Acad. Sci. U. S. A. *106*, 4453–4458. Available at: http://www.pnas.org/content/106/11/4453.full.pdf?with-ds=yes [Accessed October 25, 2017].

73. Filipski, E., Delaunay, F., King, V.M., Wu, M.W., Claustrat, B., Gréchez-Cassiau, A., Guettier, C., Hastings, M.H., and Francis, L. (2004). Effects of chronic jet lag

on tumor progression in mice. Cancer Res. *64*, 7879–7885. Available at: http://www.ncbi.nlm.nih.gov/pubmed/14612524 [Accessed October 25, 2017].

74. Aschoff, J. (1984). Circadian timing. Ann. N. Y. Acad. Sci. *423*, 442–68. Available at: http://www.ncbi.nlm.nih.gov/pubmed/6588808 [Accessed August 23, 2018].

75. Labrecque, N., and Cermakian, N. (2015). Circadian Clocks in the Immune System. J. Biol. Rhythms *30*, 277–290. Available at: http://journals.sagepub.com/doi/10.1177/0748730415577723 [Accessed August 23, 2018].

76. Hardin, P.E. The Circadian Timekeeping System of Drosophila. Available at: https://ac.els-cdn.com/S0960982205009395/1-s2.0-S0960982205009395-main.pdf?_tid=c2ef38aa-bc1a-11e7-8466-00000aacb360&acdnat=1509221058_aa45ab1663c2fc7fea4d9e4432809336 [Accessed October 25, 2017].

77. Mimi Lee, W.-C., Yoshihara, M., and Troy Littleton, J. Cytoplasmic aggregates trap polyglutamine- containing proteins and block axonal transport in a Drosophila model of Huntington's disease. Available at: http://www.pnas.org/content/101/9/3224.full.pdf [Accessed September 12, 2017].

78. Morton, A.J. (2005). Disintegration of the Sleep-Wake Cycle and Circadian Timing in Huntington's Disease. J. Neurosci. *25*, 157–163. Available at: http://www.jneurosci.org/cgi/doi/10.1523/JNEUROSCI.3842-04.2005.

79. Askenasy, J.J.M. (2001). Approaching disturbed sleep in late Parkinson's disease: First step toward a proposal for a revised UPDRS. Park. Relat. Disord. *8*, 123–131.

80. Hatfield, C.F., Herbert, J., Van Someren, E.J.W., Hodges, J.R., and Hastings, M.H. (2004). Disrupted daily activity/rest cycles in relation to daily cortisol rhythms of home-dwelling patients with early Alzheimer's dementia. Brain *127*, 1061–1074.

81. Kaneko, M., Helfrich-Förster, C., and Hall, J.C. (1997). Spatial and temporal expression of the period and timeless genes in the developing nervous system of drosophila: Newly identified pacemaker candidates and novel features of clock gene product cycling. J. Neurosci. *17*, 6745–6760.

82. Kaneko, M., and Hall, J.C. (2000). Neuroanatomy of cells expressing clock genes in Drosophila: Transgenic manipulation of the period and timeless genes to mark the perikarya of circadian pacemaker neurons and their projections. J. Comp. Neurol. *422*, 66–94. Available at: http://doi.wiley.com/10.1002/%28SICI%291096-9861%2820000619%29422%3A1%3C66%3A%3AAID-CNE5%3E3.0.CO%3B2-2 [Accessed August 23, 2018].

83. Beckwith, E.J., and Ceriani, M.F. (2015). Communication between circadian clusters: The key to a plastic network. FEBS Lett. *589*, 3336–3342. Available at: http://dx.doi.org/10.1016/j.febslet.2015.08.017.

84. Nitabach, M.N., and Taghert, P.H. (2008). Organization of the Drosophila Circadian Control Circuit. Curr. Biol. *18*, 84–93.

85. Ueda, H.R., Hayashi, S., Chen, W., Sano, M., Machida, M., Shigeyoshi, Y., Iino, M., and Hashimoto, S. (2005). System-level identification of transcriptional circuits underlying mammalian circadian clocks. Nat. Genet. *37*, 187–192.

86. Tei, H., Okamura, H., and Shigeyoshi, Y. (1997). Circadian oscillation of a

mammalian homologue of the Drosophila period gene. *389*, 512–516.

87. Allada, R., Emery, P., Takahashi, J.S., and Rosbash, M. (2001). Stopping time: the genetics of fly and mouse circadian clocks. Annu. Rev. Neurosci. *24*, 1091–1119.

88. Duong, H.A., Robles, M.S., Knutti, D., and Weitz, C.J. (2011). A molecular mechanism for circadian clock negative feedback. Science (80-.). *332*, 1436–9.

89. Gonze, D., Bernard, S., Waltermann, C., Kramer, A., and Herzel, H. (2005). Spontaneous synchronization of coupled circadian oscillators. Biophys. J. *89*, 120–9. Available at: http://www.sciencedirect.com/science/article/pii/S0006349505726643.

90. Stanewsky, R., Kaneko, M., Emery, P., Beretta, B., Wager-Smith, K., Kay, S.A., Rosbash, M., and Hall, J.C. (1998). The cryb Mutation Identifies Cryptochrome as a Circadian Photoreceptor in Drosophila. Cell *95*, 681–692. Available at: https://www.sciencedirect.com/science/article/pii/S0092867400816384 [Accessed June 4, 2018].

91. Hunter-Ensor, M., Ousley, A., and Sehgal, A. (1996). Regulation of the Drosophila protein timeless suggests a mechanism for resetting the circadian clock by light. Cell *84*, 677–685. Available at: https://www.sciencedirect.com/science/article/pii/S0092867400810466?via%3Dihub [Accessed August 24, 2018].

92. Zeng, H., Qian, Z., Myers, M.P., and Rosbash, M. (1996). A light-entrainment mechanism for the drosophila circadian clock. Nature *380*, 129–135. Available at: http://www.nature.com/doifinder/10.1038/380129a0 [Accessed August 24, 2018].

93. Sheeba, V. (2008). The Drosophila melanogaster circadian pacemaker circuit. J. Genet. *87*, 485–493.

94. Crowley, S.J., Acebo, C., and Carskadon, M.A. (2007). Sleep, circadian rhythms, and delayed phase in adolescence. Sleep Med. *8*, 602–612. Available at: http://www.ncbi.nlm.nih.gov/pubmed/17383934 [Accessed June 4, 2018].

95. Roberts, L., Leise, T.L.L., Noguchi, T., Galschiodt, A.M.M., Houl, J.H.H., Welsh, D.K.K., and Holmes, T.C.C. (2015). Light Evokes Rapid Circadian Network Oscillator Desynchrony Followed by Gradual Phase Retuning of Synchrony. Curr. Biol. *25*, 858–867. Available at: http://www.ncbi.nlm.nih.gov/pubmed/25754644 [Accessed May 4, 2018].

96. Papagiannakopoulos, T., Bauer, M.R., Davidson, S.M., Heimann, M., Subbaraj, L., Bhutkar, A., Bartlebaugh, J., Vander Heiden, M.G., and Jacks, T. (2016). Circadian Rhythm Disruption Promotes Lung Tumorigenesis. Cell Metab. *24*, 324–331. Available at: http://dx.doi.org/10.1016/j.cmet.2016.07.001 [Accessed September 12, 2017].

97. Hamada, T., LeSauter, J., Venuti, J.M., and Silver, R. (2001). Expression of period genes: Rhythmic and nonrhythmic compartments of the suprachiasmatic nucleus pacemaker. J. Neurosci. *21*, 7742–7750.

98. Yamaguchi, S., Isejima, H., Matsuo, T., Okura, R., Yagita, K., Kobayashi, M., and Okamura, H. (2003). Synchronization of Cellular Clocks in the Suprachiasmatic Nucleus. Science (80-.). *302*, 1408–1412.

99. Azzi, A., Evans, J.A., Leise, T., Myung, J., Takumi, T., Davidson, A.J., and Brown, S.A. (2017). Network Dynamics Mediate Circadian Clock Plasticity. Neuron *93*,

441–450. Available at: http://dx.doi.org/10.1016/j.neuron.2016.12.022 [Accessed December 28, 2019].

100. Evans, J.A., Leise, T.L., Castanon-Cervantes, O., and Davidson, A.J. (2013). Dynamic Interactions Mediated by Nonredundant Signaling Mechanisms Couple Circadian Clock Neurons. Neuron *80*, 973–983.

101. Quintero, J.E., Kuhlman, S.J., and McMahon, D.G. (2003). The biological clock nucleus: A multiphasic oscillator network regulated by light. J. Neurosci. *23*, 8070–8076.

102. Schaap, J., Pennartz, C.M.A., and Meijer, J.H. (2003). Electrophysiology of the circadian pacemaker in mammals. Chronobiol. Int. *20*, 171–188.

103. Moga, M.M., and Moore, R.Y. (1997). Organization of neural inputs to the suprachiasmatic nucleus in the rat. J. Comp. Neurol. *389*, 508–534.

104. Fogle, K.J., Parson, K.G., Dahm, N.A., and Holmes, T.C. (2011). Cryptochrome is a blue-light sensor that regulates neuronal firing rate. Science (80-.). *331*, 1409–1413. Available at: http://www.ncbi.nlm.nih.gov/pubmed/21385718 [Accessed May 4, 2018].

105. Sakai, K., Tsutsui, K., Yamashita, T., Iwabe, N., Takahashi, K., Wada, A., and Shichida, Y. (2017). Drosophila melanogaster rhodopsin Rh7 is a UV-to-visible light sensor with an extraordinarily broad absorption spectrum. Sci. Rep. *7*, 7349. Available at: http://www.ncbi.nlm.nih.gov/pubmed/28779161 [Accessed December 28, 2019].

106. Helfrich-Förster, C., Winter, C., Hofbauer, A., Hall, J.C., and Stanewsky, R. (2001). The circadian clock of fruit flies is blind after elimination of all known

photoreceptors. Neuron *30*, 249–261.

107. Li, M.-T.T., Cao, L.-H.H., Xiao, N., Tang, M., Deng, B., Yang, T., Yoshii, T., and Luo, D.-G.G. (2018). Hub-organized parallel circuits of central circadian pacemaker neurons for visual photoentrainment in Drosophila. Nat. Commun. *9*, 4247. Available at: http://www.nature.com/articles/s41467-018-06506-5 [Accessed June 9, 2019].

108. Roberts, L., Leise, T.L., Welsh, D.K., and Holmes, T.C. (2016). Functional Contributions of Strong and Weak Cellular Oscillators to Synchrony and Light-shifted Phase Dynamics. J. Biol. Rhythms *XX*, 1–15. Available at: http://journals.sagepub.com/doi/10.1177/0748730416649550 [Accessed May 4, 2018].

109. Hege, D.M., Stanewsky, R., Hall, J.C., and Giebultowicz, J.M. (1997). Rhythmic Expression of a PER-Reporter in the Malpighian Tubules of Decapitated Drosophila: Evidence for a Brain-Independent Circadian Clock. J. Biol. Rhythms *12*, 300–308.

110. Zerr, D.M., Hall, J.C., Rosbash, M., and Siwicki, K.K. (1990). Circadian fluctuations of period protein immunoreactivity in the CNS and the visual system of drosophila. J. Neurosci. *10*, 2749–2762.

111. Maywood, E.S., Reddy, A.B., Wong, G.K.Y., O'Neill, J.S., O'Brien, J.A., McMahon, D.G., Harmar, A.J., Okamura, H., and Hastings, M.H. (2006). Synchronization and maintenance of timekeeping in suprachiasmatic circadian clock cells by neuropeptidergic signaling. Curr. Biol. *16*, 599–605.

112. Johard, H.A.D., Yoishii, T., Dircksen, H., Cusumano, P., Rouyer, F., Helfrich-

Förster, C., and Nässel, D.R. (2009). Peptidergic clock neurons in Drosophila: Ion transport peptide and short neuropeptide F in subsets of dorsal and ventral lateral neurons. J. Comp. Neurol. *516*, 59–73.

113. Shafer, O.T., and Yao, Z. (2014). Pigment-dispersing factor signaling and circadian rhythms in insect locomotor activity. Curr. Opin. Insect Sci. *1*, 73–80.
114. Jones, J.R., Simon, T., Lones, L., and Herzog, E.D. (2018). SCN VIP neurons are essential for normal light-mediated resetting of the circadian system. J. Neurosci. *38*, 7986–7995. Available at: http://www.ncbi.nlm.nih.gov/pubmed/30082421 [Accessed December 28, 2019].
115. Seugnet, L., Suzuki, Y., Stidd, R., and Shaw, P.J. (2009). Aversive phototaxic suppression: evaluation of a short-term memory assay in *Drosophila melanogaster*. Genes, Brain Behav. *8*, 377–389. Available at: http://doi.wiley.com/10.1111/j.1601-183X.2009.00483.x [Accessed May 4, 2018].
116. Emery, P., So, W.V., Kaneko, M., Hall, J.C., and Rosbash, M. (1998). Cry, a Drosophila clock and light-regulated cryptochrome, is a major contributor to circadian rhythm resetting and photosensitivity. Cell *95*, 669–679.
117. Dolezelova, E., Dolezel, D., and Hall, J.C. Rhythm Defects Caused by Newly Engineered Null Mutations in Drosophila's cryptochrome Gene.
118. Hendricks, J.C., Finn, S.M., Panckeri, K.A., Chavkin, J., Williams, J.A., Sehgal, A., and Pack, A.I. (2000). Rest in Drosophila is a sleep-like state. Neuron *25*, 129–138.
119. Tononi, G. (2000). Correlates of sleep and waking in Drosophila melanogaster. Science (80-.). *287*, 1834–1837. Available at:

http://www.ncbi.nlm.nih.gov/pubmed/10710313 [Accessed May 4, 2018].

120. Stickgold, R., Hobson, J.A., Fosse, R., and Fosse, M. (2001). Sleep, learning, and dreams: Off-line memory reprocessing. Science (80-.). *294*, 1052–1057. Available at: http://www.ncbi.nlm.nih.gov/pubmed/11691983 [Accessed May 4, 2018].

121. Donlea, J.M., Thimgan, M.S., Suzuki, Y., Gottschalk, L., and Shaw, P.J. (2011). Inducing sleep by remote control facilitates memory consolidation in Drosophila. Science (80-.). *332*, 1571–1576. Available at: http://www.sciencemag.org/cgi/doi/10.1126/science.1202249 [Accessed May 4, 2018].

122. Shafer, O.T., Rosbash, M., and Truman, J.W. (2002). Sequential nuclear accumulation of the clock proteins period and timeless in the pacemaker neurons of Drosophila melanogaster. J. Neurosci. *22*, 5946–5954.

123. Baik, L.S., Nave, C., Au, D.D., Guda, T., Chevez, J.A., Ray, A., and Holmes, T.C. (2020). Circadian Regulation of Light-Evoked Attraction and Avoidance Behaviors in Daytime- versus Nighttime-Biting Mosquitoes. Curr. Biol., 1–8. Available at: https://doi.org/10.1016/j.cub.2020.06.010.

124. Baik, L.S., Au, D.D., Nave, C., Foden, A.J., Enrriquez-Villalva, W.K., and Holmes, T.C. (2019). Distinct mechanisms of Drosophila CRYPTOCHROME-mediated light-evoked membrane depolarization and in vivo clock resetting. Proc. Natl. Acad. Sci. U. S. A. *116*, 23339–23344.

125. Barber, A.F., Erion, R., Holmes, T.C., and Sehgal, A. (2016). Circadian and feeding cues integrate to drive rhythms of physiology in Drosophila insulin-

producing cells. Genes Dev. *30*, 2596–2606.

126. Cavanaugh, D.J., Geratowski, J.D., Wooltorton, J.R.A., Spaethling, J.M., Hector, C.E., Zheng, X., Johnson, E.C., Eberwine, J.H., and Sehgal, A. (2014). Identification of a circadian output circuit for rest: Activity rhythms in drosophila. Cell *157*, 689–701. Available at: http://dx.doi.org/10.1016/j.cell.2014.02.024.

127. Parisky, K.M., Agosto, J., Pulver, S.R., Shang, Y., Kuklin, E., Hodge, J.J.L., Kang, K., Kang, K., Liu, X., Garrity, P.A., *et al.* (2008). PDF cells are a GABA-responsive wake-promoting component of the Drosophila sleep circuit. Neuron *60*, 672–82. Available at: http://www.sciencedirect.com/science/article/pii/S0896627308009422 [Accessed May 18, 2016].

128. Guo, F., Chen, X., and Rosbash, M. (2017). Temporal calcium profiling of specific circadian neurons in freely moving flies. Proc. Natl. Acad. Sci. U. S. A. *114*, E8780–E8787. Available at: http://www.ncbi.nlm.nih.gov/pubmed/28973886 [Accessed August 24, 2018].

129. Czeisler, C.A., Duffy, J.F., Shanahan, T.L., Brown, E.N., Jude, F., Rimmer, D.W., Ronda, J.M., Silva, E.J., Allan, J.S., Jonathan, S., *et al.* (1999). Stability, precision, and near-24-hour period of the human circadian pacemaker. Science (80-.). *284*, 2177–2181.

130. Stothard, E.R., McHill, A.W., Depner, C.M., Birks, B.R., Moehlman, T.M., Ritchie, H.K., Guzzetti, J.R., Chinoy, E.D., LeBourgeois, M.K., Axelsson, J., *et al.* (2017). Circadian Entrainment to the Natural Light-Dark Cycle across Seasons and the Weekend. Curr. Biol. *27*, 508–513.

CHAPTER 4

Circadian Regulation of Light-Evoked Attraction and Avoidance Behaviors in Daytime- versus Nighttime- Biting Mosquitoes

(Baik, Nave, et al.)

Abstract

Mosquitoes pose widespread threats to humans and other animals as disease vectors [1]. Day- versus night-biting mosquitoes occupy distinct time-of-day niches [2, 3]. Here, we explore day- versus night-biting female and male mosquitoes' innate temporal attraction/avoidance behavioral responses to light and their regulation by circadian circuit and molecular mechanisms. Day-biting mosquitoes *Aedes aegypti*, particularly females, are attracted to light during the day regardless of spectra. In contrast, night-biting mosquitoes, *Anopheles coluzzii*, specifically avoid ultraviolet (UV) and blue light during the day. Behavioral attraction to/avoidance of light in both species change with time of day and show distinct sex and circadian neural circuit differences. Males of both diurnal and nocturnal mosquito species show reduced UV light avoidance in anticipation of evening onset relative to females. The circadian neural circuits of diurnal/day- and nocturnal/ night-biting mosquitoes based on PERIOD (PER) and pigment-dispersing factor (PDF) expression show similar but distinct circuit organizations between species. The basis of diurnal versus nocturnal behaviors is driven by molecular clock timing, which cycles in anti-phase between day- versus night-biting mosquitoes. Observed differences at the neural circuit and protein levels provide insight into the fundamental basis

underlying diurnality versus nocturnality. Molecular disruption of the circadian clock severely interferes with light-evoked attraction/avoidance behaviors in mosquitoes. In summary, attraction/avoidance behaviors show marked differences between day- versus night-biting mosquitoes, but both classes of mosquitoes are circadian, and light-regulated, which may be applied toward species-specific control of harmful mosquitoes.

4.1 Introduction

Mosquito-spread diseases may have contributed to the deaths of half of all the people who have ever lived [1]. Toxic pesticides are environmentally harmful in contrast to relatively safe light-based insect control approaches. However, light-based insect controls do not typically take into consideration the day versus night behavioral profiles that change with daily light:dark (LD) cycles. Insects display a wide range of short-wavelength light modulated behaviors, including attraction/avoidance [4–11]. It has been long assumed that insect responses to ultraviolet (UV) light are mediated by external photoreceptors including opsins in the eyes. Mosquitoes and flies additionally express non-opsin photoreceptors including the blue- and UV-light-sensitive CRYPTOCHROME (CRY) [12]. Recent work in flies shows that CRY mediates a wide range of behavioral responses to blue and UV light, including circadian-modulated attraction/avoidance [4–6].

Different mosquito species have evolved distinct circadian timing of behaviors according to their temporal/ecological niches. Some mosquito species are diurnal (i.e., *Aedes aegypti*) whereas others are nocturnal (i.e., *Anopheles coluzzii*). Numerous mosquito behaviors change with time of day, including flight activity, mating, oviposition, and biting [2, 3, 13–17]. Circadian clocks are light entrained and altered light timing disrupts circadian behaviors [2, 3, 10, 11, 13]. Despite their large impact on health and ecology, little is known about the basis of diurnality/nocturnality and behavioral timing in mosquitoes. We chose to investigate diurnal *Ae. aegypti* and nocturnal *An. coluzzii* mosquitoes based on comparative circadian interest and because both are anthropophilic mosquitoes that are major vectors of many human diseases.

4.2 Materials and Methods

Mosquito rearing and maintenance

Mosquitoes were reared at 27°C, 70%–80% relative humidity with a photoperiod of 12 hr:12 hr light: dark cycle. Mosquito larvae were fed Tetramin Tropical fish food (Tetra GMBH, Melle Germany). All larvae were kept in plastic containers until pupation, then transferred into a small paper cup containing deionized water and moved to a 30cm$_2$ Bugdorm mosquito cage to eclose. Emerged mosquitoes were fed 10% sucrose *ad libitum* and allowed to mate prior to all experiments.

Light Attraction/Avoidance Behavior Assay

All mosquitoes were reared in standard 12-hr: 12-hr light: dark (LD) schedule in 27°C, and 80% humidity in large cages with access to 10% sucrose diet. Adult mosquitoes (0-5 days post-eclosion) were entrained to LD schedule for minimum of 3 days prior to testing. Individual mosquitoes were each placed into 25mm diameter x 125 mm length Pyrex glass tubes (25mm diameter x 125mm length, TriKinetics) plugged with cotton “flugs” (Genesee) on either side. Flugs were soaked with 10% sucrose providing a food source, while simultaneously allowing airflow sufficient for multi-day survival of the mosquitoes in the tubes. Tubes containing individual mosquitoes were placed in humidity-, temperature-, and light-controlled incubator and allowed to acclimate for a full day. One half of the tubes were covered with infrared (IR) filters (LEE Filters 4 × 4” Infrared (87C) Polyester Filter), providing the mosquitoes with a choice of a shaded environment (IR filtered) versus light-exposed (not covered with IR filter) during the 12 hr of light (daytime). Philips TL-D Blacklight ultraviolet light (UV) source with narrow peak

wavelength of 365 nm and intensity of ~400 μW/cm$_2$ was used for UV light. Blue (450 nm, Supernight) and red (630 nm, Supernight) LED strips set at ~400 μW/cm$_2$ was used as blue and red-light sources. Light intensities were determined by a Newport 843-R Power/Energy Meter with Newport 818-UV Sensor. Additionally, IR LED strips (Infrared 850 nm 3528 LED Strip Light, 78/m, 8mm wide, by the 5 m Reel) placed on aluminum heat sink was placed under the entire setup which allowed dark imaging of mosquitoes. With each light source, same LD schedule as the LD entrainment schedule prior to experiment was continued to minimize any disturbance to the circadian time. For constant light (LL) light choice assay, the UV light was constantly left on. Webcam (Microsoft Q2F-00013 USB 2.0 LifeCam) took pictures at 10 min intervals for 3-5 days of experiment. Each mosquito's preference in the light-exposed versus shaded side of the tube was analyzed by the ImageJ program. Preference for the light-exposed or the shaded-environment, quantified as preference %. Each experiment was repeated a minimum of three times for each group. Related to Figures 1, 4, and S1.

Immunocytochemistry

All mosquitoes were reared in standard 12 hr: 12 hr light: dark (LD) schedule at 27°C, and 80% humidity in large cages, with access to 10% sucrose diet. Mosquito brains were dissected 5-10 days post-eclosion at times specified in the manuscript. All dissections, staining, and imaging were carried out in an exact same manner for all conditions for fair comparison. Brains were dissected in 1X PBS in the dark with dim red light source, fixed in 4% paraformaldehyde (PFA) for 30 min, washed 3X 10 min in PBS-Triton-X 1%, incubated in blocking buffer (10% Horse Serum-PBS-Triton-X 0.5%) at room temperature before incubation with mouse α-PDF C7, monoclonal (1:10,000) and rabbit

α-PER, polyclonal (1:1,000) antibodies overnight in 4°C. Primary antibody incubated brains were then washed 3X 10 min in PBS-Triton-X 0.5% then incubated in goat α-mouse-Alexa 488 (1:500) and goat α-rabbit-Alexa-594 (1:500) secondary antibodies in blocking buffer overnight in 4°C. Brains were washed 5X 15min in PBS-Triton-X 0.5% before mounting in VectaShield mounting media (Vector Laboratories). Microscopy was performed using Zeiss LSM700 confocal microscope. All settings for confocal microscope was kept the same across all samples, including laser power, gain, objective (20x), averaging per frame (x2), etc. Then fluorescence intensities were analyzed and represented as raw images using Imaris and ImageJ (not manipulated by Photoshop or any other photo manipulation program). All representative images in this manuscript are also raw images, not manipulated for intensity, gain, etc. unless noted otherwise in the figure legend and normalized to background fluorescence in areas outside of the imaged brain. Each condition was carried out over a minimum of 3 separate tests to further minimize any experimental variability. Related to Figures 2, 4, and S2–S4 and Table S1.

Quantification and Statistical Analysis

Mosquito preference behavior was quantified as present or not present in light-exposed versus shaded sides of the tube. This binary preference for each 10 min time points over 3-5 days was averaged per individual mosquito (n = individual mosquito). Individual preferences were then further averaged for each group. Preference behavior statistical measurements including significance were analyzed by t test using Microsoft Excel and Sigma Plot. Related to Figures 1, 4, and S1.

For immunocytochemistry, fluorescence levels were analyzed using Imaris software (Bitplane). Spherical region of interest was selected for each cell based on

anatomical location and size. Fluorescence was quantified for each region by the Imaris software. Each species time point was collected for minimum of three repetitions. Each n represents one brain. Reported quantification values reflect the average fluorescence intensity levels and error bars indicate SEM. Statistical measurements including significance was defined using t test using Microsoft Excel and Sigma Plot. Related to Figures 3, 4, S3, and S4.

4.3 Results

4.3.1 Light-Evoked Attraction/Avoidance Behaviors in Diurnal and Nocturnal Mosquitoes Are Species, Sex, and Spectrum Dependent and Change with Time of Day

To measure behavioral attraction to/avoidance of light in mosquitoes, we developed a custom-designed arena (Figure 1A). 12 h:12 h light:dark (LD) circadian-entrained young adult diurnal (*Ae. aegypti*) and nocturnal (*An. coluzzii*) mosquitoes were presented with a choice of light-exposed versus shaded environments during the subjective daytime (zeitgeber time [ZT] 0–12). Light intensity was set to 400 μW/cm$_2$, which is a relatively high intensity light that is within a natural physiological and environmental range. Light was continuously kept on during the subjective daytime (12 h; ZT 0–12) and then turned off during the subjective nighttime (12 h; ZT 12–24), maintaining the prior LD entrainment and thus the circadian clock unperturbed. Diurnal versus nocturnal mosquito species exhibit striking differences in their light-evoked attraction/avoidance behavior. Diurnal *Ae. aegypti* females are behaviorally attracted to UV light during the day and remain in the same general spatial area at night that they occupied previously during the day (Figures 1B, 1H, and 1I). In contrast, nocturnal *An. coluzzii* females strongly avoid UV light during most of the daytime and occupy the previously illuminated spatial area at night that they avoided during the day (Figures 1C, 1H, and 1I). Both species females shift behavioral attraction/avoidance as dusk approaches in anticipation of the simulated night (Figures 1B–1D and 1F). We observe this change in behavior despite the light stimulus remaining constant during the daytime, indicating that this is likely a circadian-modulated behavior in anticipation of approaching

nighttime. The “anticipatory” afternoon behavioral shift begins around midafternoon (~ZT 7) for diurnal *Ae. aegypti* females (Figures 1B and 1D). In contrast, nocturnal *An. coluzzii* females show sharp decreases in UV light avoidance starting about an hour before dusk (~ZT 11) (Figures 1C and 1F).

Mosquitoes are highly sexually dimorphic; male mosquitoes’ primary needs are to feed on nectar and to mate, whereas females additionally need to seek blood-meal hosts and oviposition sites. Male mosquitoes swarm earlier in anticipation of females [14, 15, 16]. The timing of male swarm roughly coincides with or precedes the timing of the female anticipatory behavioral shift we observed in UV light attraction/avoidance (Figures 1D and 1F) [14]. Thus, we considered the possibility of sex differences for light environmental preference. Diurnal *Ae. aegypti* males are attracted to UV light during the late subjective daytime (Figures 1B and 1E), but to a significantly lesser extent than females, which are attracted to UV light throughout the entire day. Nocturnal *An. coluzzii* males strongly avoid UV light, similar to *An. coluzzii* females (Figures 1C and 1H). Both species show sex-specific differences in timing of anticipatory behavioral shifts in attraction to/avoidance of light approaching dusk. *Ae. aegypti* light attraction peaks earlier in males (~ZT 10) than in females (~ZT 12) (Figures 1B, 1D, and 1E). Similarly, as dusk approaches, *An. coluzzii* males show an earlier behavioral shift in avoidance/attraction than females in anticipation of dusk (Figures 1C, 1F, and 1G). Sex-dependent differences persist even after the UV light is turned off, which simulates the subjective nighttime (ZT 12–24). Nighttime preference for previously UV-light-exposed environment is significantly higher in females, compared to males in both species (Figure 1I).

The color spectral preference of attraction/avoidance behavior varies between different insect species [4, 5, 8, 9, 18]. A dipteran, *Drosophila melanogaster*, avoids short-wavelength light during midday but not long-wavelength light [4, 5, 6]. We examined spectral dependence of mosquito attraction to/avoidance of light, using intensity-matched visible short-wavelength blue light and visible long-wavelength red light for comparison with UV light behavior at the same light intensity (400 μW/cm2). Diurnal *Ae. aegypti* females are attracted to both blue and red light during the day, comparable to their UV light attraction (Figures S1A, S1C, and S1E). In contrast, nocturnal *An. coluzzii* females, which strongly avoid UV light (Figure 1), avoid blue light during the day but to a significantly lesser extent than UV light (Figures S1B and S1E). Significantly different from their avoidance of blue and UV light, female *An. coluzzii* are attracted to red light (Figures S1D and S1E). During the nighttime, females of both species prefer environments with prior UV light exposure, significantly higher than their weaker nighttime preference for areas with prior blue or red light exposure (Figure S1F). We conclude that behavioral attraction to/avoidance of light are wavelength dependent and differ in both overall valence and anticipation of dusk between nocturnal and diurnal mosquito species.

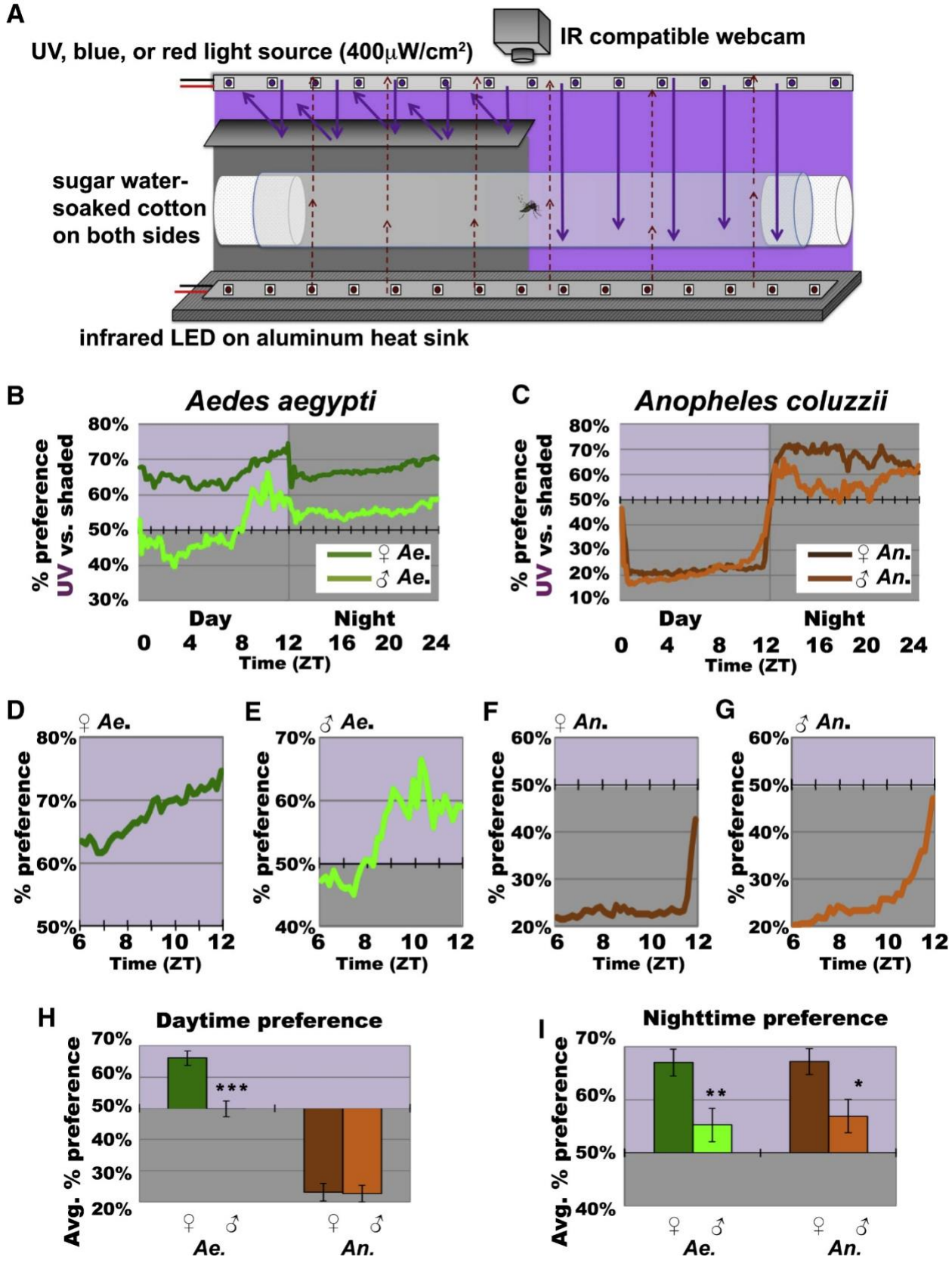
A
UV, blue, or red light source (400μW/cm²)
IR compatible webcam
sugar water-soaked cotton on both sides
infrared LED on aluminum heat sink
B
Aedes aegypti
% preference UV vs. shaded
♀ Ae.
♂ Ae.
Day
Night
Time (ZT)
C
Anopheles coluzzii
♀ An.
♂ An.
D
♀ Ae.
E
♂ Ae.
F
♀ An.
G
♂ An.
H
Daytime preference
Avg. % preference
***
Ae.
An.
I
Nighttime preference
**
*

Figure 1. UV-Light-Evoked Attraction/Avoidance Responses in Diurnal and Nocturnal Mosquitoes Are Species and Sex Dependent. (A) Schematic of mosquito light-evoked attraction/avoidance preference behavioral assay setup. (B and C) Attraction/avoidance behavior to UV light, measured by % of preference in UV-exposed versus shaded environment throughout 12 h:12 h UV light:dark (LD) for (B) female *Ae. aegypti* (dark green; n = 110) and male *Ae. aegypti* (light green; n = 61) and (C) female *An. coluzzii* (brown; n = 64) and male *An. coluzzii* (orange; n = 47). (D–G) Attraction/avoidance behavior to UV light, measured by % of preference in UV-exposed versus shaded environment during zeitgeber time (ZT) 6–12 for (D) female *Ae. aegypti*, (E) male *Ae. aegypti*, (F) female *An. coluzzii*, and (G) male *An. coluzzii*. (H and I) Average attraction/avoidance behavioral preference to UV-light-exposed versus shaded environment by *Ae. aegypti* and *An. coluzzii* female and male mosquitoes for (H) daytime (light violet background indicates illuminated area) and (I) nighttime (light violet background indicates previously illuminated area). Data are represented as mean ± SEM. $^{*}p < 0.05$, $^{**}p < 0.01$, $^{***}p < 0.001$ versus female. See also Figure S1.

4.3.2 Diurnal versus Nocturnal Mosquitoes Have Similar yet Distinct Circadian Neuronal Circuits

We anatomically mapped the circadian neuronal network in the central brain of female diurnal and nocturnal mosquitoes. Insect circadian neuronal circuits are defined by the cyclic expression of the highly conserved clock protein PERIOD (PER) that drives rhythmic changes in physiology and behavior. Pigment-dispersing factor (PDF) is a highly conserved neuropeptide co-expressed with PER in the small- and large-lateral ventral neurons (s-LNvs and l-LNvs) that modulate circadian- and light-mediated behaviors such as locomotion, sleep, arousal, and light attraction/avoidance in *D. melanogaster* [4, 5, 19, 20, 21]. Antibodies against *Drosophila* PER label circadian neurons in a broad range of other insects [22, 23, 24]. The use of *Drosophila* PER or PDF antibodies has been validated in insects that are much more distantly related to *Drosophila* than mosquitoes are (i.e., in the lepidopteran *Antheraea pernyi* silk moth and the hymenopteran *Apis mellifera* honeybee) whereas *D. melanogaster* and mosquitoes are more closely related dipterans [23, 24]. Thus, we reasoned that *Drosophila* PER, and PDF antibodies can effectively label PER and PDF proteins in mosquitoes.

We find PER and PDF are co-expressed in the lateral ventral area in both *Ae. aegypti* and *An. coluzzii* female adult brains (Figures 2 and S2; Table S1). These PDF^{+} and PER^{+} neurons can be further distinguished as l-LNvs and s-LNvs (Figures 2 and S2). Other neuronal groups include putative dorsal neurons (DNs) (Figures 2 and S2). There are large neuronal arbors in the optic lobes and dorsal projections to the DNs from the PDF^{+} LNvs [21] (Figures 2, S2, S3A–S3H, and S4A–S4H; Videos

S1 and S2). In *An. coluzzii*, the PDF+ LNv dorsal projections continue medially to the pars intercerebralis (PI) region; this projection pattern is not observed in *Ae. aegypti* (Figures 2, S3A–S3D, and S4A–S4D). Another species-specific feature is that the contralateral projection of PDF+ LNvs crosses the midline in the early daytime in *An. coluzzii* but not in *Ae. aegypti* (Figures 2, S3A–S3D, and S4A–S4D). Approximately 5 PER+/PDF− neurons found in the medial-anterior region of *Ae. aegypti* female brains, which we call medial-anterior neurons (m-ANs) here, are not detected in *An. coluzzii* (Figures 2 and S2). Another species-specific neuronal group includes ~7 PER+/PDF− neurons in the PI region in *An. coluzzii*, which are not detected in *Ae. aegypti* (Figures 2 and S2; Table S1). Thus, there are both similar and species-distinct features of the circadian neuronal circuits of diurnal *Ae. aegypti* and nocturnal *An. coluzzii*.

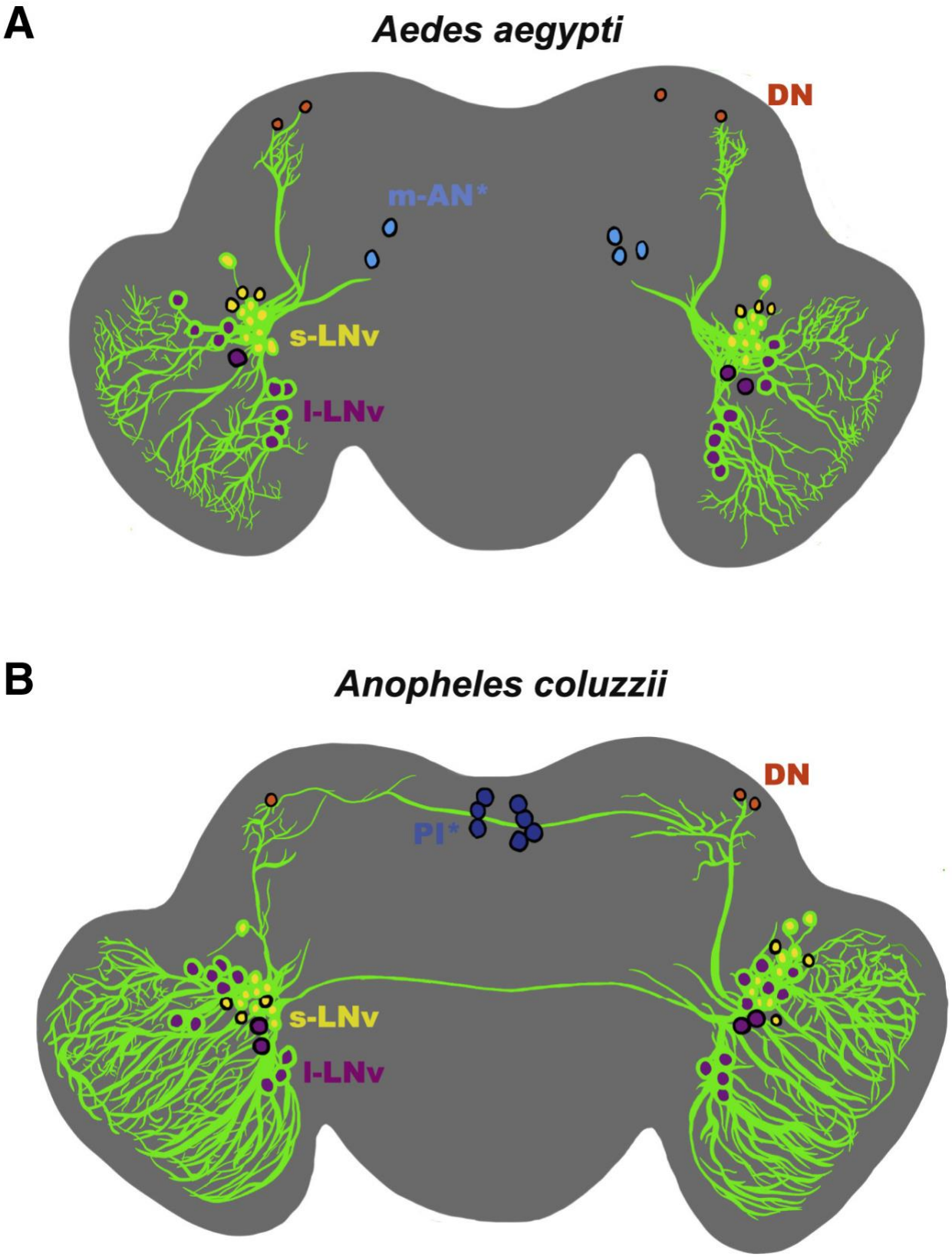
A
Aedes aegypti
DN
m-AN*
s-LNv
l-LNv
B
Anopheles coluzzii
DN
PI*
s-LNv
l-LNv
green outline = PDF+

Figure 2. Schematic Representation of *Ae. aegypti* and *An. coluzzii* Circadian Neuronal Circuits. Illustrations of representative adult female central brains and their neuronal expression of PER and/or PDF with projections depicted in black. Asterisks indicates groups distinct for each species. PDF^{+} neurons and their arbors are indicated with green outline. (A) *Ae. aegypti* s-LNv in yellow, l-LNv in violet, DNs in orange, and m-AN in light blue. (B) *An. coluzzii* s-LNv in yellow, l-LNv in violet, DNs in orange, and PI neurons in dark blue. See also Figures S2–S4, Table S1, and Videos S1 and S2.

4.3.3 Molecular Clock of Diurnal versus Nocturnal Mosquitoes in PDF+ LNv Circadian Neurons Oscillates in an Anti-Phasic Manner

To examine the timing of the molecular clock underlying diurnal and nocturnal mosquitoes, we measured PER and PDF protein oscillation over 24 h at 6-h intervals in the brains of *Ae. aegypti* and *An. coluzzii* female mosquitoes. PER protein cycles robustly in both *Ae. aegypti* and *An. coluzzii* circadian neurons. PER_{+}/PDF_{+} LNv axonal projections undergo structural remodeling with time of day for both *Ae. aegypti* and *An. coluzzii* (Figures S3A–S3D and S4A–S4D). Notably, PER oscillates in opposite phases between diurnal *Ae. aegypti* versus nocturnal *An. coluzzii* PDF_{+} LNv circadian neurons (Figure 3). PER protein levels peak in late night/early day in PDF_{+} s-LNvs and l-LNvs of the diurnal mosquito *Ae. aegypti* (Figures 3A, 3C, and 3D). In contrast, PER protein levels peak in late day/early night in PDF_{+} s-LNvs and l-LNvs of the nocturnal mosquito *An. coluzzii* (Figures 3B, 3E, and 3F). In addition to PER oscillation, PDF protein levels in s-LNvs and l-LNvs of nocturnal *An. coluzzii* oscillate with its peak expression in early night (Figures S4I and S4J). In contrast, PDF protein levels peak in early day in s-LNvs and l-LNvs of diurnal *Ae. aegypti*, but its oscillation is less clear (Figures S3I and S3J). Diurnal and nocturnal mosquitoes have distinct circadian clock protein phases and circadian neuronal architecture in the brain that suggests a possible mechanism for diurnality and nocturnality.

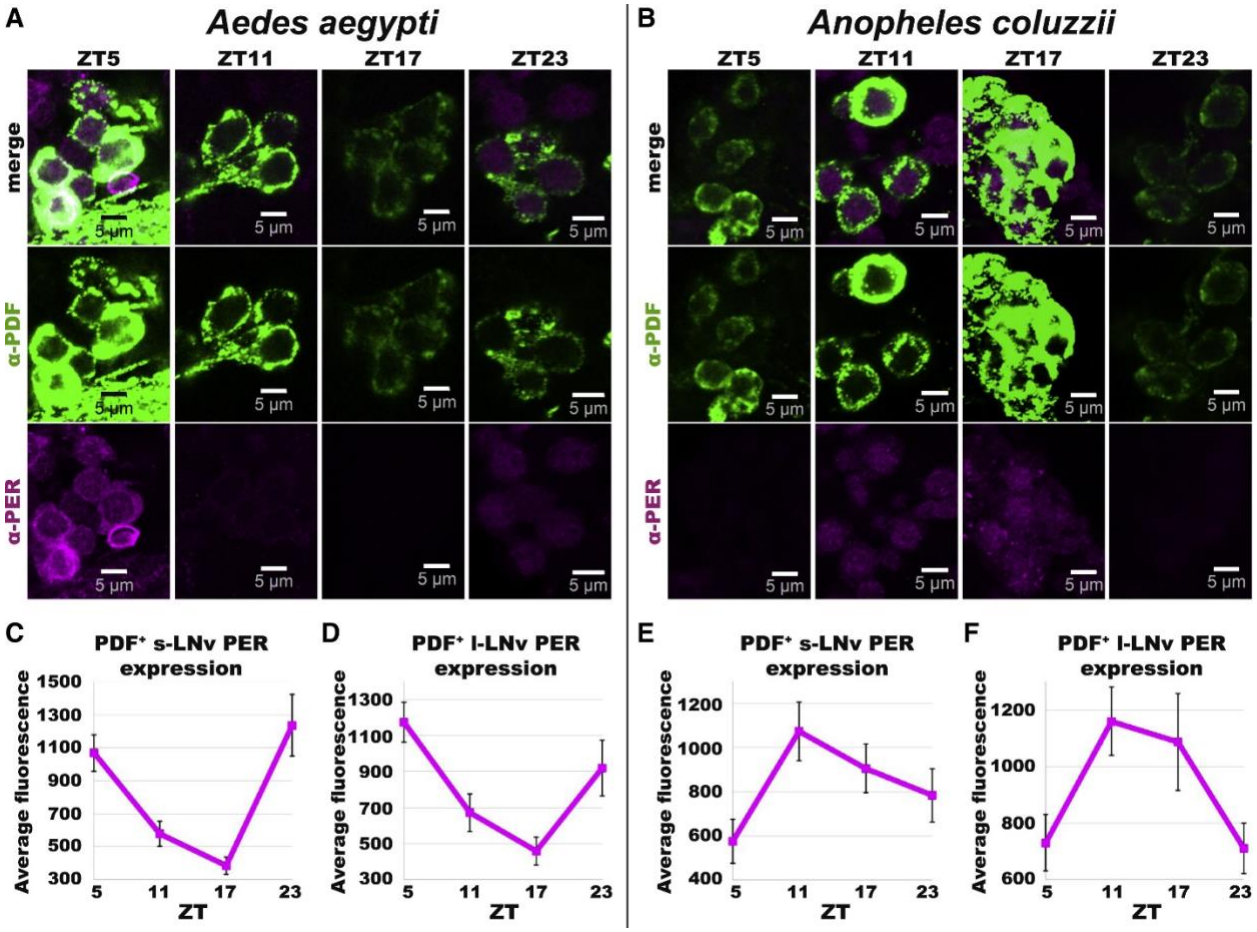

Figure 3. Diurnal versus Nocturnal Mosquito PER Expression in PDF+ LNv Neurons Oscillates in an Anti-Phasic Manner. (A and B) Representative confocal images of adult female (A) *Ae. aegypti* and (B) *An. coluzzii* mosquito LNv immunocytochemistry stained with α-PER (magenta) and α-PDF (green) antibodies at ZT 5, 11, 17, and 23. Scale bars indicate 5 μm.**.** (C–F) PERIOD expression levels over 24 h for *Ae. aegypti* (ZT 5, n = 27; ZT 11, n = 17; ZT 17, n = 6; ZT 23, n = 7) (C) s-LNv and (D) l-LNv, and *An. coluzzii* (ZT 5, n = 13; ZT 11, n = 31; ZT 17, n = 9; ZT 23, n = 8) (E) s-LNv and (F) l-LNv. Data are represented as mean ± SEM. See also Figures S2–S4 and Videos S1 and S2.

4.3.4 Constant Light Exposure Disrupts Circadian Protein Expression and the Timing of Behavioral Attraction to/Avoidance of UV Light in Mosquitoes

Constant light (LL) condition disrupts circadian clock gene expression and rhythmic behaviors in many animals, including mosquitoes [2, 3, 25, 26]. In *D. melanogaster*, LL disrupts the core clock protein oscillation, behavioral valence, and circadian timing of attraction to/avoidance of light via a circadian UV/blue light sensor, CRY [5, 6, 26]. In mosquitoes, the LL condition disrupts the cycling of core circadian genes and clock modulation of behaviors including locomotor rhythm, anticipation behavior, and timing of oviposition [3, 10, 27, 28, 29, 30].

By using LL circadian clock disruption, we tested whether the circadian clock modulates the valence and timing of behavioral attraction to/avoidance of light. Following LD entrainment, female mosquitoes were exposed to constant UV light (UV LL) for 3–5 days. Then, we measured circadian protein levels corresponding to species-specific PER peak times using anti-PER and anti-PDF immunocytochemistry. Similar to LL-induced disruption at the mRNA level [30], PER protein levels were severely reduced in mosquito brains following UV LL compared to LD in both *Ae. aegypti* and *An. coluzzii* (Figures 4A–4D). In many brains, PER protein levels in LNvs could not be quantified because there was no visible PER staining following UV LL (data not shown).

D. melanogaster has UV light avoidance that peaks in the midday, coinciding with their low locomotor activity “siesta,” followed by a behavioral shift from avoidance to attraction in anticipation of dusk, like mosquitoes. In *Drosophila*, this shift in attraction/avoidance is disrupted in flies with core clock gene knockout, circadian neuronal silencing, or LL-induced circadian clock disruptions [5, 6]. To examine the

functional link between the circadian clock and behavioral attraction to/avoidance of light, we measured the behavioral preference under the clock-disrupting UV LL condition. During UV LL, both mosquito species lack clear time-of-day-dependent changes in UV attraction/avoidance behavior, including the anticipatory behavioral shift approaching dusk (Figures 4E–4H). *Ae. aegypti* females show attraction to UV light regardless of time of day (Figures 4E and 4G). *An. coluzzii* females show loss of day-versus-night differences in avoidance/attraction, and overall lack any clear valence for either light environment under the UV LL condition (Figures 4F and 4H). LL-induced circadian clock disruption severely disrupted the timing of UV-evoked attraction/avoidance behavior in both diurnal and nocturnal mosquitoes, which strongly resembles findings in *Drosophila* using either the same LL protocol or tests of genetic clock gene nulls [5, 6].

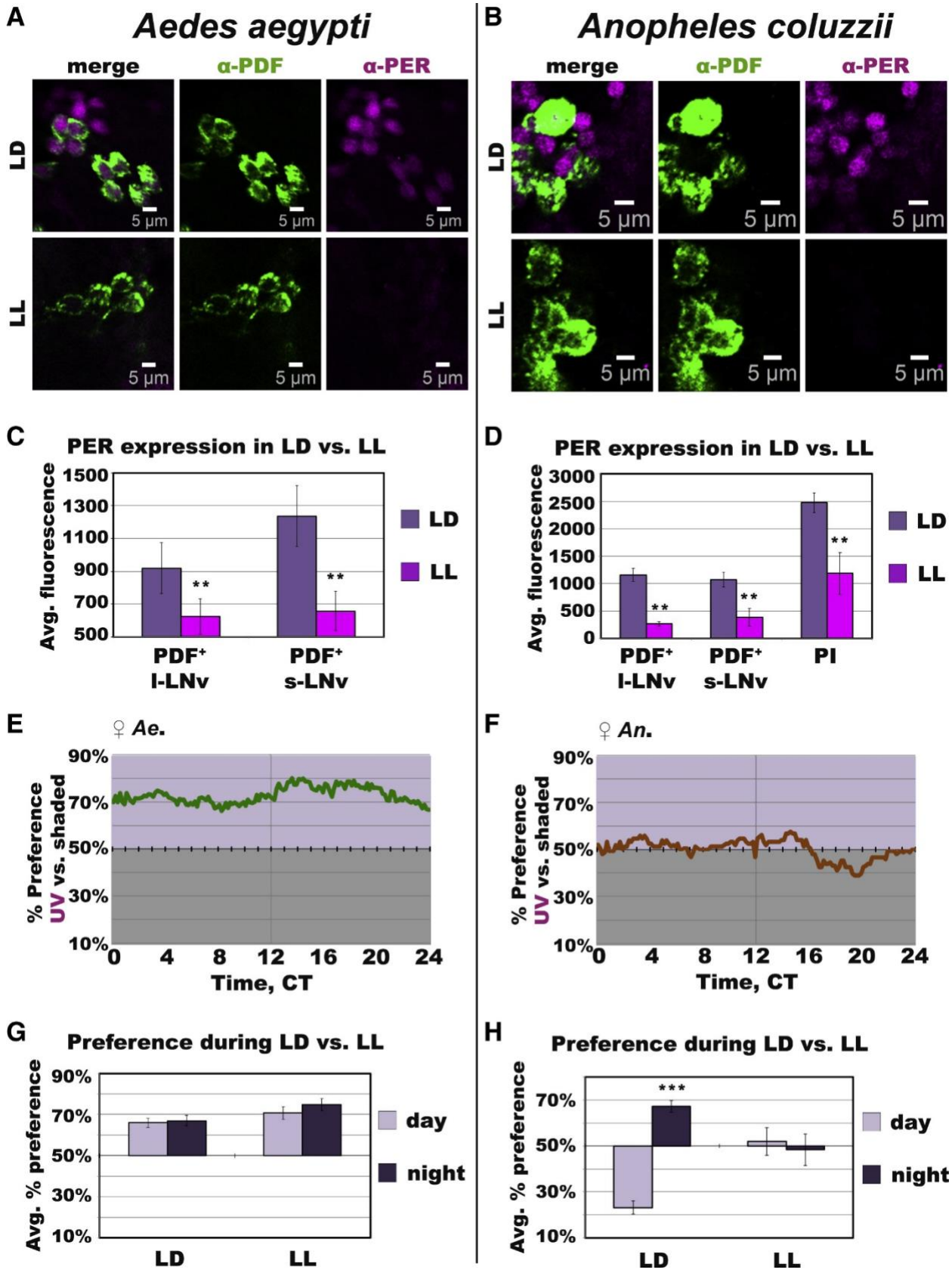
A
Aedes aegypti
merge
α-PDF
α-PER
LD
LL
5 µm
B
Anopheles coluzzii
C
PER expression in LD vs. LL
Avg. fluorescence
1500
1300
1100
900
700
500
**
PDF+ l-LNv
PDF+ s-LNv
LD
LL
D
PER expression in LD vs. LL
3000
2500
2000
1500
1000
500
0
PDF+ l-LNv
PDF+ s-LNv
PI
E
♀ Ae.
% Preference UV vs. shaded
90%
70%
50%
30%
10%
0
4
8
12
16
20
24
Time, CT
F
♀ An.
G
Preference during LD vs. LL
Avg. % preference
day
night
H
***

Figure 4. Constant UV Light (UV LL) Exposure Disrupts Circadian Protein Expression and Clock Modulation of Attraction/Avoidance Behavioral Responses to UV Light in Mosquitoes. (A and B) Representative confocal images of anti-PER (magenta) and anti-PDF (green) immunocytochemistry stained adult female mosquito brains under 12 h:12 h LD or following UV LL exposure for (A) *Ae. aegypti* and (B) *An. coluzzii*. Scale bars indicate 5 μm. (C and D) Average fluorescence intensity of circadian neurons under LD (light violet) versus LL (magenta) conditions for (C) *Ae. aegypti* ZT/CT 23 (LD, n = 7; LL, n = 13) and (D) *An. coluzzii* ZT/CT 11 (LD, n = 31; LL, n = 6). (E and F) Attraction/avoidance behavior to UV light, measured by % of preference in UV-exposed versus shaded environments during UV LL for female (E) *Ae. aegypti* and (F) *An. Coluzzii*. (G and H) Average attraction/avoidance behavioral preference to light-exposed versus shaded environments during subjective daytime (light violet) versus nighttime (dark violet) under LD or LL conditions for (G) *Ae. aegypti* and (H) *An. coluzzii* female mosquitoes.Data are represented as mean ± SEM. $^{*}p < 0.05$, $^{**}p < 0.01$, $^{***}p < 0.001$ versus LD or day. See also Figure S2.

4.4 Discussion

Different mosquito species have evolved to occupy distinct temporal niches, likely to minimize inter-species competition and optimize their chance of mating, biting, and overall survival. In addition to diurnality versus nocturnality, *Ae. aegypti* and *An. coluzzii* are behaviorally and ecologically unique. Diurnal *Aedine* mosquitoes are aggressive biters that maintain relatively high activity levels and take multiple blood meals within a same gonotropic cycle [3, 30, 31]. In contrast, nocturnal *Anopheline* mosquitoes are relatively quiescent especially during the day and mainly target defenseless hosts that are sleeping at night [2, 15]. The timing of species- and sex-specific behavioral attraction to/avoidance of light we describe here coincides with the ecological timing of these mosquito species' increased flight activity, mating, and host-seeking behaviors [2, 3, 13, 14, 15, 16, 17]. For instance, the sex-specific difference in *An. coluzzii* behavioral attraction to/avoidance of light is mainly observed in the late afternoon and nighttime, which is the most ecologically relevant and active time for this species.

We find that diurnal *Ae. aegypti* are attracted to a wide range of light spectra during the daytime whereas nocturnal *An. coluzzii* are strongly photophobic to short-wavelength light. Our results suggest that timing and spectra must be considered when targeting specific mosquitoes. For instance, the use of high-intensity UV light during the day may not be effective in attracting nocturnal mosquitoes. Controlling the timing and light spectra may allow targeting of specific mosquito species using environmentally friendly light-based approaches [32].

A wide range of behaviors in mosquitoes and other insects are temporally modulated by light, including mating, seeking a blood meal, biting, oviposition, flight

activity, and sleep [2, 3, 13, 14, 15, 16, 17]. Light treatments that alter circadian function also disrupt biting, flight activity, and oviposition behaviors in mosquitoes [2, 3, 10, 11, 13]. Both *Ae. aegypti* and *An. coluzzii* exhibit behavioral shifts in attraction/avoidance in anticipation of dusk, despite no change in the light stimulus itself. Our characterization of light-evoked attraction/avoidance behavior in mosquitoes shows timing features that suggest that these processes are under circadian regulation, similar to that of *D. melanogaster* [4, 5, 6]. The disruption of circadian protein expression and loss of UV-evoked attraction/avoidance anticipatory behavior under the clock-disrupting LL condition are clear evidence that UV attraction/avoidance are circadian-clock-modulated behaviors. The timing of the anticipatory behavioral shift in UV avoidance/attraction is distinct between diurnal versus nocturnal mosquitoes, supporting the idea that change in avoidance/attraction behavior may contribute to temporal niches occupied by each species.

In the more extensively studied circadian neural network, that of *D. melanogaster*, there are ~150 circadian neurons [33]. In comparison, we find that *Ae. aegypti* and *An. coluzzii* have only about ~80–90 circadian neurons in total. The largest difference between *D. melanogaster* and mosquitoes is that both mosquitoes have only a few DNs (~90 DNs in flies versus only ~4 in the two mosquito species tested). LNvs, on the other hand, are much more abundant in both mosquitoes tested than in *D. melanogaster* (~10 or 11 LNvs in flies versus ~25–30 in mosquitoes). Other interesting groups of neurons are the mosquito-species-specific neuronal groups m-ANs of *Ae. aegypti* and PI neurons of *An. coluzzii*, which are not PER+ in *Drosophila*. PI neurons in many other insect species express PER (reviewed in [34]). In *D. melanogaster*, PI neurons are not PER+ yet are

circadian rhythmic due to clock neuronal inputs [35, 36]. PDF is a critical neural peptide in circadian neuronal signaling working in close neuronal proximity. In *D. melanogaster*, PDF^+ s-LNv axon terminal structures undergo temporal oscillation to modulate circadian neural signaling [36, 37]. Similarly, we find that axon terminals of PDF^+ LNvs of both mosquito species undergo structural remodeling according to time of day. Further investigation of the circadian neural circuit dynamics may reveal the principles of the clock-coding mechanism of mosquitoes.

In addition to circuit-level differences, PER protein oscillates in an anti-phasic manner between diurnal and nocturnal mosquitoes. Anti-phasic oscillation is not observed at the DNA and mRNA levels [30, 31, 38, 39]. It has been demonstrated in cyanobacteria, *Drosophila*, and mice that post-translational modification of core circadian proteins modulates protein stability, phasic expression, and nuclear translocation, which are essential in the timing of the clock and its behavioral outputs [26, 40, 41, 42, 43, 44, 45, 46]. Our qualitative analysis suggests nuclear PER peaks at opposite times between diurnal versus nocturnal mosquitoes: PER peaks in the late nighttime (~ZT 23) in *Ae. aegypti* versus in the late daytime (~ZT 11) in *An. coluzzii* (Figure 3), which can be further confirmed with nuclear markers. Furthermore, the circadian clock in non-suprachiasmatic nucleus neurons and periphery tissues cycles in opposite phases in diurnal versus nocturnal mammals [47, 48, 49]. These findings along with our findings of the circuit-level differences and anti-phasic oscillation of core circadian proteins point to a potential mechanism underlying diurnal versus nocturnal behaviors.

4.5 Supplementary Figures

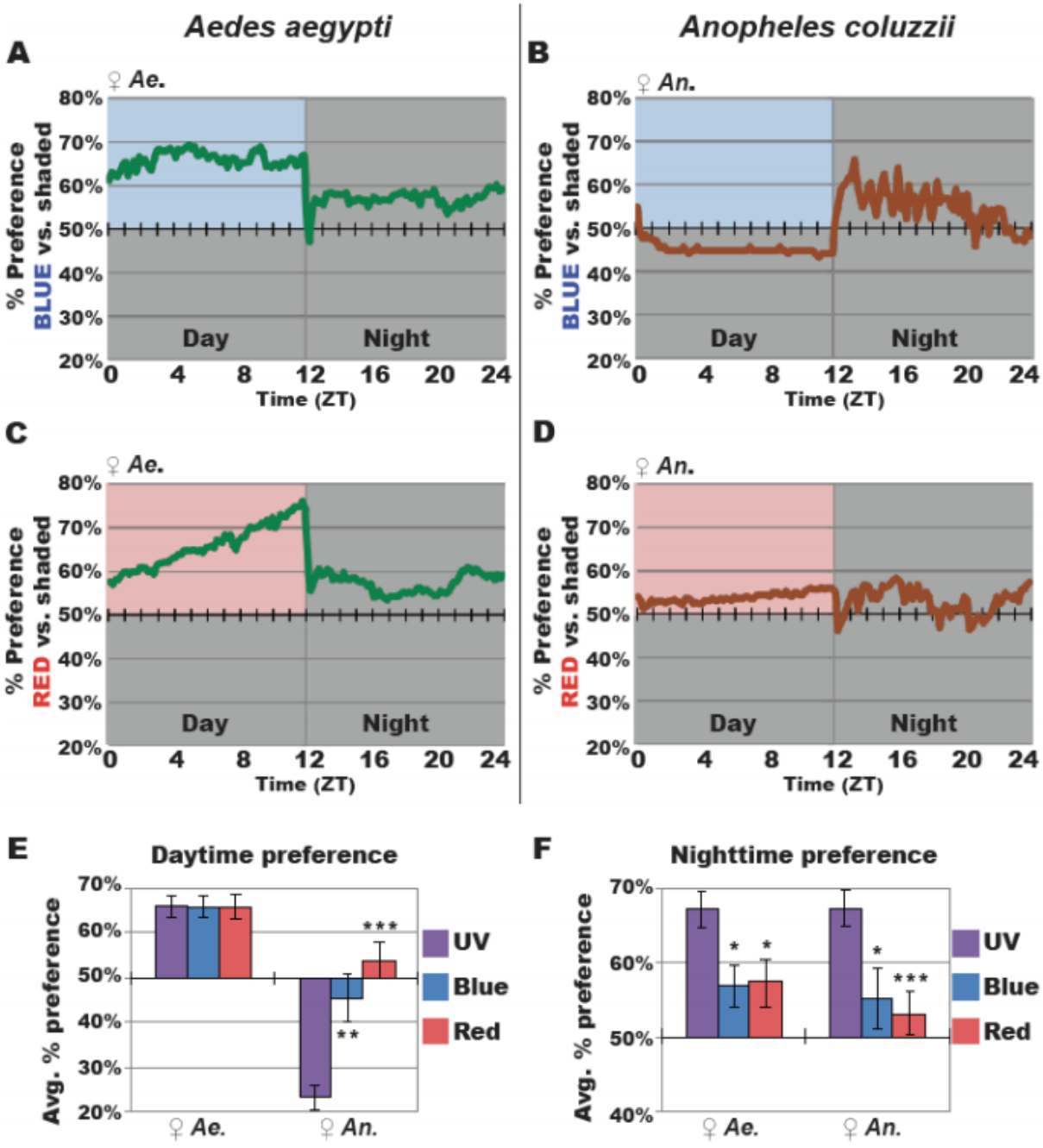

Figure S1. Mosquito light-evoked attraction/avoidance behavior is wavelength-specific, Related to Figure 1. (A-B) Attraction/avoidance behavior to blue light (450 nm LED, 400 μW/cm2), measured by % preference in blue light-exposed versus shaded environment throughout 12 hr: 12 hr blue light: dark for female (A) *Ae. aegypti* (n=78) and (B) *An. coluzzii* (n=34). (C-D) Attraction/avoidance behavior to red light (620 nm LED, 400 μW/cm2), measured by % preference in red light-exposed versus shaded environment throughout 12hr: 12hr red light:dark for female (C) *Ae. aegypti* (n=62) and (D) *An. coluzzii* (n=52). (E-F) Average attraction/avoidance behavioral preference to light-exposed (UV, blue and red) versus shaded-environment for (E) daytime and (F) nighttime in *Ae. aegypti* and *An. coluzzii* female mosquitoes. Data are represented as mean ± S.E.M. *p < 0.05; **p < 0.01; ***p < 0.001 vs. UV.

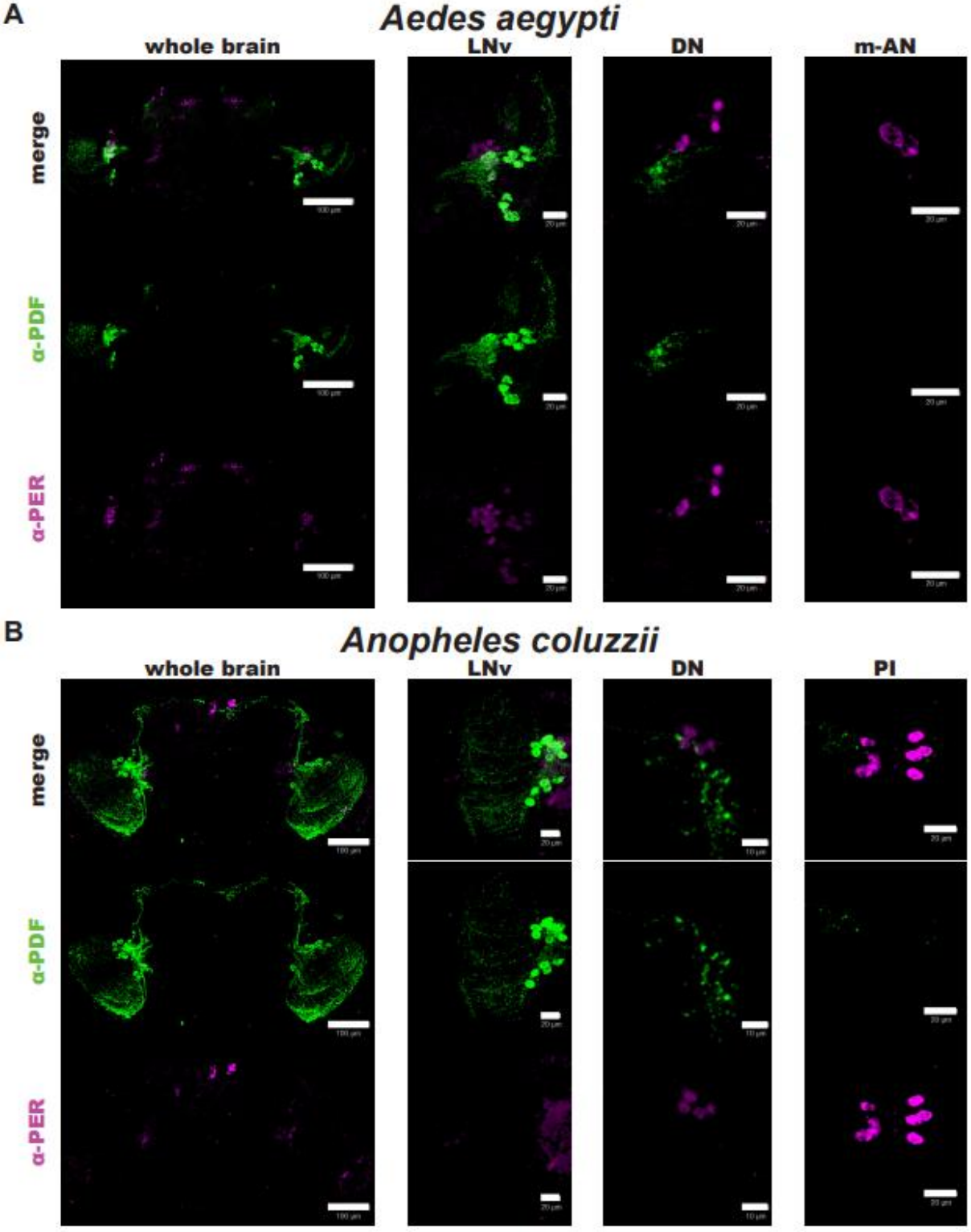
A
Aedes aegypti
whole brain
LNv
DN
m-AN
merge
α-PDF
α-PER
B
Anopheles coluzzii
whole brain
LNv
DN
PI
merge
α-PDF
α-PER

Figure S2. Circadian neuronal circuit of diurnal and nocturnal mosquito brains, Related to Figure 2, Figure 3 and Figure 4. (A-B) Representative confocal images of adult female (A) *Ae. aegypti* and (B) *An. coluzzii* mosquito brains immunocytochemistry stained with α–PER (magenta) and α–PDF (green) antibodies. Similar to *Drosophila*, neurites from PDF+ LNv neurons project dorsally towards the DNs in *Ae. aegypti*. In *An. coluzzii* brains, PDF+ LNv neurites project dorsally towards to the DNs and then extend medially towards the PER+ PI neurons. Images shown in whole brain panels were collected from single brain samples using a “tiling” option during image acquisition to capture the entire image field of the whole brain sample (2 tiles of 1024 x 1024 pixels). Post-acquisition images were enhanced uniformly throughout the entire image field for intensity and contrast to show the full extent of the arbors and cell bodies. *Scale bars indicate 100µm for whole brains, 10µm for *An. coluzzii* DN, and 20µm all others.

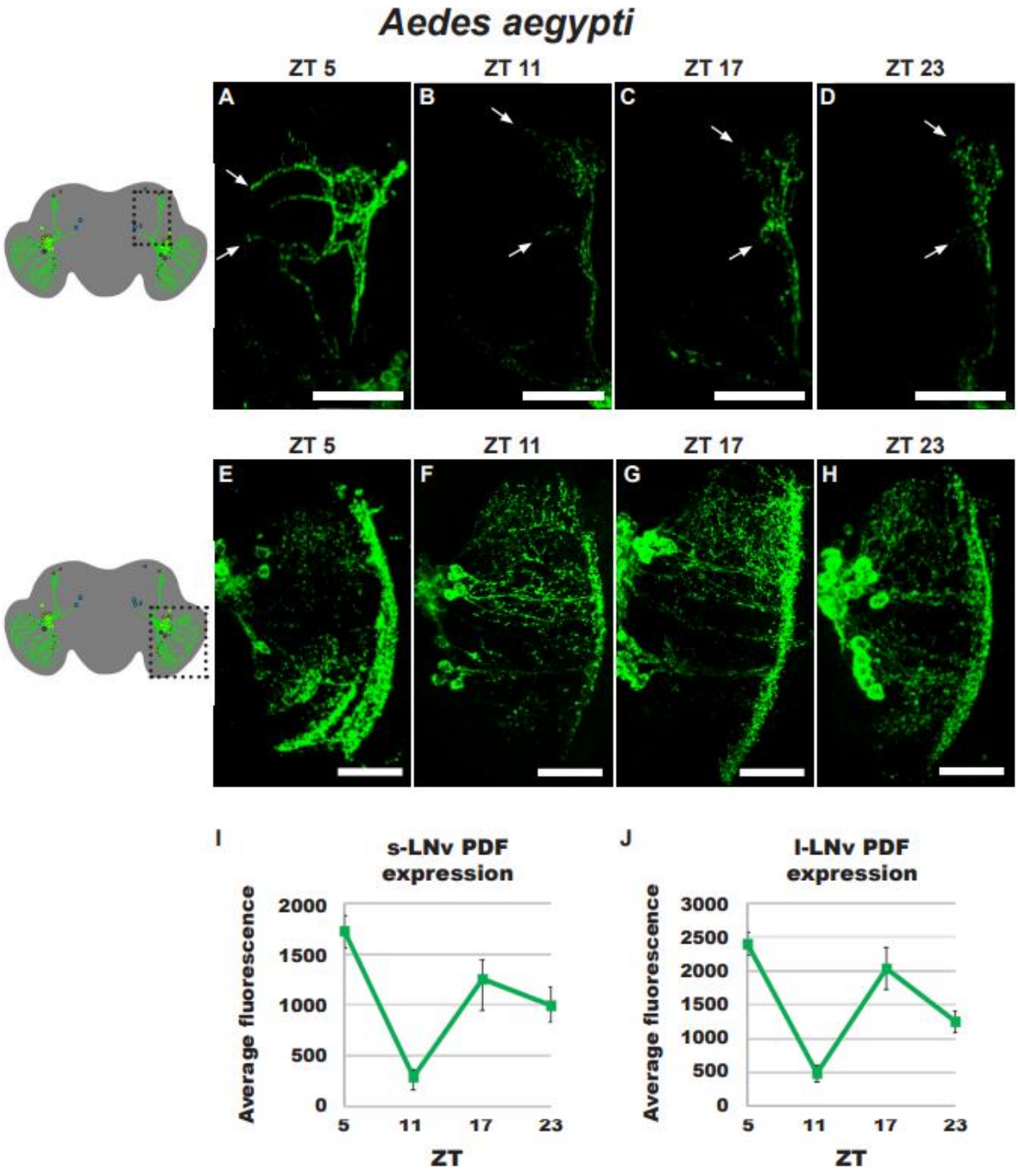

Figure S3. PDF+ neurons and in *Aedes aegypti* female brains, Related to Figure 2 and Figure 3. (A-D) Representative confocal images of adult female *Ae. aegypti* brains immunocytochemistry stained with α–PDF (green) antibody, zoomed in on LNv dorsal

projections at (A) ZT5, (B) ZT11, (C) ZT17, and (D) ZT23. White arrows indicate the ends of LNv neuronal arbors. These images were enhanced for intensity and contrast to better show the ends of the arbors. *Scale bars indicate 50 µm. (E-H) Representative confocal images of adult female *Ae. aegypti* brains immunocytochemistry stained with α–PDF (green) antibody, zoomed in on an optic lobe at (E) ZT5, (F) ZT11, (G) ZT17, and (H) ZT23. These images were enhanced for intensity and contrast to better show the ends of the arbors. *Scale bars indicate 50 µm. (I-J) PDF expression levels over 24 hrs time for *Ae. aegypti* (ZT5, n=27; ZT11, n=17; ZT17, n=6, ZT23, n=7) (I) s-LNv and (J) l-LNv. Data are represented as mean ± S.E.M.

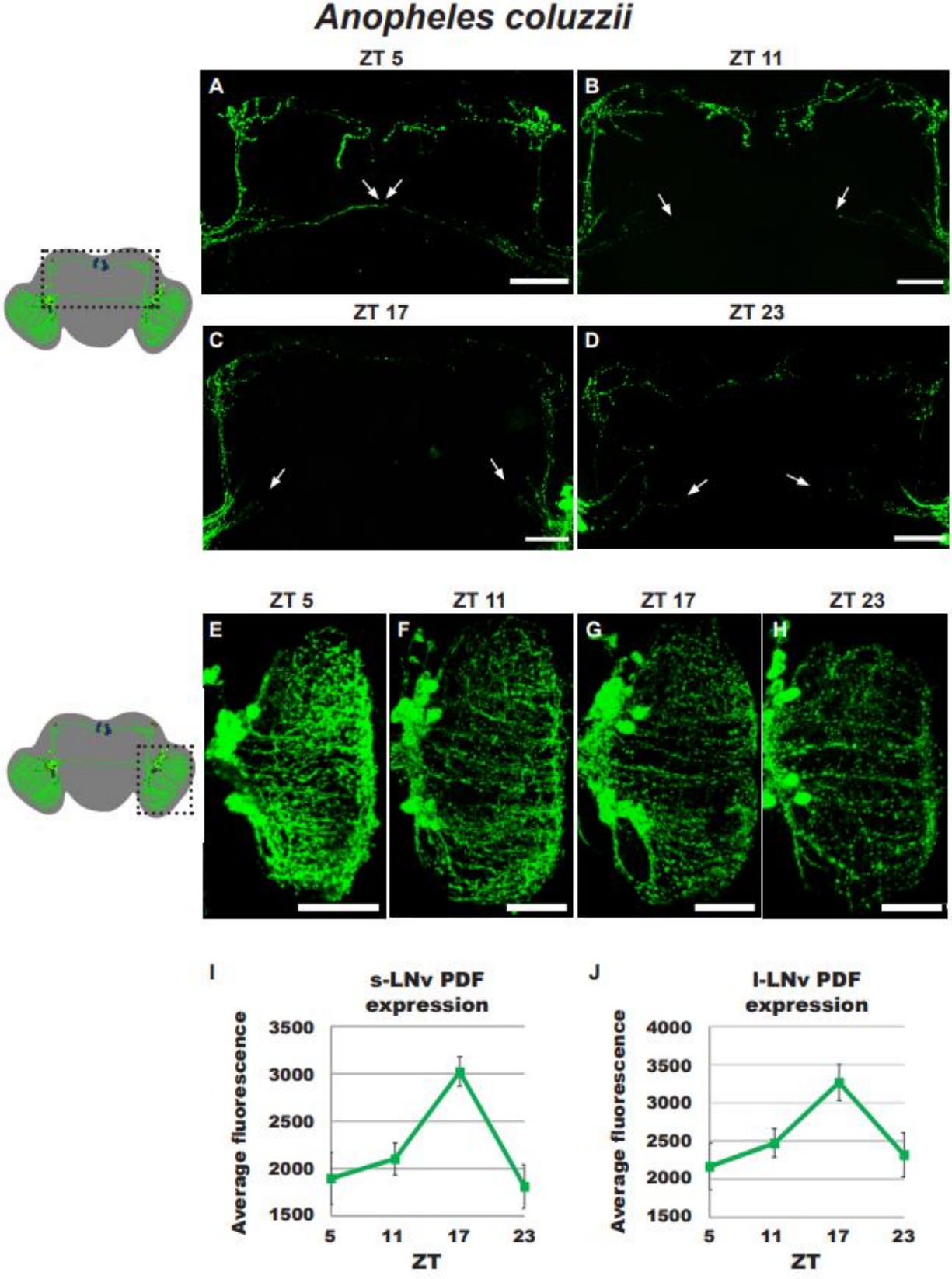
Anopheles coluzzii
ZT 5
ZT 11
ZT 17
ZT 23
A
B
C
D
E
F
G
H
I
s-LNv PDF expression
Average fluorescence
3500
3000
2500
2000
1500
5
11
17
23
ZT
J
l-LNv PDF expression
Average fluorescence
4000
3500
3000
2500
2000
1500
5
11
17
23
ZT

Figure S4. PDF+ neurons and in *Anopheles coluzzii* female brains, Related to Figure 2 and Figure 3. (A-D) Representative confocal images of adult female *An. coluzzii* brains immunocytochemistry stained with α–PDF (green) antibody, zoomed in on LNv dorsal projections at (A) ZT5, (B) ZT11, (C) ZT17, and (D) ZT23. White arrows indicate the ends of LNv neuronal arbors. Images shown in panels A-D were collected from single brain samples using a "tiling" option during image acquisition to capture the entire image field of the whole brain sample (2 tiles of 1024 x 1024 pixels). Post-acquisition images were enhanced uniformly throughout the entire image field for intensity and contrast to show the full extent of the arbors. *Scale bars indicate 50 µm. (E-H) Representative confocal images of adult female *An. coluzzii* brains immunocytochemistry stained with α–PDF (green) antibody, zoomed in on an optic lobe at (E) ZT5, (F) ZT11, (G) ZT17, and (H) ZT23. These images were enhanced for intensity and contrast to better show the ends of the arbors. *Scale bars indicate 50 µm. (I-J) PDF expression levels over 24 hrs time for *An. coluzzii* (ZT5, n=13; ZT11, n=31; ZT17, n=9, ZT23, n=8) (I) s-LNv, and (J) l-LNv. Data are represented as mean ± S.E.M.

	Avg. number of neurons per hemisphere				Avg. number of neurons per brain		
	PDF$^+$ l-LNv	PDF$^+$ s-LNv	PDF$^-$ l-LNv	PDF$^-$ s-LNv	DNs	PI Neurons	m-ANs
Aedes aegypti	8.6 ± 0.4 (n= 18)	9.3 ± 0.5 (n= 18)	3.1 ± 0.4 (n= 19)	5.8 ± 1.1 (n= 19)	4.1 ± 0.3 (n= 30)	-	4.8 ± 0.4 (n= 31)
Anopheles coluzzii	10 ± 0.5 (n= 20)	9.8 ± 0.5 (n= 21)	3.5 ± 0.7 (n= 8)	5.2 ± 0.8 (n= 8)	3.3 ± 0.4 (n= 26)	7.3 ± 0.1 (n= 22)	-

Table S1. Average number of PERIOD-expressing neurons. Related to Figure 2. Average number of PERIOD-expressing neurons ±SEM (n= #) in *Ae. aegypti* and *An. coluzzii* female brains, per hemisphere for PDF+ or PDF- large- and small-LNvs, and per whole brain for DNs, m-ANs, and PI neurons. Female *Ae. aegypti* brains have approximately 8-9 PDF+ l-LNvs and 9-10 PDF+s-LNvs, while female *An. coluzzii* brains have approximately 10 PDF+ l-LNvs and 9-10 PDF+ s-LNvs per hemisphere. Both species of mosquitoes have larger number of LNvs compared to *Drosophila melanogaster*, which has 5-6 l-LNvs and 4-5 PDF+ s-LNvs, but otherwise their neuroanatomical features are highly similar to *Drosophila melanogaster* and other insects. In the lateral ventral region amongst the LNv, there are PER+/PDF- neurons, again, consistent with a PER+/PDF- “5th s-LNv” neuron seen in flies. We find approximately 3 PDF- putative l-LNvs and 6 PDFputative s-LNvs in female *Ae. aegypti*, and approximately 3-4 PDF- putative l-LNvs and 4- 6 PDF- putative s-LNvs in female *An. coluzzii* in each side of the brain.

4.6 Supplementary Movies

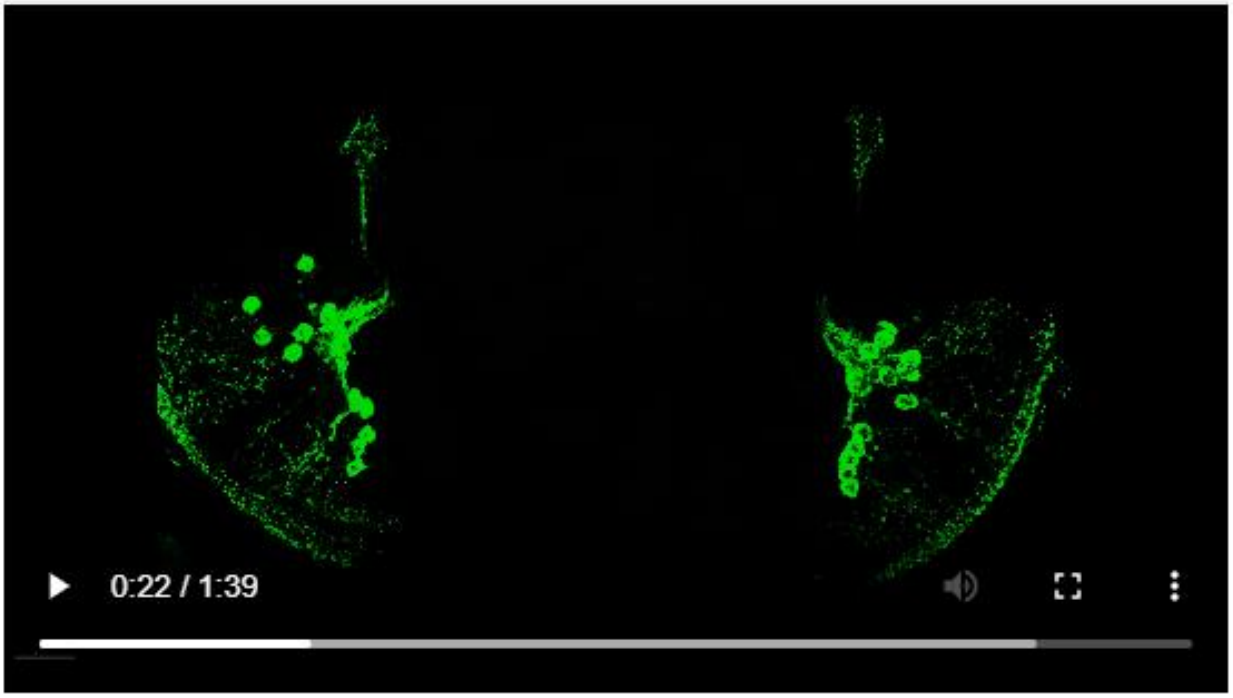

Movie S1. 3D Rendering of PDF Neurons and Projections in the *Ae. aegypti* Female Brain, Related to Figures 2 and 3 3D animation of anti-PDF stained *Aedes aegypti* female brain showing individual z-slice progressing from anterior to posterior, then posterior to anterior, followed by building of z stack, and z stacked brain rotated in multiple directions (+180° around x axis and back, −180° around x axis and back, −180° around the y axis and back, −180° around y axis and back).

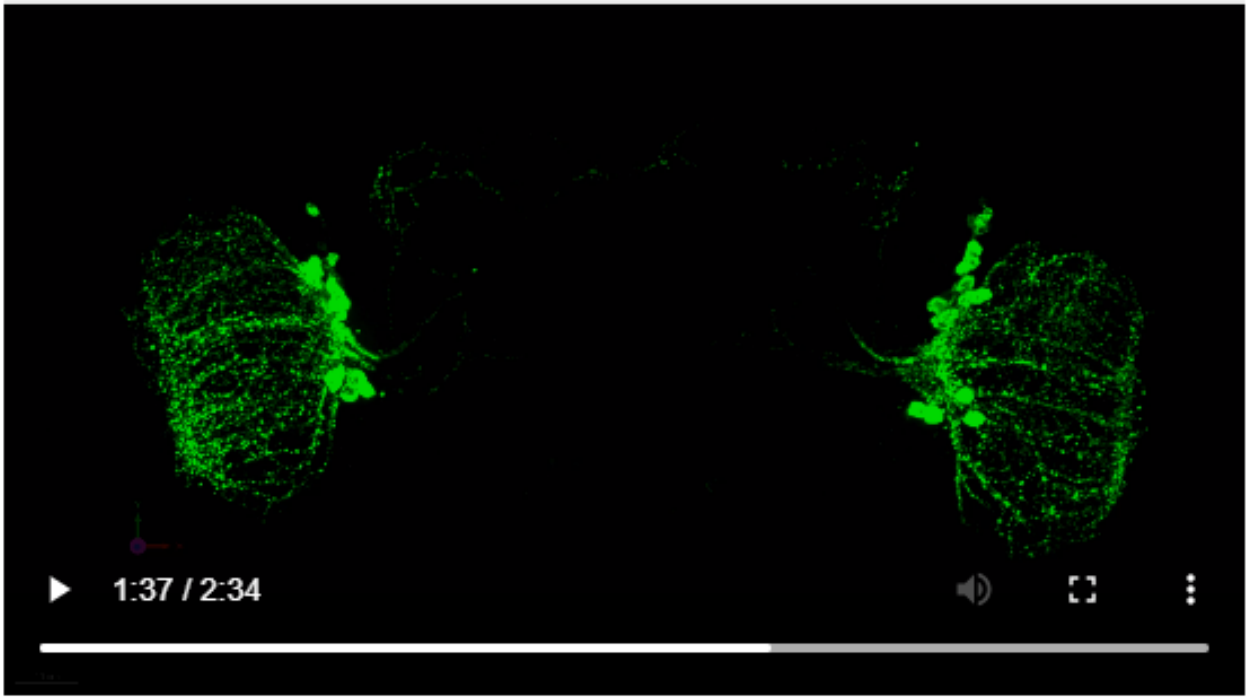

Movie S2. 3D Rendering of PDF Neurons and Projections in the *An. coluzzii* Female Brain, Related to Figures 2 and 3 3D animation of anti-PDF stained *Anopheles coluzzii* female brain showing individual z-slice progressing from anterior to posterior, then posterior to anterior, followed by building of z stack, and z stacked brain rotated in multiple directions (+180° around x axis and back, −180° around x axis and back, −180° around the y axis and back, −180° around y axis and back).

4.7 References

1. Whitfield, J. (2002). Portrait of a Serial Killer: A Roundup of the History and Biology of the Malaria Parasite (Nature Publishing Group).

2. Jones, M.D., Hill, M., and Hope, A.M. (1967). The circadian flight activity of the mosquito *Anopheles gambiae*: phase setting by the light regime. J. Exp. Biol. 47, 503–511.

3. Taylor, B., and Jones, M.D. (1969). The circadian rhythm of flight activity in the mosquito *Aedes aegypti* (L.). The phase-setting effects of light-on and light-off. J. Exp. Biol. 51, 59–70.

4. Baik, L.S., Fogle, K.J., Roberts, L., Galschiodt, A.M., Chevez, J.A., Recinos, Y., Nguy, V., and Holmes, T.C. (2017). CRYPTOCHROME mediates behavioral executive choice in response to UV light. Proc. Natl. Acad. Sci. USA 114, 776–781.

5. Baik, L.S., Recinos, Y., Chevez, J.A., and Holmes, T.C. (2018). Circadian modulation of light-evoked avoidance/attraction behavior in *Drosophila*. PLoS ONE 13, e0201927.

6. Baik, L.S., Recinos, Y., Chevez, J.A., Au, D.D., and Holmes, T.C. (2019). Multiple phototransduction inputs integrate to mediate UV light-evoked avoidance/attraction behavior in *Drosophila*. J. Biol. Rhythms 34, 391–400.

7. Knop, E., Zoller, L., Ryser, R., Gerpe, C., Horler, M., and Fontaine, C. (2017). Artificial light at night as a new threat to pollination. Nature 548, 206–209.

8. Tokushima, Y., Uehara, T., Yamaguchi, T., Arikawa, K., Kainoh, Y., and Shimoda, M. (2016). Broadband photoreceptors are involved in violet light preference in the parasitoid fly Exorista japonica. PLoS ONE 11, e0160441.

9. Green, C., and Cosens, D. (1983). Spectral responses of the tsetse fly, Glossina morsitans morsitans. J. Insect Physiol. 29, 795–800.

10. Farnesi, L.C., Barbosa, C.S., Araripe, L.O., and Bruno, R.V. (2018). The in- fluence of a light and dark cycle on the egg laying activity of *Aedes aegypti* (Linnaeus, 1762) (Diptera: Culicidae). Mem. Inst. Oswaldo Cruz 113, e170362.

11. Sheppard, A.D., Rund, S.S.C., George, G.F., Clark, E., Acri, D.J., and Duffield, G.E. (2017). Light manipulation of mosquito behaviour: acute and sustained photic suppression of biting activity in the *Anopheles* gambiae malaria mosquito. Parasit. Vectors 10, 255.

12. Liu, B., Liu, H., Zhong, D., and Lin, C. (2010). Searching for a photocycle of the cryptochrome photoreceptors. CurrOpin. Plant Biol. 13, 578–586.

13. Das, S., and Dimopoulos, G. (2008). Molecular analysis of photic inhibition of blood-feeding in *Anopheles* gambi*Ae.* BMC Physiol. 8, 23.

14. Sawadogo, S.P., Costantini, C., Pennetier, C., Diabate', A., Gibson, G., and Dabire', R.K. (2013). Differences in timing of mating swarms in sympatric populations of *Anopheles coluzzii* and *Anopheles* gambiae s.s. (formerly *An.* gambiae M and S molecular forms) in Burkina Faso, West Africa. Parasit. Vectors 6, 275.

15. Rund, S.S., Lee, S.J., Bush, B.R., and Duffield, G.E. (2012). Strain- and sex-specific differences in daily flight activity and the circadian clock of *Anopheles* gambiae mosquitoes. J. Insect Physiol. 58, 1609–1619.

16. Araripe, L.O., Bezerra, J.R.A., Rivas, G.B.D.S., and Bruno, R.V. (2018). Locomotor activity in males of *Aedes aegypti* can shift in response to females' presence. Parasit. Vectors 11, 254.

17. Sumba, L.A., Okoth, K., Deng, A.L., Githure, J., Knols, B.G., Beier, J.C., and Hassanali, A. (2004). Daily oviposition patterns of the African malaria mosquito *Anopheles* gambiae Giles (Diptera: Culicidae) on different types of aqueous substrates. J. Circadian Rhythms 2, 6.

18. Coombe, P. (1982). Visual behaviour of the greenhouse whitefly, Trialeurodes vaporariorum. Physiol. Entomol. 7, 243–251.

19. Sheeba, V., Fogle, K.J., Kaneko, M., Rashid, S., Chou, Y.T., Sharma, V.K., and Holmes, T.C. (2008). Large ventral lateral neurons modulate arousal and sleep in *Drosophila*. Curr. Biol. 18, 1537–1545.

20. Parisky, K.M., Agosto, J., Pulver, S.R., Shang, Y., Kuklin, E., Hodge, J.J., Kang, K., Liu, X., Garrity, P.A., Rosbash, M., and Griffith, L.C. (2008). PDF cells are a GABA-responsive wake-promoting component of the *Drosophila* sleep circuit. Neuron 60, 672–682.

21. Renn, S.C., Park, J.H., Rosbash, M., Hall, J.C., and Taghert, P.H. (1999). A pdf neuropeptide gene mutation and ablation of PDF neurons each cause severe abnormalities of behavioral circadian rhythms in *Drosophila*. Cell 99, 791–802.

22. Giebultowicz, J.M. (2000). Molecular mechanism and cellular distribution of insect circadian clocks. Annu. Rev. Entomol. 45, 769–793.

23. Sauman, I., and Reppert, S.M. (1996). Circadian clock neurons in the silk moth Antheraea pernyi: novel mechanisms of Period protein regulation. Neuron 17, 889–900.

24. Bloch, G., Solomon, S.M., Robinson, G.E., and Fahrbach, S.E. (2003). Patterns of PERIOD and pigment-dispersing hormone immunoreactivity in the brain of the European honeybee (Apis mellifera): age- and time- related plasticity. J. Comp. Neurol. 464, 269–284.

25. Konopka, R.J., Pittendrigh, C., and Orr, D. (1989). Reciprocal behaviour associated with altered homeostasis and photosensitivity of *Drosophila* clock mutants. J. Neurogenet. 6, 1–10.

26. Zerr, D.M., Hall, J.C., Rosbash, M., and Siwicki, K.K. (1990). Circadian fluctuations of period protein immunoreactivity in the CNS and the visual system of *Drosophila*. J. Neurosci. 10, 2749–2762.

27. Haddow, A.J., and Gillett, J.D. (1957). Laboratory observations on the oviposition-cycle in the mosquito *Aedes* (Stegomyia) africanus Theobald. Ann. Trop. Med. Parasitol. 51, 170–174.

28. Nayar, J.K., and Sauerman, D.M., Jr. (1971). The effect of light regimes on the circadian rhythm of flight activity in the mosquito *Aedes* taeniorhynchus. J. Exp. Biol. 54, 745–756.

29. Pandian, R.S. (1994). Circadian rhythm in the biting behaviour of a mosquito Armigeres subalbatus (Coquillett). Indian J. Exp. Biol. 32, 256–260.

30. Rivas, G.B.S., Teles-de-Freitas, R., Pavan, M.G., Lima, J.B.P., Peixoto, A.A., and Bruno, R.V. (2018). Effects of light and temperature on daily activity and clock gene expression in two mosquito disease vectors. J. Biol. Rhythms 33, 272–288.

31. Gentile, C., Rivas, G.B., Meireles-Filho, A.C., Lima, J.B., and Peixoto, A.A. (2009). Circadian expression of clock genes in two mosquito disease vec- tors: cry2 is different. J. Biol. Rhythms 24, 444–451.

32. Liu, Y.N., Liu, Y.J., Chen, Y.C., Ma, H.Y., and Lee, H.Y. (2017). Enhancement of mosquito trapping efficiency by using pulse width modulated light emitting diodes. Sci. Rep. 7, 40074.

33. Rieger, D., Shafer, O.T., Tomioka, K., and Helfrich-Forster, C. (2006). Functional analysis of circadian pacemaker neurons in *Drosophila melanogaster*. J. Neurosci. 26, 2531–2543.

34. Helfrich-Forster, C., Nitabach, M.N., and Holmes, T.C. (2011). Insect circadian clock outputs. Essays Biochem. 49, 87–101.

35. Barber, A.F., Erion, R., Holmes, T.C., and Sehgal, A. (2016). Circadian and feeding cues integrate to drive rhythms of physiology in *Drosophila* insulin-producing cells. Genes Dev. 30, 2596–2606.

36. Cavanaugh, D.J., Geratowski, J.D., Wooltorton, J.R., Spaethling, J.M., Hector, C.E., Zheng, X., Johnson, E.C., Eberwine, J.H., and Sehgal, A. (2014).

Identification of a circadian output circuit for rest/activity rhythms in *Drosophila*. Cell 157, 689–701.

37. Gorostiza, E.A., Depetris-Chauvin, A., Frenkel, L., P´ırez, N., and Ceriani, M.F. (2014). Circadian pacemaker neurons change synaptic contacts across the day. Curr. Biol. 24, 2161–2167.

38. Rund, S.S., Hou, T.Y., Ward, S.M., Collins, F.H., and Duffield, G.E. (2011). Genome-wide profiling of diel and circadian gene expression in the malaria vector *Anopheles* gambi*Ae.* Proc. Natl. Acad. Sci. USA 108, E421– E430.

39. Leming, M.T., Rund, S.S., Behura, S.K., Duffield, G.E., and O'Tousa, J.E. (2014). A database of circadian and diel rhythmic gene expression in the yellow fever mosquito *Aedes aegypti*. BMC Genomics 15, 1128.

40. Hirano, A., Fu, Y.H., and Ptacek, L.J. (2016). The intricate dance of post-translational modifications in the rhythm of life. Nat. Struct. Mol. Biol. 23, 1053–1060.

41. Li, Y.H., Liu, X., Vanselow, J.T., Zheng, H., Schlosser, A., and Chiu, J.C. (2019). O-GlcNAcylation of PERIOD regulates its interaction with CLOCK and timing of circadian transcriptional repression. PLoS Genet. 15, e1007953.

42. Chiu, J.C., Ko, H.W., and Edery, I. (2011). NEMO/NLK phosphorylates PERIOD to initiate a time-delay phosphorylation circuit that sets circadian clock speed. Cell 145, 357–370.

43. Nakajima, M., Imai, K., Ito, H., Nishiwaki, T., Murayama, Y., Iwasaki, H., Oyama, T., and Kondo, T. (2005). Reconstitution of circadian oscillation of cyanobacterial KaiC phosphorylation in vitro. Science 308, 414–415.

44. Shafer, O.T., Rosbash, M., and Truman, J.W. (2002). Sequential nuclear accumulation of the clock proteins Period and Timeless in the pacemaker neurons of *Drosophila melanogaster*. J. Neurosci. 22, 5946–5954.

45. Nawathean, P., and Rosbash, M. (2004). The doubletime and CKII kinases collaborate to potentiate *Drosophila* PER transcriptional repressor activity. Mol. Cell 13, 213–223.

46. Yagita, K., Tamanini, F., Yasuda, M., Hoeijmakers, J.H., van der Horst, G.T., and Okamura, H. (2002). Nucleocytoplasmic shuttling and mCRY-dependent inhibition of ubiquitylation of the mPER2 clock protein. EMBO J. 21, 1301–1314.

47. Mure, L.S., Le, H.D., Benegiamo, G., Chang, M.W., Rios, L., Jillani, N., Ngotho, M., Kariuki, T., Dkhissi-Benyahya, O., Cooper, H.M., and Panda, S. (2018). Diurnal transcriptome atlas of a primate across major neural and peripheral tissues. Science 359, eaao0318.

48. Lemos, D.R., Downs, J.L., and Urbanski, H.F. (2006). Twenty-four-hour rhythmic gene expression in the rhesus macaque adrenal gland. Mol. Endocrinol. 20, 1164–1176.

49. Ramanathan, C., Nunez, A.A., and Smale, L. (2008). Daily rhythms in PER1 within and beyond the suprachiasmatic nucleus of female grass rats (Arvicanthis niloticus). Neuroscience 156, 48–58.

Chapter 5

Conclusions and Final Remarks

Circadian rhythms play an important role in governing daily physiology and behavior. For thousands of years humans had evolved to synchronize their internal biological clocks to the rising and setting of the sun. This process, called entrainment, ensures that our internal molecular mechanisms perform their optimal processes at the right times of the 24-hr day. Many studies have shown that disruption of circadian rhythms lead to many downstream repercussions. The disruption of the biological clock lead to detrimental conditions ranging from issues with sleeping, irritability, overt tiredness, and to more serious conditions such as increased risk of heart disease, risk of type 2 diabetes, and the promotion of certain cancers. Here we sought to shed light on the mechanism that controls the biological clock. We developed a method to capture real-time disruption of the biological clock by tracking the molecular components that are key players to circadian rhythms. Additionally, we study a protein complex that directly impact the behaviors of the molecular clock as well as downstream circadian-mediated locomotor behaviors. Last, we shed light on how circadian rhythms affect diurnality/nocturnality and characterize the molecular mechanisms on two different mosquito species which control daytime and nighttime behaviors. Together, we show evidence of the importance of circadian rhythms on day-to-day physiology and behavior, and (1) suggest possible ways to alleviate the detrimental effects of weekend light shift on the general public, (2) improve on the general knowledge on the mechanisms governing circadian rhythms, and (3)

elucidate and show comparison in circadian mechanisms between daytime and nighttime biting mosquitoes.

In Chapter 2, we developed a light/dark entrainment protocol (*LD Strobe*) to allow for bioluminescence imaging of the entire circadian neural circuit. This tool provides us the ability to obtain real-time bioluminescence imaging of the clock protein, PER, in the entire *Drosophila* circadian neural circuit. By doing so, we modified the *LD Strobe* protocol simulate light shifts experienced by the general populace during the transition from a weekday work week schedule, to delayed light exposure experienced during weekends (WLS). We found that WLS leads to significant disruption of the clock protein oscillation characterized by desynchronization of oscillations between circadian neuron subgroups, as well as the oscillations within these subgroups. Additionally, we modified the *LD Strobe* entrainment to obtain bioluminescence to show proof of principle in tracking (1) TIMELESS under a consistent LD schedule, (2) behaviors of the molecular clock under constant light (LL), and (3) provided evidence that the circadian neural circuit is autonomous outside of external photoreceptors (i.e. the compound eye) and the fly brain can directly entrain to environmental light signals. Lastly, we provide evidence that a simulation of one weekend phase shifting light schedules lead to detriments to sleep patterns and learning and memory in flies.

The technology developed to obtain the data for chapter 2 can be carried out to investigate countless studies inquiring about how the biological clock is affected. For example, the *LD Strobe* entrainment can be used to study the effects of neurodegenerative diseases (i.e. Alzheimer's and Huntington's disease) on the daily dynamics of clock oscillations. Furthermore, we could speculate how oscillations of clock

proteins are challenged in the presence of light disruptions. The experimental procedures used in Chapter 2 could potentially shed light on the interplay between neurodegenerative diseases and circadian clock behaviors, as well as circadian-modulated outputs that are characteristic of said diseases.

In Chapter 3, we characterized the novel MTGO protein. Earlier work shows that MTGO binds to the TRiC/CCT3 complex to perform important tasks in *Drosophila* larval development. Syed et al., show that MTGO is key to the formation of neuromuscular junctions, larval locomotion, pupal eclosion, and much more. Here we show that MTGO provides input in the mediation of circadian-modulated behaviors in adult *Drosophila.* We find that in adult flies, mutations to *mtgo* lead to an absence of locomotor activity under LD and DD conditions. Furthermore, this downplay of movement reflects a disruption in circadian rhythmicity, in that locomotion does not indicate circadian-modulated morning and evening anticipatory behaviors. MTGO mutants exhibit an inversion in the expression of the clock protein, PERIOD, supporting our observations in defects in locomotor behaviors. Lastly, because our goal is to characterize the relationship of MTGO with the biological clock, we determined that the MTGO protein, itself, oscillates throughout the 24-hour day. This suggests that MTGO may be in a feedback loop along with the circadian clock, where the molecular clock provides input into the temporal expression of the MTGO protein, but that MTGO, itself, provides input into the molecular clock, seen by the disruption in PER expression observed in MTGO mutants. Although we have sufficient evidence to conclude that MTGO affects the circadian clock behaviors, further studies are needed to confirm the direct relationship between MTGO and the molecular clock. For example, one factor missing is how does MTGO interact with the key circadian proteins,

if at all. Experiments providing MTGO binding to clock components would provide concrete evidence and justification to the evidence we've presented.

Lastly, in Chapter 4, we provided insights on the mechanisms that govern circadian rhythmicity between daytime and nighttime-biting mosquitoes. Our findings provided insights on the circadian-modulated locomotor behaviors that vary between the two species *Aedes aegypti and Anopheles coluzzii.* We found that light attraction and circadian modulated light avoidance behavior is dependent upon species, sex of the mosquitoes, spectra of light used, and the time of the day. Furthermore, we show, for the first time, circadian clock behaviors comparing nighttime- and daytime-biting mosquitoes, anti-phasic oscillations of the clock protein PER. Our findings provide valuable information on the mediation of circadian rhythmicity between diurnal and nocturnal species of animals suggesting the optimization of behaviors on a time-dependent manner.

Together, our findings build on the foundation of shedding light on the importance of circadian rhythms in daily physiology and behavior. We developed novel methods in determining the molecular and locomotor behaviors upon circadian disruption. We provided insights on a novel protein complex that suggests it interacts with the molecular clock, and that disruption of this protein leads to a detriment to circadian rhythmicity. Finally, we add to the knowledge base of circadian modulation in diurnal and nocturnal species of mosquitos. We contribute our findings with a mindset of shedding light on the importance of circadian rhythms in our daily lives.